Summer 6-24-2019

The Collison Floating Evaporation Pan: Design, Validation, and Comparison

Jacob William Collison

Jacob William Collison
Candidate

Civil, Construction & Environmental Engineering
Department

This dissertation is approved, and it is acceptable in quality and form for publication:

Approved by the Dissertation Committee:

Mark Stone, Chairperson

Julie Coonrod

Jan Boll

Ricardo Gonzalez-Pinzon

The Collison Floating Evaporation Pan: Design, Validation, and Comparison

by

Jacob William Collison

B.S., Civil Engineering, University of New Mexico, 2011

M.S., Civil Engineering, University of New Mexico, 2013

DISSERTATION

Submitted in Partial Fulfillment of the

Requirements for the Degree of

Doctor of Philosophy in Engineering

The University of New Mexico

Albuquerque, New Mexico

July, 2019

DEDICATION

To my amazing wife, Kathryn!
This project would have never panned out without your support!

ACKNOWLEDGMENTS

I would like to thank my friend and mentor, Mark Stone, for all your feedback and help through the years. Taking your Fluid Mechanics class back in 2009 started me on this path. I am grateful that you have been there for me for all these years.

I am grateful for the invaluable feedback from my committee members, Mark Stone, Julie Coonrod, Jan Boll, and Ricardo Gonzalez-Pinzon.

I would like to thank Dagmar Llewellyn for her support through the years and helping to secure funding for this project through U.S. Bureau of Reclamation Science and Technology program.

Finally, I want to thank my wife, Kathryn, for being the lucky individual to read my first drafts…

The Collison Floating Evaporation Pan: Design, Validation, and Comparison

by

Jacob William Collison

B.S., Civil Engineering, University of New Mexico, 2011

M.S., Civil Engineering, University of New Mexico, 2013

Ph.D., Civil, Construction & Environmental Engineering, University of New Mexico, 2019

ABSTRACT

Accurate tracking of open-water evaporative losses, one of the largest consumptive uses of water in the Southwestern USA, is increasingly important with anticipated climate shifts toward longer and more severe droughts. A new open-water evaporation technique, the Collison Floating Evaporation Pan, (CFEP), was tested on Cochiti Lake, New Mexico, USA for one year with objectives being: identify the limitations and potential solutions to evaporation techniques; deploy, test the reliability, and validity of the CFEP and evaluate uncertainties in standard evaporation techniques; and improvements over prior evaporation techniques. The CFEP provided reliable evaporation measurements during sustained winds greater than 20 m/s. The accuracy of the CFEP was validated with an averaged percent difference of 1.72 of actual. The CFEP provided more accurate evaporation measurements than the five methods it was compared to with the Class A Pan underestimating evaporation by 910 acre-feet from May 13 through November 30, 2018.

Contents

Chapter 1: Introduction

1.1 Motivation

Accurate tracking of lake and reservoir evaporative losses, one of the largest consumptive uses of water in the Southwestern United States (Bureau of Reclamation, September 2012; Wurbs and Ayala, 2014), is becoming increasingly important with anticipated climate shifts toward higher temperatures, less available open water, and longer, more severe droughts (Friedrich et al., 2018; Hurd and Coonrod, 2008; Udall and Overpeck, 2017). As projected water supplies fail to meet increasing demands, modifications to where and when water is stored based on the reduction of evaporative losses can have a significant positive impact on total water supplies (Bureau of Reclamation, December 2012). Understanding where and when lake and reservoir evaporation rates are the highest/lowest can help water managers reduce evaporative losses by using the conservation at the source methodology (Friedrich et al., 2018). This methodology requires accurate and precise open-water evaporation knowledge in order to be best implemented, but acquiring such knowledge can be very expensive when using current state-of-science evaporation estimation techniques.

The high costs associated with state-of-science evaporation estimation techniques results in less accurate state-of-practice evaporation estimation techniques being used instead. An example of the difference in error rates associated with these two different evaporation estimation methodologies is represented by how evaporation is determined on the two largest reservoirs on the Colorado River, USA. Lake Mead and Lake Powell evaporate an estimated combined 1,400 MCM (million cubic meters; or 1,135 million acre-feet) annually, which is over five times the water usage of Denver, Colorado, USA (Bureau of Reclamation, December

2012; Friedrich et al., 2018). The annual evaporation rate of Lake Mead is 720 MCM, with an average estimated error of 47 MCM (5-8%) using the state-of-science techniques eddy covariance and Bowen ratio energy budget (Moreo and Swancar, 2013); the annual evaporation rate of Lake Powell is 680 MCM, with an average estimated error of 153 MCM (15-30%) using a state-of-practice technique, water budget (Winter, 1981; Myers, 2013). From this, it is clear that the state-of-science technique used on Lake Mead has a much smaller error rate than the more commonly used state-of-practice technique used on Lake Powell. However, while the eddy covariance and Bowen ratio energy budget state-of-science techniques used to estimate Lake Mead's evaporation rate are considered one of the most accurate open-water evaporation estimation techniques (Baldocchi, 2003; Blanken et al., 2000; Foken, 2008; Moreo and Swancar, 2013; Stannard et al., 2013), they are also limited to well-funded, short-in-duration scientific studies due to their high cost and complexity of use. In contrast, the state-of-practice water budget technique used to estimate Lake Powell's evaporation rate is commonly used by water resource managers in conjunction with a Class A Pan due to its low cost, ease of use, and long, reliable records, but it is also considered to be one of the least accurate open-water evaporation estimation techniques (Duan, 2014; Kumambala and Ervine, 2010; Piper et al., 1986; Rientjes et al., 2011; Russell and Johnson, 2006; Sena, 2000; Setegn et al., 2011; Sivapragasam et al., 2009; Velpuri et al. 2012). The large difference in error rates between the evaporation estimation techniques exemplifies the gap between state of science and state of practice.

In total, state-of-science evaporation estimation techniques have been completed on approximately 25-35 lakes and reservoirs within the USA. It is estimated that there are approximately 31,000 lakes and reservoirs greater than 10,000 m^2 in the USA that are used for drinking/irrigation water (National Inventory of Dams, 2019; U.S. Environmental Protection Agency, 2009). Thus, these accurate state-of-science techniques have only been completed on approximately 0.1% of the lakes and reservoirs whereas the majority of the remaining 99.9% of lakes and reservoirs use state-of-practice techniques. This gap between accurate and inaccurate techniques continues to grow as more accurate evaporation techniques are created, but are rarely implemented by water resource managers.

The main underlying reason for the gap in accurate, but rarely used and inaccurate, but commonly used evaporation estimation techniques is the associated costs of each technique. State-of-science techniques are estimated to cost between $150-300k+ per year for one location whereas state-of-science techniques generally cost between $10-30k per year (based on a review of eddy covariance and Bowen ratio energy budget techniques funded by the National Science Foundation). Additionally, state-of-science techniques are technically and computationally complicated, requiring a considerable amount of training and postprocessing of acquired data in order to determine evaporation rates (Mauder and Foken, 2006).

This study aimed to investigate a novel technology, the U.S. patented (Collison, 2018) Collison Floating Evaporation Pan (CFEP) as a possible solution that can bridge the gap between state-of-science and state-of-practice evaporation estimation techniques. Specifically, the CFEP is designed to be easily applied like state-of-practice techniques, and as or more accurate and substantially lower in cost than state-of-science techniques. The CFEP is designed around the simplistic premise of a Class A Pan, where a decrease in water level is the evaporation rate, while overcoming the accuracy drawbacks of the Class A Pan. Additionally, the CFEP is designed to be fully automated with onboard telemetry for remote access, reducing the need for field visits. Lastly, the accuracy of the CFEP was verified with a hemispherical evaporation chamber (dome), considered one of the most accurate techniques for measuring in-situ open-water evaporation (Crilley and Collison, 2015; Garcia et al., 2008; Masoner and Stannard, 2010; Stannard, 1988).

1.2 Current Limitations of Evaporation Estimation Techniques

The vast majority of lake and reservoir evaporation is estimated with a Class A Pan within the United States, Europe, and Australia (Doorenbos and Pruitt, 1977; Famsworth et al., 1982; Rayner, 2005), even though it is considered one of the least accurate techniques (Alvarez et al., 2006; Chu et al., 2012; Eichinger et al., 2003; Follansbee, 1934; Grayson et al., 1996; Tanny et al., 2008; Trask, 2007). The Class A Pan's widespread use is due to its low cost and reliability as well as being easily applied. It is inaccurate due to a few reasons, including its small thermal mass, which is susceptible to diurnal variations in air temperature (Hounam, 1973; Jovanovic et al., 2008; Morton, 1979), and its placement outside the atmospheric boundary layer (ABL) influence of a body of water.

Large bodies of water absorb solar energy in the spring, resulting in reduced evaporation rates, and then release the stored energy in the fall, resulting in increased evaporation rates (Penman, 1948). The Class A Pan and its smaller thermal mass is coupled to diurnal variations in air temperature, resulting in higher evaporation rates in the spring/early summer and lower evaporation rates in the fall (Hounam, 1973; Jovanovic et al., 2008; Morton, 1979). This major limitation for Class A Pans, as well as other state-of-practice evaporation estimation techniques that do not account for stored energy, results in higher uncertainties and reduced accuracy of measurements. State-of-science evaporation techniques are able to capture the effects of stored energy on evaporation rates, which increases their annual and monthly accuracy.

In addition to the stored energy problems of the Class A Pan, another major limitation of the Class A Pan and other state-of-practice evaporation estimation techniques is collecting atmospheric variables (air temperature, relative humidity, net radiation, and wind speed) and/or placement of equipment outside the atmospheric boundary layer influence of a body of water (Winter et al., 2003). The ABL overlying a lake or reservoir is caused by the higher rates of open-water evaporation and can be imagined as a "bubble" of cool and moist air that impedes evaporation (Friedrich et al., 2018; Kaimal and Finnigan, 1994; Kormann and Meixner, 2001; Stewart, 1979; Troen and Mahrt, 1986). This ABL is more significant in arid/semiarid environments due to the vast difference in available water for evaporation from a body of water in comparison to the water-limited land surrounding the body of water. Collecting data outside the influence of the ABL will result in higher estimated evaporation rates requiring a corrective value being applied, like the Class A Pan coefficient of 0.7, which reduces the Class A Pans estimated evaporation rate by 30% (Follansbee, 1934; Kohler, 1954). State-of-science techniques have to be placed within the ABL influence of the body of water to function properly, meaning a corrective coefficient does not need to be applied.

The major limitation for state-of-science evaporation estimation techniques, other than their high cost and complexity, is the requirement of adequate fetch. The general rule for acquiring adequate fetch is having a homogeneous surface surrounding the weather station at 100 to 1,000 times the instrument height depending on atmospheric stability, stable verses unstable, respectively (Horst and Weil, 1994; Moreo and Swancar, 2013). Not meeting this fetch requirement in arid/semiarid environments will result in hot and dry air surrounding the body of water and interfering with atmospheric measurements, resulting in a higher estimated evaporation rates, unless this inaccurate data is removed during extensive postprocessing

(Mauder and Foken, 2006). Meeting this requirement is considerably difficult on all but the largest lakes and reservoirs, especially on lakes and reservoirs in arid/semiarid environments where the shape of these bodies of water tend to be narrow and long. The dams used to impound these bodies of water are typically built in narrow-deep sections (e.g., canyons), producing narrow, long, and deep bodies of water where the fetch requirement is rarely met from all directions. Additionally, the limitation of adequate fetch distances prevents the understanding of the effect of shore-to-water and water-to-shore winds on evaporation rates in arid/semiarid environments.

The last major limitation for both state-of-science and state-of-practice evaporation estimation techniques is applying a single evaporation estimation to the whole lake or reservoir, which remote sensing studies have shown to be an inaccurate assumption, as evaporation rates vary throughout a reservoir based on varying surface water temperatures (Duan, 2014; Ebaid and Ismail, 2010; Hassan, 2013; Herting et al., 2004; Lenters et al., 2013). The large fetch distances needed for state-of-science and state-of-practice techniques preclude quantification of spatially varying evaporation rates.

1.3 Overcoming Limitations

The CFEP is designed to overcome the limitations of high cost, complexity of use, and adequate fetch requirements associated with state-of-science techniques as well as the limitations of stored energy, placement outside the ABL, and inaccuracy associated with state-of-practice techniques. The cost of the CFEP is estimated to range between $40-75k per year, depending on site specific requirements. The low cost of the CFEP is due in part to its fully automated design, reducing expensive site visits; in addition, the robustness of the design allows for long-term use, further reducing costs (see section 3.2.2 for more information).

Overcoming the high costs associated with state-of-science techniques will allow for accurate evaporation data at more locations and for longer durations.

The CFEP is designed to provide a straightforward but accurate approach to measuring evaporation, where a decrease in water level within the evaporation pan equals the evaporation rate (see section 3.2.2 for more information). This clear-cut process provides real-time evaporation rates as no postprocessing of the data is required, in contrast to state-of-science techniques which require a significant amount of postprocessing in order for an evaporation rate to be determined (Mauder and Foken, 2006). Additionally, how the CFEP measures evaporation is identical to that of a Class A Pan, allowing for straightforward adoption by water resource managers who are already familiar with this way of measuring evaporation.

The CFEP is designed to overcome the limitation of adequate fetch, as it requires no fetch distances since the water level within the evaporation pan is identical to the surrounding lake or reservoir water level (see section 3.2.2 and 3.3.1 for more information). Adequate fetch is required for both state-of-science and state-of-practice techniques in order to allow for air overlying the water to equilibrate to the lake or reservoir ABL through atmospheric mixing before being measured by various atmospheric sensors (Horst and Weil, 1994; Moreo and Swancar, 2013). As no adequate fetch distance is required for the CFEP, it can be deployed in fetch-limited locations, such as small coves, small lakes/reservoirs, and/or narrow channels, presently inaccessible with other evaporation estimation techniques, allowing for a greater range of deployment locations.

In addition to allowing for more deployment locations, requiring no adequate fetch allows the CFEP to measure spatially varying evaporation rates. Evaporation rates within the CFEP's evaporation pan can be associated with different wind directions; therefore, spatially varying evaporation rates as a function of wind direction can be determined. Being able to deploy a CFEP near the shore of a lake or reservoir will increase the knowledge of evaporation rates during shore-to-water winds and water-to-shore winds in arid/semiarid environments where it is assumed that the air over the shore has a lower vapor pressure than the air over the body of water.

The CFEP is designed to capture the effects of stored energy on evaporation in a large body of water. The CFEP was built with aluminum alloy 6061, which has a thermal conductivity six times greater than stainless steel, a material that the Class A Pan and other floating evaporation pans use. This higher thermal conductivity allows for the water temperature within the CFEP's evaporation pan to be influenced by the water surrounding it. The increased temperature of the lake or reservoir water during the fall, due to stored solar energy from the spring and summer, will influence the water within the CFEP's evaporation pan, providing a more accurate evaporation measurement (see section 3.3.3. for more information). Additionally, when the CFEP is placed within the ABL of a lake or reservoir, the influence of the ABL will affect the CFEP equally as the water surrounding it, increasing accuracy.

The CFEP is designed to overcome the limitations associated with state-of-science and state-of-practice evaporation estimation techniques, allowing for deployment at locations previously unavailable to prior techniques as well as quantifying spatially varying evaporation rates, enhancing hydrologic sciences' knowledge about evaporation rates in fetch-limited locations. Additionally, the uncomplicated and inexpensive design provides water resource managers an accurate and affordable evaporation estimating tool, allowing for deployment at a wider range of locations providing a great benefit for broader impacts.

1.4 Objectives

With funding from the U.S. Bureau of Reclamation and the U.S. Army Corps of Engineers, this study tested the CFEP on Cochiti Lake, located in central New Mexico, USA, a 61.7 MCM (50,000-acre-foot) flood-control reservoir from November 2017 through December 2018. The goal of this research was to advance knowledge of spatial and temporal evaporation processes in lakes and reservoirs through an improved measurement technique based on the hypotheses that a properly designed floating evaporation pan will provide near-actual evaporation rates. This goal was met by addressing the following three objectives:

1. Identify the limitations and potential solutions to evaporation estimation techniques;
2. Design, deploy, and test the reliability and validity of the CFEP and evaluate uncertainties in standard evaporation estimation techniques; and
3. Patented improvements over prior evaporation estimating techniques.

These objectives were completed during November 2017 through December 2018, where different design iterations were adapted to fix problems of waves overtopping the evaporation pan. The addition of additional buoyancy and an outer splash guard resulted in zero wave overtopping of the evaporation pan from May 13, 2018 through the end of the study. The accuracy and precision of the CFEP was determined with a dome on three separate dates. The CFEP was within 2% of the dome measurements, with the dome shown to be within ±5% of actual evaporation (Reicosky and Peters, 1977; Reicosky, 1981; Reicosky et al., 1983). The results from the CFEP were compared to the following equations and techniques: the Hargreaves-Samani equation (Hargreaves and Samani, 1985), the Hamon equation (Hamon, 1961), the U.S. Weather Bureau equation (Kohler et al., 1955), the Penman equation (Penman, 1948), and an onsite Class A Pan.

1.5 Overview of Dissertation

Chapter 2 focuses on the limitations of current state-of-science and state-of-practice evaporation estimation techniques. This chapter elucidates the barriers that prevent widespread adoption of state-of-science techniques and why water resource managers continue to use less accurate state-of-practice techniques instead. Additionally, this chapter offers potential solutions to this problem by either simplifying state-of-science techniques, increasing the accuracy of inaccurate state-of-practice techniques, and/or developing a new technique, the CFEP.

Chapter 3 focuses on the major objectives of this study: design, validation, and comparison of the CFEP to other techniques. The design period of the study was from November 2017 through April 2018, where modifications were applied to the CFEP to produce a reliable evaporation measurement. Three separate dome validation tests were completed, and, finally, the CFEP's evaporation data was compared to standard evaporation techniques.

Chapter 4 is an overview of the "Floating Evaporation Pan with Adjustable Freeboard and Surrounding Wave-Guard," U.S. 10,082,415 B1 patent (Collison, 2018). Detailing the improvements over a prior U.S. floating evaporation pan patent by Masoner and Christenson (2007) that were incorporated into the CFEP design, being the wave-guard surrounding the evaporation pan, which added reliability and a wider range of deployment locations.

Chapter 5 provides a summary of the dissertation's chapters and their main conclusions, improvements to hydrologic sciences, broader impacts, and recommendations for future research.

Chapter 2: An Examination of the Limitations of Current Evaporation Techniques

2.1 Introduction

Within the continental United States of America, there are approximately 31,000 lakes and reservoirs greater than 10,000 m^2 that are designated for drinking water or are accessible for drinking water use (National Inventory of Dams, 2019; U.S. Environmental protection Agency, 2009). At the majority of these 31,000 locations, open water evaporation losses are estimated using various evaporation estimation techniques, ranging from simpler techniques, like the Class A Pan, to more complicated techniques, like eddy covariance. Open water evaporative loss information is used to help inform water resource management decisions, such as those concerning water compact deliveries, modification of water credits and/or debits, and water storage locations. The more accurately evaporation losses are estimated, the more efficiently the water system can be managed, which further results in more water available for beneficial uses; currently, however, the most accurate techniques are limited to well-funded, short-in-duration scientific studies at limited locations.

These well-funded scientific studies on open-water evaporation rates typically consist of either eddy covariance or Bowen ratio energy budget technique costing between $150-300k per year with durations rarely longer than four years (Lowe, 2009; and based on a review of eddy covariance and Bowen ratio energy budget techniques funded by the National Science Foundation). The high costs associated with both of these techniques has limited detailed evaporation estimates to approximately 25-35 lakes and reservoirs in the USA, which is 0.1%

of the 31,000 lakes and reservoirs used for drinking water. The evaporation rate on the remaining lakes and reservoirs, if required, is estimated by less accurate techniques, leading to uncertainties in compact water allocations and inefficiencies in water resource management.

The most widespread open-water evaporation estimation technique is the Class A Pan, a technology invented in the early 1880's that is commonly used throughout the United States, Europe, and Australia (Doorenbos and Pruitt, 1977; Famsworth et al., 1982; Rayner, 2005). The Class A Pan (see section 2.2.1 for more information) was recommended as the standard evaporation estimation technique in the 1930's due to its simplicity of use, inexpensive cost, and reliability, even though it was the least accurate technique tested (Follansbee, 1934). Reliability was the main deciding factor for the Class A Pan becoming the standard in the 1930's, as the accuracy difference between the techniques compared in Follansbee (1934) was less than 7%. The inaccuracy of the Class A Pan has become more apparent as more accurate techniques have been invented, providing evidence that the Class A Pan can be off by 20-75% in arid environments and is one of the least accurate evaporation estimation techniques available (Alvarez et al., 2006; Chu et al., 2012; Eichinger et al., 2003; Follansbee, 1934; Grayson et al., 1996; Tanny et al., 2008; Trask, 2007). While it has been shown repeatedly that the Class A Pan is not very accurate, it is still the standard state of practice even as more accurate state-of-science techniques have become available.

This gap in accuracy between the state-of-practice and state-of-science evaporation estimation techniques continues to grow as the state-of-science techniques become more accurate; further, they are rarely adopted by water resource managers, mainly due to high costs and complexity of use. The eddy covariance and Bowen ratio energy budget techniques both require a significant investment in sensitive and expensive instrumentation, significant postprocessing of collected data, and an extensive knowledge of how these techniques operate (Mauder and Foken, 2006). In contrast, the state-of-practice evaporation estimation techniques include Class A Pans, one-to-four variable atmospheric evaporation estimation equations, and simple water budget techniques, all of which are very easily applied, require minimal training, and are inexpensive in practice.

A modification of current techniques and/or a new technique that is accurate, easily applied, affordable, and adoptable by water resource managers is needed to bridge the gap between state of science and state of practice. One potential benefit of such a technique would be increased evaporation knowledge at more locations, leading to improved water management practices, such as conservation at the source. Conservation at the source relies on accurate evaporation rates to determine when and where it is best to store water to reduce evaporative losses and thus provide more water for beneficial use (Friedrich et al., 2018). Another advantage of such a technique would be more accurate accounting of water losses within a system, leading to more accurate water operation models and adaptive water management practices (Huntjens et al., 2011; Pahl-Wostl, 2007). Adaptive water management is a data-driven process which relies on accurate data of all the gains and losses within a system in order to improve water management policies and make the system more efficient.

2.2 State of Practice for Open-Water Evaporation Estimation Techniques

State-of-practice evaporation estimation techniques typically consist of easily applied and inexpensive methods, such as Class A Pans, water budgets, and simple equations that require minimal atmospheric variables. The accuracy of these techniques is sacrificed for their simplicity of use, resulting in estimated evaporation rates being off by as much as 75% in arid environments (Eichinger et al., 2003). Although, simplicity of these techniques helps ensure high reliability of their measurements, with data sets greater than a hundred years at some locations. Reliable and consistent measurements, although inaccurate, provide daily data that are needed for water management. The atmospheric variables required for the simple evaporation estimation equations are typically air temperature, wind speed, relative humidity, and some form of solar radiation derived from the declination of the sun.

Solar radiation, relative humidity, wind speed, and the vapor pressure gradient are the core mechanics that drive evaporation. Solar radiation is the major driving force of air temperature on a daily basis and water temperature on a seasonal basis. As the water temperature rises, the erratic movement of water molecules increases, leading to a greater diffusion rate based on Fick's laws of diffusion. Greater diffusion rates lead toward higher evaporation rates, especially during windy conditions, as the wind causes turbulent mixing of non-saturated air with saturated air located directly above the water surface. Lastly, the vapor pressure gradient which is the gradient from saturated air at the water surface to non-saturated air farther above the lake or reservoir, also drives evaporation (Bowen, 1926). The drier the overlying air, the steeper the gradient, increasing evaporation rates (Troen and Mahrt, 1986). The increased vapor pressure overlying a lake or reservoir caused by the evaporating water forms a "bubble" of cool and moist air that impedes evaporation, with this "bubble" being referred to as the atmospheric boundary layer (Friedrich et al., 2018; Kaimal and Finnigan, 1994; Kormann and Meixner, 2001; Stewart, 1979; Troen and Mahrt, 1986).

The air within an atmospheric boundary layer (ABL) over lakes and reservoirs has a greater vapor pressure than the surrounding land in arid/semiarid environments due to limited precipitation and sources of water (Agam and Berliner, 2006). Evaporation rates and the forces that drive evaporation vary from within the ABL and outside the ABL, with evaporation estimation techniques conducted within the ABL being similar to that of the lake or reservoir (Winter et al., 2003). The vast majority of all evaporation estimation techniques that use atmospheric data to estimate evaporation collect data outside the ABL due to difficulties associated with collecting these data from a floating weather station. Evaporation estimation techniques conducted outside the ABL often require a corrective coefficient that reduces the estimated evaporation rate, such as the pan coefficient for the Class A Pan technique.

2.2.1 Land-Based Evaporation Pan Techniques

The most common and standard form of land-based evaporation pans is the Class A Evaporation Pan, invented in the early 1890's and established as the standard in 1934 (Follansbee, 1934). The Class A Pan consists of a 22-gauge galvanized iron pan, typically 1.22 m in diameter and 0.254 m deep, on a wood base 0.152 m above the ground. The Class A Pan's water level is typically measured once each day in the morning and the pan is typically filled once a week or if the water level drops below a certain level. By filling the pan once a week, the thermal mass associated with the water in the pan decreases throughout the week, allowing the water to be more susceptible to diurnal temperature changes later in the week, which affects evaporation rates (Hounam, 1973; Jovanovic et al., 2008; Morton, 1979). The heat capacity of Class A Pans varies substantially from the lakes and reservoirs for which they are estimating evaporation. The available energy within a land-based pan for evaporation is susceptible to diurnal variations in air temperature whereas in larger bodies of water, the available energy for evaporation varies on a seasonal basis, with the body of water absorbing energy in the spring and then releasing the stored energy in the fall (Penman, 1948). This difference in heat capacity further decreases the ability of land-based pans to estimate lake or reservoir evaporation accurately on a daily and monthly basis, with monthly estimated evaporation varying as much as 75% in arid-environments (Eichinger et al., 2003), whereas yearly evaporation values have been shown to be within 20% of actual (Harwell, 2012). In order to overcome the overestimation of evaporation from land-based pans, due to the pan being placed outside the ABL of the lake or reservoir, a pan coefficient needs to be applied. Typically, a yearly pan coefficient around 0.70 is used (Follansbee, 1934; Kohler, 1954), reducing the evaporation rate measured by the Class A Pan by 30%.

The Class A Pan's simplicity of use and low cost ($20-30k per year) has led to its widespread adoption. However, there are key limitations associated with its use, the first being its placement outside the influence of the lake or reservoir's ABL, which is more problematic in arid/semiarid environments due to the large difference in vapor pressure between the ABL and surrounding land, resulting in a greater evaporation rate from the Class A Pan. This limitation can be partially overcome by placing the Class A Pan adjacent to the lake or reservoir in non-arid/semiarid environments. The second major limitation is the small thermal mass of the water within the evaporation pan, which results in evaporation rates being a product of diurnal air temperature changes whereas the lake or reservoir's water temperature varies on a seasonal basis. Due to this limitation, Class A Pans typically overestimate evaporation in the spring when the reservoir is storing solar radiation, and underestimate evaporation in the fall when the reservoir is releasing the stored energy through evaporation (Gianniou and Antonopoulos, 2007). This limitation can be partially overcome by using varying monthly pan coefficients, but this requires another evaporation estimation technique to determine what these coefficients need to be. Table 2.1 below lists some comparison studies completed with the Class A Pan and the associated error between the Class A Pan and more accurate techniques.

Table 2.1: Uncertainty of different evaporation techniques

Quotes from various scientific papers	Techniques[1]	Source
"Environmental factors can cause as much as **77 percent** over measurement in an arid environment as compared to a well-irrigated environment in the same climatic zone, such as the San Joaquin Valley west side."	Class A pan in different environments	Johnson et al., 1979
"In most instances, except for four instances, the floating pan to land pan [Class A pan] differences were positive, with the land pan measurements exceeding floating pan measurements **91 percent** of the time."	Class A Pan to Floating Pan	Masoner and Stannard, 2010
"Evaporation from a rinsed floating pan differed from a Class A pan by **14 to 29 percent** on a monthly basis, and **22 percent** for a six-month period. Pan to lake coefficients have been shown to vary from about **0.4 to 2.0 for monthly** data, and from **0.5 to 0.9 for annual** data."	Class A Pan to Floating Pan	Winter, 1981
Recommended Pan Coefficients for Class A Pans placed in dry fallow areas with < 40% Relative Humidity: **0.35 to 0.7** (Table 5)	Class A Pan Coefficients	Allen et al., 1998
"The long-term pan measurements greatly overestimate the amount of evaporation, especially during the summer. On a daily basis, the average error is on the order of **50% to 75%**."	Class A Pan to Eddy Covariance	Eichinger et al., 2003
"The modified Hamon method estimates of annual reservoir evaporation were always **within 20 percent** of annual reservoir evaporation from pan data."	Class A Pan to Mass Transfer	Harwell, 2012
"The adjusted FAO-56 Penman-Monteith equation predicted pan evaporation with an average error of **6.2 percent** and the adjusted ASCE equation predicted pan evaporation with an average error of **10.1 percent**."	Class A Pan to Energy Budget	Harwell, 2012
"The USWB [U.S. Weather Bureau] method estimates of annual lake evaporation also have been shown to frequently be **within 20 percent** of energy-budget and water-budget estimates."	Energy Budget to Energy Budget and Water Budget	Harwell, 2012
"Percentage errors between the USWB method and water-budget estimates at the three locations ranged from **4.4 percent** at Lake Hefner to **14.4 percent** at Lake Okeechobee."	Energy Budget to Water Budget	Harwell, 2012 Kohler et al., 1955
"Kohler concluded that annual lake evaporation could be estimated within **10-15 percent** by applying the annual coefficient 0.70 to Class A pan evaporation."	Class A Pan to Water Budget	Jensen, 2010 Kohler, 1954

[1] Comparison of technique X to technique Y

2.2.2 Water Budget Technique

The water budget technique is conceptually straightforward and estimates evaporation by accounting for lake or reservoir storage volume variations caused by changes in inflow volumes (surface water, ground water, and precipitation) and outflow volumes (surface water, ground water, and evaporation). The surface water inflows and outflows are measured by stream gaging stations that convert the height of the stream to discharge volumes based on channel characteristics and historical measurements and observations, which has an error rate between 5-10% (Turnipseed and Sauer, 2010). Precipitation events that create inflows from non-gaged side channels are a major unknown for this technique, such that water budgets are typically calculated during periods of no precipitation. The largest unknowns in the water budget technique are the amount of ground water flux (inflows and outflows) and evaporation. The ground water flux portion of the water budget is sometimes assumed as negligible, leaving evaporation as the only unknown of the budget, but with high uncertainties (Duan, 2014; Kumambala and Ervine, 2010; Piper et al., 1986; Rientjes et al., 2011; Russell and Johnson, 2006; Sena, 2000; Setegn et al., 2011; Sivapragasam et al., 2009; Velpuri et al. 2012). The uncertainties associated with how to measure or ignore ground water fluxes reduces the accuracy of water budget techniques' estimation of evaporation rates (Harwell, 2012; Kohler, 1954: Lenters et al., 2005). The most significant water budget study occurred on Lake Hefner, OK, USA, in the early 1950's where the unknowns associated with ground water fluxes were accounted for by a ground water well network of 68 test holes and wells (Kohler, 1954). Detailed water budget studies like the 1950's Lake Hefner study are rare and costly and are typically not completed in a stand-alone study, but in conjunction with other evaporation estimation techniques.

The major limitation of using the water budget technique to determine evaporation rates is accounting for unknown ground water fluxes, especially in situations where there are no nearby ground water wells. Another limitation of the water budget technique is accounting for inflow from ephemeral streams that are not gaged, adding further uncertainties of the changing volume of water within the system. Although conceptually simple, acquiring the necessary data to do an accurate water budget can be very costly, as stream gaging stations can cost between $40-75k per year, in addition to the costs associated with monitoring ground water wells adjacent to the body of water, and/or the cost of installing ground water monitoring wells if none are accessible. However, using the water budget technique for determining evaporation rates can be simplified if ground water fluxes are known from prior studies and there is only one inflow and outflow from the body of water. In ideal instances, the water budget technique has been shown to be within 20% of more accurate techniques (Harwell, 2012; Kohler, 1954; Kohler et al., 1955).

2.2.3 Evaporation Estimation Equations

This category of evaporation estimation techniques requires either one or a few of the following atmospheric parameters: air temperature, water-surface temperature, wind speed, wind direction, vapor pressure (ambient air and at water surface), and solar radiation. The simplest of these techniques requires only onsite air temperature measurements in conjunction with a solar radiation input that is based on the declination of the sun in order to estimate evaporation, such as the Hargreaves-Samani equation (Hargreaves and Samani, 1985) and the Hamon equation (Hamon, 1961). Both of these equations were originally developed to estimate evapotranspiration in rural areas lacking robust datasets of atmospheric parameters and have been shown to be within 20% of energy-budget techniques and a close approximation to weighing lysimeters (Brower, 2018; Hargreaves and Samani, 1985; Harwell, 2012).

Slightly more complicated evaporation estimation equations include measurements of wind speed, vapor pressure, air temperature, and a form of solar radiation. One example of this type of equation is the U.S. Weather Bureau equation (USWB; Kohler et al., 1955, Harwell, 2012). The USWB equation is a modification of the Penman equation (Penman, 1948), where evaporation from a theoretical Class A Pan is used in the Penman equation and is then reduced by a pan coefficient value of 0.7. The increased atmospheric variables required in these two equations require dedicated weather stations costing between $30-50k for initial installation and another $20-50k per year for maintenance, data collection, and postprocessing.

The major limitations of these equations is that they do not incorporate seasonally stored/released energy from the body of water, which results in overestimated evaporation in the spring and underestimated evaporation in the fall. Further, the weather stations needed to collect the variables required for these equations are typically placed outside the ABL of the body of water, further reducing accuracy. With the proper calibration (empirically derived fitting coefficients) by more accurate techniques, these equations have been shown to be within 20% of the more accurate technique on an annual basis (Harwell, 2012; Winter, 1981).

2.3 State of Science for Open-Water Evaporation Estimation Techniques

State-of-science evaporation estimation techniques typically consist of (1) energy budget, where all energy fluxes surrounding as well as to and from a lake or reservoir are accounted for; (2) eddy covariance, where the vertical transfer of water vapor from a lake or reservoir is measured; (3) remote sensing, where water surface temperature data is collected by satellites and/or UAVs; and (4) floating evaporation pans, where an evaporation pan is floated on a lake or reservoir. These techniques are described in depth below.

2.3.1 Energy Budget Technique

The most common energy budget technique for estimating lake and reservoir evaporation is the Bowen ratio energy budget (Bowen, 1926). This evaporation estimation technique requires accurate accounting of all energy gains and losses within a system in order to determine the amount of latent-heat energy used to evaporate water. The energy budget technique requires the following information: incoming and reflected short wave radiation; incoming and reflected long wave radiation; latent heat of vaporization; sensible heat flux conducted to and from the atmosphere from the body of water; energy advected to and from the body of water; and changes in stored energy within the body of water (Lee and Swancar, 1997; Lenters et al., 2005; Moreo and Swancar, 2013; Rosenberry et al., 2007). In order to calculate all the aforementioned parameters, the following information needs to be gathered: water temperature and flow rate entering and leaving the body of water; water temperature profiles throughout the body of water; surface water temperature throughout the body of water; net radiation (four components); solar radiation; air temperature; humidity; barometric pressure; and wind speed and direction. The Bowen ratio part of the energy budget calculates the ratio of sensible heat to latent heat, which is based on the difference between water temperature and water surface temperature divided by the difference between saturated vapor pressure at the water surface and vapor pressure in the air. Simply put, all the energy sources into and leaving a system are measured, with the energy used for evaporation (latent heat) being calculated as the closure term to balance the energy inputs and outputs.

The major limitations of this technique are the amount of data that needs to be collected from many different sources simultaneously and the costs associated with all the instrumentation, installation, maintenance, and significant postprocessing of all the collected data (Mauder and Foken, 2006; Winter et al., 2003). A recent review of funded Bowen ratio energy budget for lakes and reservoirs by the National Science Foundation indicates this technique costs between $150-300k per year, depending on the number of deployed weather stations on land and floating and site-specific requirements. In addition to the high costs associated with equipment, the difficulty in obtaining accurate net advected energy into lakes and reservoirs with multiple inflows and calculating accurate changes in stored energy in large lakes and reservoirs are major limiting factors for the application of the Bowen ratio energy budget (Elsawwaf et al., 2010).

The major advantage of this technique is the increased accuracy over the techniques discussed in the State of Practice section, with annual accuracies within 5-20% of actual being reported (Lee and Swancar, 1997; Lenters et al., 2005; Moreo and Swancar, 2013; Rosenberry et al., 2007; Winter et al., 2003). This accuracy declines when calculating evaporation on a monthly time interval due to the unknown amount of advected energy from unmonitored side channels and varying water temperature profiles on large bodies of water. Lastly, the deployment location of the instruments used in this technique are within the ABL of the body of water, eliminating the need for a corrective coefficient which enhances the accuracy of this technique.

2.3.2 Eddy Covariance Technique

The eddy covariance technique estimates evaporation by calculating the latent-heat flux from the water surface using the vertical component of wind speed and corresponding water vapor density at 10 Hz through a process called turbulent transport or mass-transfer (Brutsaert, 1982; Harbeck, 1962). Eddies created by wind turbulence and convective heat flow transfer mass (water vapor) and energy (heat) between the surface and the atmosphere. The eddy covariance technique is considered one of the most accurate open-water evaporation techniques and is commonly reported as actual evaporation rates (Baldocchi, 2003; Blanken et al., 2000; Foken, 2008; Moreo and Swancar, 2013; Stannard et al., 2013). This technique requires less instrumentation than the Bowen ratio energy budget technique, with the main instrumentation being a 3D sonic anemometer and krypton hygrometer. Although relatively straightforward, this technique requires a significant amount of postprocessing of data, especially in situations where adequate homogeneous fetch in not met in all directions (Mauder and Foken, 2006; Winter et al., 2003).

Acquiring adequate homogeneous fetch in all directions is the major limiting factor for this technique, with adequate fetch being defined by a homogeneous surface (water surface) in all directions where the air has had sufficient distance to become equilibrated to the surface conditions. The general rule for adequate fetch requirements is 100 times the instrument height for stable atmospheric conditions and substantially greater (1,000 to 2,000 times instrument height) for unstable conditions (Horst and Weil, 1994; Moreo and Swancar, 2013). Instrument height, depending on technique and instrument type, can range between 1 m to over 20 m, requiring at least 100 to 2,000+ m of fetch depending on atmospheric stability. Meeting this requirement is considerably difficult on all but the largest lakes and reservoirs, especially on lakes and reservoirs in arid/semiarid-environments where the shape of these bodies of water tend to be narrow and long. The dams used to impound these bodies of water are typically built in narrow-deep sections (e.g., canyons), producing narrow, long, and deep bodies of water where the fetch requirement is rarely met from all directions. Not meeting the fetch requirement from all wind directions will produce data that vary with wind direction, further adding to the uncertainty of evaporation estimates and substantially increasing the amount of postprocessing required (Moreo and Swancar, 2013).

The ideal deployment location for an eddy covariance system is at the center of a large, round lake where fetch requirements are met from all wind directions. Deploying an eddy covariance system on a barge is a potential solution to meet adequate fetch, but wave-induced rocking of the barge can add wind direction uncertainties that reduce the accuracy of the measurement and need to be removed in postprocessing. Placing an eddy covariance system on a fixed tower is the recommended strategy, but the water depths of many lakes and reservoirs prevent the placement of such towers. An alternate solution is placing the weather tower at the edge of the body of water, but depending on the prevailing wind direction, some or the majority of the wind data might need to be removed during postprocessing. Another potential placement location is on small islands that meet adequate fetch, which was done in Lake Mead by Moreo and Swancar. A total of four different small rock-outcrop islands were used during the duration of their study on Lake Mead, with the eddy covariance tower being moved as Lake Mead water levels changed seasonally.

The last major limitation of this technique is the high costs associated with the equipment, routine maintenance, and the considerable amount of postprocessing of the data (Mauder and Foken, 2006; Winter et al., 2003). The annual costs of this technique are similar to that of the Bowen ratio energy budget, around $150-300k per year. Weekly or bi-monthly cleaning of the sensitive 3D sonic anemometer and krypton hygrometer is required for accurate readings. Due to the costs associated with the equipment, installation, maintenance, data processing needs, and deployment limitation, this technique is typically limited to short-term, 2-3 years, scientific studies on a few lakes and reservoirs.

2.3.3 Remote Sensing Techniques

Remotely sensed data from satellites, specifically the thermal bands, is being used to estimate spatially varying evaporation rates from lakes and reservoirs. Remote sensing studies use the thermal bands to determine the skin-surface water temperature in conjunction with an on-site weather station, an evaporation estimate can be determined (Cleugh et al., 2006; Ebaid and Ismail, 2010; Hassan, 2013; Herting et al., 2004). Two of the more common types of remote sensing evaporation estimation are regional-scale studies and site-specific studies (e.g., lakes and reservoirs). Regional-scale studies typically use MODIS data, which has a ground sampling distance of 1,000 m^2 and rely on large scale inputs, such as minimum and maximum air temperature averages, over large distances (Allen et al., 2007; Savoca et al., 2013; Senay et al., 2013). Site-specific studies use smaller ground sampling distances, 30 m^2 or smaller, to determine evaporation spatially throughout a body of water. The distinction between regional and site-specific studies is the ground sampling distance, 1,000 m^2 versus sub-30 m^2, respectively, where the larger ground sampling distances of regional studies are only applicable on large lakes and reservoirs (e.g., Lake Mead, Lake Powell, the Great Lakes). One of the most commonly used data for site-specific studies is from the Landsat series of satellites operated by the USGS.

One major limitation of this technique is accounting for pixels that contains both open water and the shore. Because of the lower specific heat capacity of the shore compared to the open water, any pixel containing the shore will have a higher thermal value associated with it. Depending on the size of the ground sampling distance (pixel size), a significant portion of pixels will have to be removed that contain shore thermal interference. Additionally, accurate remote sensing applications require field verifications and calibrations by weather stations within the study area. These weather stations ideally need to be in the center of the reservoir to meet fetch requirements and be within the ABL, but due to the difficulty of maintaining a floating weather station this is typically not done, creating uncertainties in evaporation estimates.

The major advantage of open-water evaporation determined through remote sensing is the low cost of data (free if using LandSat or MODIS data), but the costs of on-site weather stations, especially floating stations, can substantially increase the cost of this technique. The free data sources for remotely sensed data have a large ground sampling distance, reducing the accuracy of the technique. This can be overcome by using data with smaller ground sampling distance, such as commercially owned satellites that charge per square kilometer or by using unmanned aerial vehicles but this data can be costly, $50k-150k+ depending on the system (Koh and Wich, 2012).

2.3.4 Floating Evaporation Pan Techniques

In order to overcome the major drawback of land-based evaporation pans, the positive correlation of evaporation rates to mean air temperature (Jovanovic et al., 2008), evaporation pans have been modified to float, where the water surrounding the evaporation pan will reduce the diurnal temperature variations. Another major advantage with a floating evaporation pan is its placement within the atmospheric boundary layer of the body of water, ideally resulting in no correction coefficient. Additionally, the water surrounding the floating evaporation pan will allow for the seasonally changing water temperature of the body of water to influence the water temperature within the evaporation pan, thus allowing the floating evaporation pan to capture the effects of stored energy on evaporation rates.

Recently, Klink (2006) and Masoner and Stannard (2010) used a floating evaporation pan to estimate evaporation of a lake and lagoon, respectively. Klink (2006) built a wooden platform that was supported by four plastic floats with a stainless-steel evaporation pan situated in the middle. This study encountered problems with the structure flexing and bending due to wave action, causing the evaporation pan to become tilted, preventing accurate water-level depth measurements. Additionally, measurements of the water levels in the evaporation pan were subject to errors from diurnal temperature variations affecting the pressure transducer because submerged and vented pressure transducers can vary as much as 7 mm daily due to diurnal water temperature change (Liu and Higgins, 2015).

In Masoner and Stannard (2010), floats were added to a standard Class A Pan that was then floated on a small lagoon. Masoner and Stannard (2010) also incorporated a hemispherical evaporation chamber (Stannard, 1988), for validation of the evaporation rates from their floating evaporation pan. This study demonstrated that through the use of a hemispherical evaporation chamber near-actual evaporation rates can be measured in-situ and compared well (97% of actual) to an on-site floating evaporation pan. The major drawback of this study was the design of the floating evaporation pan, as the evaporation pan had no protection from human and/or wind produced waves, reducing the reliability of measurements during windy conditions. Lastly, both of these floating evaporation pan studies had a duration of around two months, which is not long enough to establish reliability of the device. Further, with no wave protections built into their respective designs both of these floating evaporation pans could not be placed on a larger lake or reservoir.

The major limitations of floating evaporation pans are the reliability of the evaporation measurement. In the 1930's study that established the Class A Pan as the standard evaporation technique, a small floating evaporation pan was tested but was deemed unreliable due to the inability to account for wave action interfering with the water level within the evaporation pan, splashing of water into or out of the evaporation pan (Follansbee, 1934). The interference from wave action can be overcome by surrounding the evaporation pan with adequate wave guards. A wave guard can be used to prevent most waves on lakes and reservoirs, but larger waves on lakes like the Great Lakes cannot be prevented and will swamp the evaporation pan. Another limitation is that the addition of a wave guard can increase the costs of a floating evaporation pan, with estimates of $40-70k per year, depending on location and site-specific requirements.

An advantage of a floating evaporation pan is the relatively simple and straightforward way evaporation is measured. Like the Class A Pan, a decrease in water level is the evaporation rate, requiring minimal, if any, postprocessing of the data. Additionally, redundancy in evaporation measurements can be incorporated by including a weather station attached to the floating evaporation pan thus recording atmospheric variables concurrently. Another major advantage of a floating evaporation pan is the lack of fetch requirement, as the water level within the evaporation pan is at the same level of the surrounding water. No fetch requirement allows for a floating evaporation pan to be deployed in situations unfavorable for other state-of-science techniques that require substantial fetch distances.

2.4 Potential Solution

The gap between the state of science and state of practice for evaporation estimation techniques continues to grow as more accurate, yet complicated and expensive, techniques are conceived, but water resource managers continue using less accurate techniques due to their inexpensive cost and simplicity of use. As the climate shifts towards hotter and drier conditions in the Southwestern USA (Friedrich et al., 2018; Udall and Overpeck, 2017), conditions in which Class A Pans tend to greatly overestimate evaporation (Eichinger et al., 2003; Jovanovic et al., 2008), a replacement technique that is more accurate than the current state-of-practice technique, easier to use than the state-of-science techniques, and similar in cost to the current state-of-practice techniques is needed. In order to meet these requirements, modifications of existing techniques and/or a new technique are necessary.

One solution is simplifying state-of-science techniques, making them less expensive and easier to apply. Companies like Campbell Scientific Inc. and LI-COR are supplying complete eddy covariance kits and the supporting software that simplifies this complex technique. These complete packages include step-by-step instructions that cover installation and setup as well as software for postprocessing of the data. These kits cost between $50-100k, depending on deployment application and site requirements. Although these kits do simplify the eddy covariance technique, the costs associated with routine site maintenance, especially with floating systems, and postprocessing of the data can substantially increase the annual costs of this technique. These kits make deploying these systems easier, but the required adequate fetch conditions for eddy covariance technique greatly limits potential deployment locations.

Another potential solution is taking a simple, but inaccurate technique like the Class A Pan and adding further corrections to improve its accuracy. The Texas Water Development Board and the National Oceanic and Atmospheric Administration-National Weather Service (NOAA-NWS) manages and operates over 100 Class A Pans in and around Texas, USA. Instead of using one state-wide annual pan coefficient to correct the Class A Pan's evaporation rate, different pan coefficients are used at each site on a monthly basis. These pan coefficients were derived from the "Evaporation Atlas for the Contiguous 48 United States" completed by NOAA in 1982, which was based on Class A Pan and limited weather station data collected between 1956-1970 (Famsworth et al., 1982). The Texas Water Development Board's use of spatial and temporal varying pan coefficients increases the accuracy of lake and reservoir estimated evaporation from Class A Pans, but their estimated evaporation values are still based on uncertainties and limitations associated with the Class A Pan at its core (Harwell, 2012).

The evolving technology of unmanned aerial vehicles, drones, adds an alternative to expensive remotely sensed data from satellites. The costs of a drone and supporting imaging equipment and software can vary from simple, inexpensive fixed-wing drones, which cost around $5k, to more advanced multi-rotor drones, which cost $30-65k (Chapman, 2016; Koh and Wich, 2012). Drones are capable of gathering images with sub-centimeter ground sampling distance depending of the camera system installed on a drone. Small ground sampling distances overcomes one of the major disadvantages of remotely sensed satellite data, shore thermal interference. After the initial cost of the drone and supporting equipment, the only costs associated with this technique is labor, which, depending on the number of site visits, can range greatly. Like remotely sensed satellite data, a weather station with at least air temperature, relative humidity, and wind speed is required on site for accurate evaporation estimates, ideally placed within the ABL of the body of water. The added costs of a weather station and labor costs associated with drone operation and postprocessing of the images can substantially increase the costs of using drones (Koh and Wich, 2012). If a lake or reservoir already has a weather station in use, then the addition of periodic drone surveys of water surface temperatures can enhance the evaporation estimation by including spatially varying evaporation rates for minor additional costs.

A recent U.S. patented design for an improved floating evaporation pan technique was issued in September, 2018: the Collison Floating Evaporation Pan (CFEP), U.S. Patent 10,082,415 (Collison, 2018). The CFEP is designed to overcome problems associated with prior floating evaporation pans, specifically their reliability. Reliability is increased with the inclusion of an outer wave guard surrounding the evaporation pan, protecting the evaporation pan from wave overtopping. Additionally, the CFEP includes an adjustable height baffle within the evaporation pan to prevent water from sloshing out of the pan. Unaccountable water entering and leaving a floating evaporation pan were the main reliability problems cited in Follansbee (1934), leading to the Class A Pan being recommended as the standard technique. The CFEP's wave guard and adjustable height baffle remedy these aforementioned reliability difficulties.

The accuracy of the CFEP is verified with monthly or quarterly hemispherical evaporation chamber validation tests (Stannard, 1988) similar to those used in Masoner and Stannard (2010). As the CFEP is also located within the ABL of the body of water, no corrective coefficient is required, providing an accurate, real-time estimation of evaporation with minimal data postprocessing. Additionally, the CFEP is also fully equipped with a complete micrometeorological weather station, adding a redundant evaporation estimation calculation if the evaporation pan is overtopped by water. This atmospheric data collected by the on-board weather station can be used in conjunction with remotely sensed data, either from satellites or drones, allowing for spatially varying evaporation rates to be determined. The fully automated and telemetry-equipped CFEP technique reduces maintenance and field visit costs and allows for real-time acquisition of evaporation estimates. The annual costs associated with this technique range between $45-70k, depending of the number of validation tests and site-specific requirements.

2.5 Summary

As drinking water demands increase every year (Federal Energy Management Program, 2017) and supplies decrease (Friedrich et al., 2018; Udall and Overpeck, 2017), accurate accounting of lake and reservoir evaporation, one the largest losses (Wurbs and Ayala, 2014), is needed. Better accounting of evaporative losses from lakes and reservoirs will provide justification for improved water management techniques, such as adaptive water management (Huntjens et al., 2011; Pahl-Wostl, 2007) and conservation at the source (Friedrich et al., 2018; Pelz, 2017). Both of these management techniques rely on accurate data, which is currently lacking on all but a few lakes and reservoirs, due mainly to the costs associated with the accurate state-of-science evaporation estimation techniques. Water resource managers, at no fault of their own, currently use inaccurate and inexpensive evaporation estimation techniques such as the Class A Pan because an alternative to the expensive state-of-science techniques is unavailable. A new open-water evaporation estimation technique, the CFEP, was designed to fill the gap between inexpensive and easily applied, but inaccurate, and expensive and complicated, but accurate evaporation estimation techniques. The CFEP technique overcomes the accuracy limitations of the state-of-practice techniques by being within the atmospheric boundary layer of a body of water and the high costs of state-of-science techniques by being fully automated and easily applied. Accurate accounting of evaporative losses on the majority of lakes and reservoirs will lead to better water management policies, making water systems more efficient, reducing evaporative losses, and providing more water for beneficial use.

Chapter 3: The Collison Floating Evaporation Pan: Design, Validation, and Comparison

3.1 Introduction

Estimating evaporation rates is fraught with complications due to the difficulty in obtaining various atmospheric variables that affect open-water evaporation rates (Alkaeed et al., 2006; Harwell, 2012; Rosenberry et al., 2007). Water resource managers need accurate and precise estimates of evaporation rates in order to apply adaptive water management techniques and efficiently manage water resources (Huntjens et al., 2011; Pahl-Wostl, 2007), but due to budget constraints, accuracy and precision are sacrificed for ease of use and reliability, limiting the accessible evaporation estimation techniques.

The most common and widely used technique for estimating evaporation from lakes and reservoirs is the Class A Pan, a technology invented in the early 1880s that has changed very little since its first iteration. This technique is commonly used throughout the United States, Europe, and Australia (Doorenbos and Pruitt, 1977; Famsworth et al., 1982; Rayner, 2005). The Class A Pan technique is inexpensive and easily applied, and has provided reliable evaporation measurements for over a hundred years in some areas, but it is also one of the least accurate ways of estimating open-water evaporation (Alvarez et al., 2006; Chu et al., 2012; Follansbee, 1934; Grayson et al., 1996; Tanny et al., 2008; Trask, 2007). The magnitude and timing of evaporation estimated by Class A Pans is questionable (Alvarez et al., 2006; Chu et al., 2012; Hounam, 1973; Morton, 1979) due in part to both its position outside the reservoir's atmospheric boundary condition (Stewart, 1979) and a positive correlation between mean air temperature and evaporative rates (Jovanovic et al., 2008).

More accurate, state-of-the-art techniques for estimating lake and reservoir evaporation are available, with the Bowen ratio energy budget and eddy covariance techniques considered two of the most accurate (Blanken et al., 2000; Bowen, 1926; Brutsaert, 1982; Foken, 2008; Lenters et al., 2005; Moreo and Swancar, 2013; Rosenberry et al., 2007; Stannard et al., 2013), but the major limitations of these two techniques are their high cost and complexity of use, constraining their use to well-funded and short-duration scientific studies. An alternative to inexpensive and easily applied, but inaccurate or expensive and complicated, but accurate evaporation estimation techniques is explored in this study.

More accurate estimates of lake and reservoir evaporation rates can affect compact deliveries and accrued credits or debits. For example, the Rio Grande Compact (Rio Grande Compact, 1938) states that any excess water delivered to Texas from New Mexico will be counted as a credit and that the evaporation rate from Elephant Butte Reservoir, New Mexico, USA directly reduces any such credit. An overestimation of evaporation from Elephant Butte Reservoir will decrease delivery credits at a greater rate than they were accrued, benefiting Texas, but the converse would benefit New Mexico. The annual evaporation on Elephant Butte Reservoir ranges from 61.7 MCM (50,000 acre-feet) to 308 MCM (250,000 acre-feet), dependent mostly on the quantity of stored water (Papadopulos and Associates, 2000). The technique for estimating evaporation from Elephant Butte Reservoir, the Class A Pan, has been shown to be within 20 to 75% (Eichinger et al., 2003) of actual evaporation in arid environments, resulting in an uncertainty of annually estimated evaporation on Elephant Butte Reservoir between ±1.2 MCM (10,000 acre-feet) and ±231 MCM (187,500 acre-feet).

Enhancing the knowledge of evaporation rates of different lakes and reservoirs (spatially and temporally) within the same basin can lead to improved water management by changing the paradigm of storing water where it is convenient to where it is most efficient based on reductions in evaporation losses. Currently, the vast majority of water within the Rio Grande Basin in New Mexico, USA is stored in Elephant Butte Reservoir per Rio Grande Compact requirements while under Article VII (Rio Grande Compact, 1938). Elephant Butte Reservoir is the largest southernmost reservoir on the Rio Grande in New Mexico and has an annual evaporation rate, as measured by a Class A Pan, of 2.86 m. In comparison, the northernmost reservoir within the same system is Heron Reservoir, which has an annual evaporation rate of 1.32 m, less than half of the evaporation rate of Elephant Butte Reservoir (DRI, 2019). A recent article by WildEarth Guardians, "The Rio Grande, rethinking rivers in the 21st century" (Pelz, 2017), proposed storing water in the northern reservoirs in the Rio Grande basin instead of the southern reservoirs. The potential water savings due to reduction in evaporative losses range from 49.3 MCM (40,000 acre-feet) in dry years to 105 MCM (85,000 acre-feet) in average precipitation years. To put these potential savings into context, 1,233 m^3 (1 acre-foot) of water is enough to supply a family of four for a year (Pelz, 2017). The proposed plan by WildEarth Guardians is based around the concept of conservation at the source.

The premise behind the concept of conservation at the source is knowing accurate evaporation rates associated with different lakes and reservoirs within the same system, which can lead to modifications of where and when water is stored based on the reduction of evaporation losses. Conservation at the source is based on the following two methods: 1) classifying lakes and reservoirs based on their evaporation rates and storing water where there will be less evaporative losses, and 2) using suppressive evaporation techniques by way of geoengineering, such as shade balls, monolayer films, etc. (Friedrich et al., 2018). Conservation at the source is focused on making a water resource system more efficient, which will reduce losses associated with storing water in a lake or reservoir and provide more water. Additionally, enhanced lake and reservoir evaporation knowledge has the potential of preventing compact delivery misallocations, resulting in costly litigation. Both of the aforementioned benefits of enhanced evaporation knowledge require accurate evaporation rates in order to be properly implemented. Thus, a new open-water evaporation technique that is cost effective, easily applied, and as or more accurate than current state-of-the-art techniques is needed.

3.1.1 Study Objectives

The goal of this research was to advance knowledge of spatial and temporal evaporation processes in lakes and reservoirs through an improved measurement technique, the Collison Floating Evaporation Pan (CFEP), U.S. Patent 10,082,415 (Collison, 2018, Figure 3.1), for in-situ measurements of evaporation from lakes and reservoirs. This goal was met by addressing the following three objectives:

1. Design, deploy, and test the reliability of the CFEP for in-situ measurements of evaporation from lakes and reservoirs;
2. Investigate the validity (accuracy and precision) of the CFEP using accepted best practices; and
3. Evaluate the limitations in standard evaporation measurement techniques.

The first objective of this study was to finalize the design of a floating evaporation pan that would provide reliable open-water evaporation estimates. Prior floating evaporation pans had reliability issues; specifically, there were no safeguards in place to prevent wave overtopping or the loss of water within the evaporation pan during large wave events, leading to a loss of data (Follansbee, 1934; Klink, 2006; Masoner and Stannard, 2010). The novelty of the CFEP is the outer wave guard that prevents wave overtopping of the evaporation pan, increasing the reliability of evaporation measurements, as seen in Figure 3.1.

Figure 3.1: Collison Floating Evaporation Pan (CFEP) on Cochiti Lake, New Mexico, USA.

The second objective of this study was to investigate the validity (i.e., accuracy and precision) of CFEP using an accepted best-practices in-situ evaporation estimation technique. This study used a hemispherical evaporation chamber (Stannard, 1988; henceforth referred to as "dome") to validate the CFEP by measuring evaporation rates adjacent to the CFEP, see

Figure 3.2. The dome evaporation measurements were used to tests the accuracy of the CFEP (the closeness to near-actual evaporation) and the precision of the CFEP (statistical variability in CFEP evaporation measurements).

Figure 3.2: Hemispherical Evaporation Chamber (dome) during a validation test on September 30, 2018 on Cochiti Lake, New Mexico, USA.

The third objective of this study was to evaluate the limitations in standard evaporation estimation techniques in comparison to the CFEP. The evaporative estimation techniques investigated in this study include the Hargreaves-Samani equation (Hargreaves and Samani, 1985), the Hamon equation (Hamon, 1961), the U.S. Weather Bureau equation (Kohler et al., 1955), the Penman equation (Penman, 1948) and an onsite Class A Pan (managed by the U.S. Army Corps of Engineers Cochiti Lake Ranger Station). This study focused on the aforementioned equations because they are more commonly used in conjunction with Class A Pans' evaporation estimation or when Class A Pans are not present (Harwell, 2012). These equations are discussed in detail in section 3.2.4 below.

The original premise for floating an evaporation pan in water was to overcome the inadequacies of land-based pans, particularly their positive correlation of evaporation rate to daily mean air temperatures (Hounam, 1973; Jovanovic et al., 2008; Morton, 1979). The available energy for evaporation within a land-based Class A Pan is susceptible to diurnal variations in air temperature, whereas in larger bodies of water, the available energy for evaporation varies on a seasonal basis, with the body of water absorbing energy in the spring and then releasing the stored energy in the fall through evaporation. This storage and subsequent release of the stored energy from lakes and reservoirs are not captured by land-based evaporation pans or land-based atmospheric instrumentation.

3.1.2 Open-Water Evaporation Processes

The physical process of evaporation is well known, well established, and based on Fick's laws of diffusion (Bird et al., 2007; Fick, 1855): as water temperature increases, the water molecules become more excited (larger, swifter motion), which allows for a higher diffusion rate into the air overlying the water. During windy conditions, the saturated air adjacent to the water surface is replaced by non-saturated air through turbulent mixing (Brutsaert, 1982), increasing the diffusion rate. The drier the air that mixes with the saturated air, the greater the diffusion rate, which leads to an increase in evaporation.

The other major physical process controlling evaporation from lakes and reservoirs is the vapor pressure gradient. The vapor pressure gradient is defined as the gradient between the saturated vapor pressure at the water surface to the actual vapor pressure of the overlying air (Bowen, 1926). The larger the lake or reservoir, the smaller the slope of this gradient; conversely, the smaller the lake or reservoir, the steeper the slope of this gradient, with steeper gradients associated with a higher evaporation rate (Troen and Mahrt, 1986). The vertical height of the vapor pressure gradient overlying a lake or reservoir is referred to as the atmospheric boundary layer (Friedrich et al., 2018; Kaimal and Finnigan, 1994; Kormann and Meixner, 2001; Stewart, 1979; Troen and Mahrt, 1986). The shape of the atmospheric boundary layer overlying a lake or reservoir can be described as a bubble of cooler air with higher vapor pressure compared to the surrounding land's air temperature and vapor pressure, which impedes evaporation rates.

Evaporation estimation techniques that use atmospheric variables or are controlled by atmospheric variables that are not placed within this atmospheric boundary layer will have uncertainties related to their accuracy because they are measuring atmospheric variables associated with the land surrounding the lake or reservoir. Atmospheric variables include the following: air temperature, humidity, wind speed and direction, solar radiation, and barometric pressure. The general rule for evaporation estimation techniques that rely upon atmospheric variables is to have a homogeneous fetch in all directions around the weather station at a distance of at least 100 times the height of the sensor in stable atmospheric conditions and 1000+ times the height of the sensor in unstable conditions (Horst and Weil, 1994; Moreo and Swancar, 2013). Obtaining adequate fetch is difficult in arid and semi-arid environments where lakes and especially reservoirs are long and narrow, limiting suitable deployment locations and adding accuracy uncertainties for techniques that require adequate fetch.

3.1.3 State of Science and State of Practice

Reliable and accurate accounting of the gains and losses of water from a lake or reservoir is crucial for operational water management, especially since evaporation is one of the largest losses, sometimes even exceeding consumptive usage (Friedrich et al., 2018). With the transition toward more adaptive water management (Huntjens et al., 2011; Pahl-Wostl, 2007), driven in part by data, reliability of said data is paramount for proper management of water resources, where consistent data of questionable accuracy is better than sparse data of high accuracy. Additionally, the costs associated with Class A Pans is two to three orders of magnitude less than more accurate and complex state-of-the-art techniques, which rely on many expensive and delicate instrumentation working concurrently in order to estimate evaporation.

Two examples of evaporation estimation techniques that are considered to be the most accurate are the Bowen ratio energy budget (Bowen, 1926) and eddy covariance (Baldocchi, 2003; Blanken et al., 2000; Brutsaert, 1982; Foken, 2008; Harbeck, 1962; Moreo and Swancar, 2013; Stannard et al., 2013). Both of these techniques require extensive field measurements with expensive and delicate instrumentation as well as significant postprocessing of field data in order to estimate evaporation (Mauder and Foken, 2006), which limits implementation to well-funded scientific studies at just a few locations. Additionally, these two accurate evaporation estimation techniques are typically deployed for only two to three years with only a few studies having a duration greater than five years, including Lenters et al. (2005) with ten years and Winter et al. (2003) with six years in duration. Due to the costly and complex nature of state-of-the-art evaporation estimation techniques, an alternative evaporation estimation technique, floating evaporation pans have been investigated.

Two recent floating evaporation pan studies were completed by Klink (2006) and Masoner and Stannard (2010), which estimated the evaporation of a lake and lagoon, respectively. Klink (2006) built a rectangular wooden platform that was supported by four plastic floats with a semi-submerged, stainless-steel evaporative pan placed in the center. He encountered problems with the wooden structure flexing and bending due to wave action, which would cause the evaporation pan to be non-parallel with the water surface, causing inaccurate water level measurements. Further, measurement of the water levels in the evaporation pan was subject to errors from diurnal temperature variations affecting the pressure transducer because submerged and vented pressure transducers can vary as much as 7 mm daily due to diurnal water temperature change (Liu and Higgins, 2015).

Masoner and Stannard (2010) added three floats to a normal Class A Pan and deployed the modified Class A Pan in a small lagoon, 450 m by 20 m, and measured the water level change within the evaporation pan with a float attached to a linear potentiometer. The lagoon was small enough where wave overtopping of the evaporation pan was not a concern, so no wave protection was included with their design. This study provided reliable evaporation estimation from a floating evaporation pan, but their pan cannot be placed in large bodies of water where wind or human-derived waves are present, limiting the deployment of such a device to only small bodies of water. Klink (2006) and Masoner and Stannard (2010) both improved the field of floating evaporation pans, but both had limitations inherent with their designs, as mentioned above. Both studies were also very short in duration, around two months each, which is not a significant enough time period to establish the reliability of the devices.

In total, these state-of-the-art evaporation estimation studies have occurred on approximately 25-35 lakes and reservoirs throughout the USA, which is 0.1% of 31,000 lakes and reservoirs greater than 10,000 m^2 in the USA (National Inventory of Dams, 2019; U.S. Environmental Protection Agency, 2009). All other evaporation estimates are based on state of practice techniques. The most common of these techniques is the Class A Pan, which has been shown to have error rates as high as 75% in arid environments (Eichinger et al., 2003), but are inexpensive and easily applied, leading to wide-spread usage.

The gap between the more accurate techniques to measure lake and reservoir evaporation (state of science) and what is commonly used in operational water management (state of practice) constrains the advancement of hydrologic sciences by limiting state-of-the-art evaporation estimation techniques to only well-funded scientific studies (Lowe et al., 2009). This limits the number of locations where a detailed evaporation analysis has occurred. Water resource managers do not have the necessary funds to implement state-of-the-art evaporation estimation techniques, as they can cost between $150-300k+ per year for one location (based on a review of eddy covariance and Bowen ratio energy budget techniques funded by the National Science Foundation). Accessibility, ease of use, and lower costs for water resource managers are crucial to expanding the knowledge of accurate evaporation to more than just 0.1% of the accessible 31,000 lakes and reservoirs in the USA. A greater understanding of evaporation rates at more locations will lead to better water management, enhanced water management models, and ultimately changes in decision making allowing methodologies like conservation at the source to be utilized (Friedrich et al., 2018).

3.2 Methods

3.2.1 Study Location and Deployment Details

The CFEP was deployed on Cochiti Lake in New Mexico, USA in November 2017 through December 2018 (see Figure 3.3). Cochiti Lake is a flood-control reservoir constructed in 1965 and controlled by the U.S. Army Corps of Engineers; it has a permanent recreation pool of 61.7 MCM (50,000 acre-feet) with the surface area forming an approximate rectangle 2,500 m by 1,200 m in a north-northwest orientation. Cochiti Dam was constructed on Pueblo de Cochiti Indian Reservation, thus limiting public access. Cochiti Lake was chosen for this study due to its proximity to Albuquerque, no-wake lake status, limited public access, nearly constant stage (except during flood conditions), and a safe deployment location near the reservoir's outlet. Additionally, Cochiti Lake consistently experiences high winds, which provided ideal conditions for testing the durability and reliability of the CFEP during high wave action. Further, the U.S. Army Corps of Engineers operates a Class A Pan at their Cochiti Lake Ranger Station, which is their primary technique for estimating Cochiti Lake evaporation. This Class A Pan is located on the crest of a hill 1,200 m from and 70 m above Cochiti Lake and has provided continuous evaporation data since 1975.

The CFEP was installed on Cochiti Lake on November 17, 2017. The period from installation to May 13, 2018 was used to trouble-shoot the CFEP, including the following (now solved) problems: a small leak in the pan due to a failed weld that was difficult to detect, difficulties measuring the water level within the pan due to instrumentation malfunction, and constant swamping of the evaporation pan during high wave events. The CFEP on Cochiti Lake collected evaporation data every 15-minute from May 13 through November 30, 2018, with the end date chosen because of frozen surface water conditions in December. During this time period there were only two gaps in data. A data gap occurred on August 1 at 18:00 through August 2 at 11:15 due to a failed software update. The second gap, where only the evaporation pan water level measurements were not recorded, occurred on August 8 at 19:00 through August 14 at 23:15, due to a disconnected electrical wire.

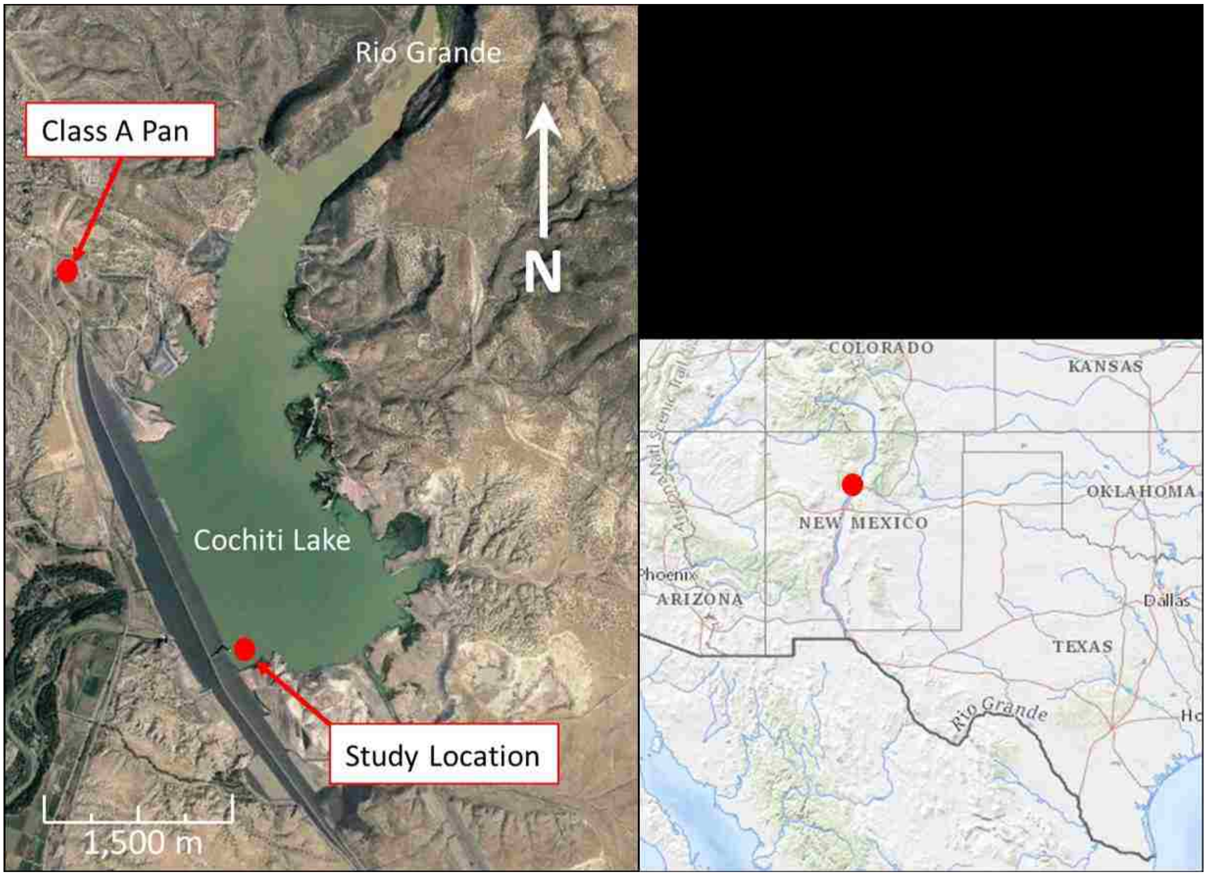

Figure 3.3: Cochiti Lake, on the Rio Grande in central New Mexico, USA, with the CFEP study location and on-site Class A Pan noted by the red dot (Source: Google Earth ©, and USGS National Map).

3.2.2 Collison Floating Evaporation Pan

The design of the CFEP incorporates several novel features that represent a substantial advancement from prior floating evaporative pans, including the following: 1) the CFEP is semi-submerged to minimize the difference in water temperature between the pan and the surrounding lake or reservoir; 2) the CFEP is designed to have minimal influence on the atmospheric boundary layer overlying the pan relative to the reservoir; 3) the CFEP has a wave guard surrounding the evaporation pan, protecting it from wave overtopping; and 4) the CFEP is made entirely out of aluminum alloy 6061, providing a strong, lightweight, and corrosion-resistant pan with good malleability and weldability as well as high thermal conductance.

CFEP Design

The CFEP's evaporation pan is 2.44 m in diameter and 0.61 m deep surrounded by a 4.88-m-diamter outer wave guard consisting of a half A-frame wave breaker (Hales, 1981) that prevents large reservoir waves from overtopping the evaporation pan. The CFEP's evaporation pan and the outer wave guard are connected by six, 1.22-m-long bracing members (see Figure 3.1). The wave guard on the CFEP consists of a 0.61-m tall vertical wall that forms a circle surrounding the evaporation pan with a 0.31-m wide horizontal top extending away from the CFEP (see Figure 3.1 and 3.4). The thermal conductivity of aluminum is four times that of steel (205.0 W/m K vs 50.2 W/m K; Young and Sears, 1992). This increased thermal conductivity rate is key to reducing the water temperature difference from the floating evaporation pan and the surrounding reservoir water, as noted in prior floating evaporation pan studies (Klink 2006; Masoner and Stannard, 2010).

The round shape of the outer wave guard is essential in reducing the forces acting upon the CFEP by wave and wind action. A study by Kamath et al. (2015) showed that force from water waves acting on a rectangular-shaped object (along the long axis) to be 57% higher than on a cylindrical object. Allowing the waves to diffract around an object instead of being reflected orthogonally away from the object results in a lower force on the object, thus reducing the stress on the CFEP and leading to a more stable water level within the evaporation pan. Floating evaporation pans from prior studies (Follansbee, 1934; Klink, 2006) were typically rectangular in shape, and in each of these studies, the floating evaporation pans began to deteriorate or deform after a few weeks of deployment. Additionally, the wave guard protects the interior evaporation pan from unwanted wave over-toppings, improving the reliability of evaporation measurements.

Figure 3.4: Horizontal wave guard on Collison Floating Evaporation Pan.

The outer wave guard has adjustable depth buoyancy floats that provide an extra 12,500 N of buoyancy force, allowing for the CFEP's buoyancy to be adjusted in order to level out the CFEP (offsetting the weight of micrometeorological instrumentation). Being able to adjust the buoyancy of the CFEP allowed for the freeboard height, the height of the CFEP above the water, to be adjusted throughout the study. The optimal freeboard height will be one that minimizes wave overtopping and also minimizes water surface wind disturbance, with 0.2 m being the optimal height determined during this study.

An adjustable height baffle is located within the evaporation pan, that helps prevent the sloshing of water within the evaporation pan during high wave events, therefore reducing the risk of water sloshing out of the evaporation pan. An added benefit of the baffle is that the water within the evaporation pan simulates a mass damper, with a weight of 1,900 kg when 0.41 m deep. The baffle impedes the oscillation of water within the evaporation pan so that the water's frequency oscillation is delayed compared to the oscillation frequency of the entire

CFEP. This difference in frequency acts as a mass damper coupled with the large inertia of the water within the evaporation pan, further reducing the overall rocking of the whole CFEP. Additionally, the CFEP was designed to have the majority of mass (wave guard, buoyancy floats, and weather station) on the outer edges in order to produce a large moment of inertia around the central axis to increase resistance to rocking motions during wave events. The anchoring of the CFEP in Cochiti Lake consisted of three independent mooring anchors every 120 degrees, keeping the CFEP's orientation constant during calm and windy conditions.

CFEP Instrumentation and Equipment

The change in water level height within the CFEP's evaporation pan was measured with a linear potentiometer (see Table 3.1) attached to a float, with the float being attached to a 0.9-m long horizontal arm with a hinge on one end, restricting the float to vertical movement. Because the float's path is an arc and not perpendicular to the water surface, a correction from arc measurements to perpendicular measurements was considered but not used because the amount of error introduced in the water level measurement due to the path of an arc was less than 0.001%.

The CFEP was also equipped with atmospheric sensors (see Table 3.1), with data from these sensors collected every 15 minutes. The data collected by these sensors were used to estimate evaporation using different evaporation estimation techniques and to calculate potential evaporation indicators such as vapor pressure deficit. The difference between the amount of vapor pressure in the air (relative humidity) and the maximum amount of vapor pressure in the air (saturated vapor pressure), which is a function of air temperature, is called vapor pressure deficit, VPD, where VPD is calculated as follows:

$$VPD = \left(1 - \frac{RH}{100}\right) * SVP \tag{3.1}$$

where:

VPD	is the vapor pressure deficit, kPa,
RH	is the relative humidity, %,
SVP	is the saturated vapor pressure, kPa.

Saturated vapor pressure is calculated as follows from Allen et al. (2005):

$$SVP = 0.6108 * \exp\left(\frac{17.27 * T}{T + 237.3}\right) \tag{3.2}$$

where:

T	is air temperature, °C.

The water surface temperature in the CFEP's evaporation pan and the water surface temperature adjacent to the CFEP were measured by two different infrared thermal radiometers (see Table 3.1), but due to consistent infestations of spider nests within the field of view of these radiometers, the data were suspect and unreliable and not used in any analysis. The CFEP was also equipped with a precipitation sensor in order to decouple water-level depths in the evaporation pan from precipitation amounts.

Wind speed was collected as an average over a 15-minute period and wind direction was collected as a sample once every 15 minutes. Hourly and daily averages of wind speed and direction were computed by first turning the 15-minute values of wind speed and wind direction into a vector (magnitude and direction), applying the desired averaging interval, and then turning the vectors back into separate parameters, wind speed and wind direction. Additionally, due to the placement of the CFEP near the southern shore of Cochiti Lake, adequate fetch was not available in all directions. Winds coming from between 84 to 300 degrees (where north is 0 degrees) were classified as southerly winds with inadequate fetch and winds coming from between 0 to 83 degrees and between 301 to 360 degrees were classified as northerly winds with adequate fetch.

The CFEP was equipped with a camera that had the CFEP's evaporation pan in the field of view, allowing for quick assessment of errant water levels within the evaporation pan. The CFEP was also equipped with a 4G cellular modem for remote download and upload of information to and from the installed CR1000 data logger. Finally, the water level within the evaporation pan was maintained by two pumps (see Table 3.1). One pump was set to fill the pan every night at midnight to a set level of 0.41 m so that every day the evaporation pan would start out at the same water level and same thermal mass. A second pump was set to drain the evaporation pan to a set level if it became swamped by a wave.

Minor adjustments to the evaporation pan's water level data consisted of removing site visit disturbances, bird landings on and leaving the pan, and periods of high variance water level data from high winds/waves from the north. In order to correct for the latter, a linear evaporation rate using the water level before the winds increased and the water level after the winds subsided was applied. These linear rates were only applied to periods of similar wind direction. If the wind changed direction during a windy period, then a new linear rate was applied to the new wind direction. Each linear rate was between 0.05 mm per 15 minutes to 0.2 mm per 15 minutes, which is consistent with evaporation rates during windy periods when the water level within the evaporation pan did not experience high variance.

Table 3.1 Instrumentation and equipment installed on the CFEP

Type of measurement	Company Name	Instrument and model number	Placement above water surface (m)
Evaporation pan water level	Unimeasure	HX-PA-24	1.0
Air temperature/humidity	Campbell Scientific	EEE181	2.0
Wind speed and direction	R.M Young	5103	2.0
Precipitation	R.M Young	50202	2.2
Barometric Pressure	Serta Systems	278	1.8
Solar radiation	Apogee Instruments	SP-110	2.4
Surface water temperature	Apogee Instruments	SI-111-SS	1.0 (interior) and 0.8 (exterior)
Net Radiation	Kipp and Zonen	NR-Lite2	1.0
Data logger	Campbell Scientific	CR1000	1.8
Digital Camera	Campbell Scientific	CC5MPX	2
Cell Modem	Sierra Wireless	AirLink RV50	1.8
Pump	Yescom	1100GPH	-0.5 (interior & exterior)

3.2.3 Hemispherical Evaporation Chamber (Dome) and Calibration

The hemispherical evaporation chamber is the most accurate technique for measuring in-situ open-water evaporation (Crilley and Collison, 2015; Garcia et al., 2008; Masoner and Stannard, 2010; Stannard, 1988). The specific hemispherical evaporation chamber (henceforth referred to as “dome”) used in this study was invented by Dave Stannard (Stannard, 1988), see Figure 3.2. It was originally invented to measure evapotranspiration (ET) over agricultural crops as a substitute to larger, more expensive, and more difficult to use rapid ET chambers (Greenwood and Beresford, 1979; Kock et al., 1971; Puckridge, 1978; Saugier, 1976). The rapid ET chamber measurements were compared to an adjacent weighing lysimeter, with a ±5 percent agreement between the two different techniques (Reicosky and Peters, 1977; Reicosky, 1981; Reicosky et al., 1983). One drawback of the dome technique is that the dome cannot be left out for continuous measurements and has to be used for periodic measurements ranging from a few hours to a full day (Crilley and Collison, 2015; Garcia et al., 2008; Masoner and

Stannard, 2010; Stannard, 1988). The dome has to be aired out (de-gassed) between measurements and routinely cleaned to ensure clear transmission of solar radiation through the acrylic dome for accurate and precise evaporation measurements.

The 1-m diameter acrylic dome that Dave Stannard created had the accuracy of larger rapid ET chambers but the added benefit of being usable by one person (Stannard, 1988). These rapid ET chambers work by measuring the vapor density increase within the enclosed space, with the vapor density increase being proportional to ET or evaporation rates, depending on the environment being enclosed by the chamber. The dome was originally developed for ET measurements (Crilley and Collison, 2015; Garcia et al., 2008; Stannard, 1988), but a recent study by Masoner and Stannard (2010) used the dome to measure open-water evaporation with great success. The dome is calibrated by measuring the vapor density of water evaporating from a container on a balance (the same principle of a weighing lysimeter); therefore, using the dome over open water instead of over vegetation does not affect the accuracy of the dome's measurements.

Dome Design and Calibration

The dome used in this study was made out of 6.35 mm thick acrylic with an interior diameter of 0.905 m with a 38 mm lip, with the final thickness of 3 mm after being molded. The acrylic dome was manufactured by California Quality Plastics, Ontario, CA. A 75 mm thick and 55 mm wide buoyancy foam ring was attached to the bottom of the dome for buoyancy, with the joint between the dome and the buoyancy foam ring sealed with silicone. In order to prevent gaps between the dome's bottom buoyancy foam ring and the water surface during wave action, the amount of buoyancy force from the foam ring was determined such that the foam ring would be submerged by 7 cm while still providing adequate buoyancy for the dome. A 10-mm inside diameter, 0.8-m long, coiled, polyethylene hose was inserted through the side of the dome 22 cm from the bottom. The coiled hose dissipated the sudden increase in pressure inside the dome when placed on the water surface due to 7 cm of the dome being submerged (see Figure 3.1), where increased air pressure decreased evaporation rates (Özgür and Koçak, 2015).

Ambient wind conditions outside the dome were reproduced within the dome with two variable-volt direct-current (0-24 V) fans with 100 mm diameter blades. Following the advice in Stannard (1988), the fans were mounted at a height 1/4 of the diameter of the dome, 22.5 cm. The fans were mounted opposite of each other to maximize air flow and were aimed 5 degrees above the horizon and 27 degrees to the right of the center axis of the dome. Wind speed produced by the fans inside the dome was determined by placing the dome on a flat surface with nine equal grids. In each of the grids, a hand-held anemometer (Wintronic 2, Kaindl Electronic, Rohrbach, Germany) was secured such that the anemometer cups were 0.2 m above the flat surface. Voltages of 6, 12, 18, and 24 were applied to the fans for two minutes and the resulting wind speed for each of the different voltages was measured in every grid cell. The wind speed for each voltage was averaged over all nine grid cells and a linear least-squares regression (R^2 = 0.998) was used to determine the voltage-wind speed relationship:

$$y = 0.212 * x + 0.188 \tag{3.3}$$

where:

y	average wind speed inside chamber, m/s,
x	fan supply voltage, V.

During validation tests the wind speed inside the dome was controlled in real time by a 3-cup anemometer (model 03101, Campbell Scientific, Logan, UT) placed 2 m away from the dome and 1 m above the water surface, and connected to a datalogger (CR1000, Campbell Scientific, Logan UT). The datalogger was programmed with a step function to reproduce Equation 3.3.

The vapor density changes inside the dome were calculated by measuring air temperature and relative humidity every two secs with an air temperature and relative humidity sensor that was inserted through the side of the dome at a height of 0.3 m (model HygroClip S, Rotronic Instrument Corp., Hauppauge, NY). When the dome is placed over vegetation, or in this case open water, the vapor density begins to increase quickly during the first 30-45 s and then it slows down around 60 s as it asymptotically approaches maximum vapor pressure. The evaporation rate is determined by the rate of change in vapor density, with the steepest 11-point moving slope being the instantaneous evaporation rate calculated by the following equation (Stannard, 1988):

$$E = 86.4\left(\frac{M*V*C}{A}\right) \quad (3.4)$$

where:

E	evaporation rate, mm/day,
M	the steepest slope of vapor density, $\mathrm{g}/(\mathrm{m}^3 * \mathrm{s})$,
V	the volume inside the chamber, m^3,
C	the calibration factor for the Dome, unitless,
A	the area of surface covered by the Dome, m^2,
86.4	a conversion factor that converts $\mathrm{g_{water}}/\mathrm{m}^2 sec$ to $\mathrm{mm_{water}}/\mathrm{day}$.

The volume of the dome (V) was 0.226 m^3, the area covered by the dome (A) was 0.643 m^2, and the calibration factor (C) was 1.0419.

The calibration factor (C) is used to account for the water vapor absorbed by the acrylic and poor air mixing by the fans within the dome. The process for dome calibration in this study followed the steps described by Stannard (1988). A pot of water was placed on a balance (model MS 32001L, Mettler Toledo, Columbus, OH) that had a 120-volt AC heating element controlled by a water temperature probe. The dome was placed over the pot once a set temperature was established and remained in place for three minutes. The water temperature in the pot was set to 16, 22, 28, and 35 °C, and wind speeds of 0.76 and 2.18 m/s were tested at each temperature. Higher wind speeds were tested, but the wind turbulences on the surface of the water interfered with the balance readings. At least three calibration runs were completed at each temperature and at each wind speed setting. The results of the calibration tests are shown in Figure 3.5 below, with a linear least-squares regression line through the origin used to determine the dome calibration factor, C = 1.0419.

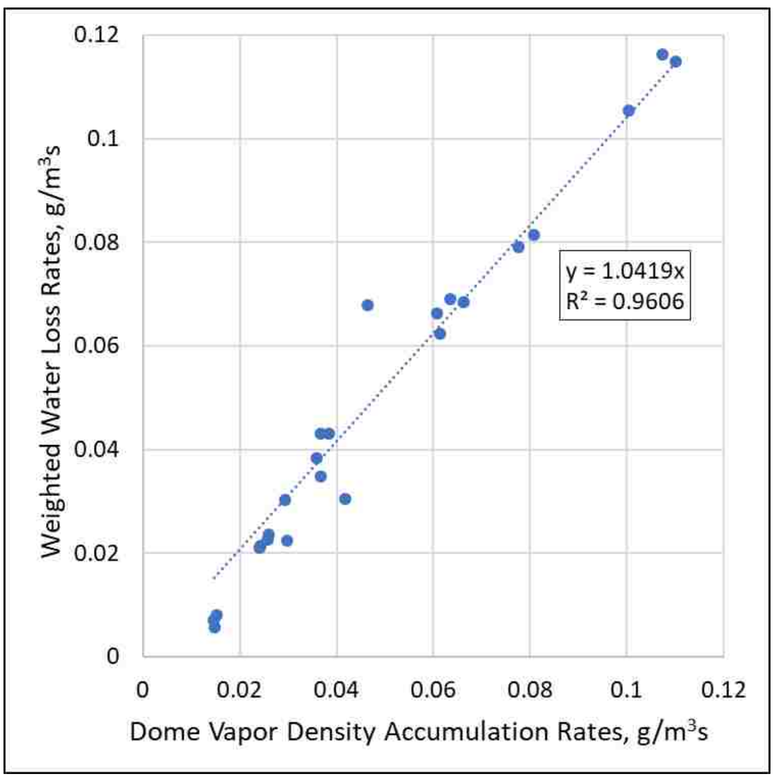

Figure 3.5: Hemispherical evaporation chamber calibration factor determination, C = 1.04.

Dome Validation Tests

Three validation tests with the dome were completed on September 30, October 19, and October 21, 2018 with the tests conducted between 7:40 and 14:50, 9:30 and 18:50, and 8:30 and 18:10, respectively. Each validation test consisted of taking dome measurements every ten minutes adjacent to the CFEP, with each test having a duration of two minutes. After the dome was lifted off the water surface, it was aired out for eight minutes to remove the built-up vapor pressure within the dome and to allow the air temperature and relative humidity probe to equilibrate back to ambient air temperatures and humidity levels.

The entire process was automated by a program that required the following connected equipment: a high ampere (26 A, 24 V) direct current motor with worm-gear reductions to lift and lower the dome; two switches to turn the motor off at set locations (dome on the water, dome in the air); a three-cup anemometer to control the fans inside the dome in real time; an air temperature and relative humidity sensor installed in the dome; an infrared radiometer; five solid state relays (one for the motor and four for each wind speed setting); two fans in the dome; and two 12-volt batters to power both the logger with 12 V and the fans and motor with 24 V. For each dome measurement, the program consisted of the following process: 0 seconds, turn on fans to current ambient wind speed (based on equation 3.3); 30 s, lower dome onto water; 120 s, lift dome off water; 240 s, turn off fans; repeat every 600 s.

Dome Relative Humidity Sensor Calibration

The dome's relative humidity (RH) sensor (model HygroClip S) experiences drift over time (Bell et al., 2017) and hence was calibrated with a CFEP RH sensor (model EE181) that was still within factory calibration. The black dots in Figure 3.6 represent corrected dome RH values and the red dots represent uncorrected RH values. A linear adjustment of the dome RH values in the form of $RH_{calibrated} = m * RH_{measured} + b$ was applied. The adjustment factors, m and b, were calculated such that the slope of a linear least-squared regression line for the corrected data would be equal to one with a y-intercept of zero. This adjustment procedure was followed for each of the three dome tests with the m and b adjustment factors as follows: 1.503 and -12.975, 1.527 and -21.01, and 1.537 and -18.57 for test dates September 30, October 19, and October 21, respectively. The close agreement of m and b adjustment factors from the three different dome tests highlights the consistent drift of the dome RH sensor, with the correction of the September 30, 2018 validation test shown in Figure 3.6 to illustrate the uncorrected and corrected differences.

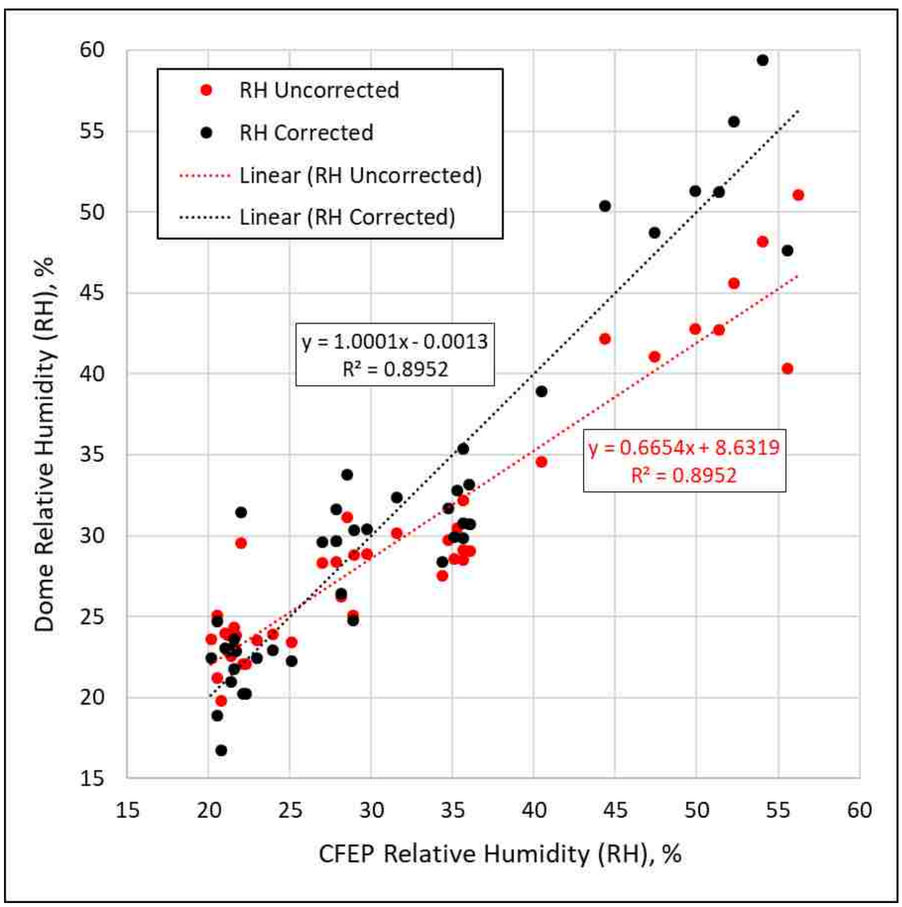

Figure 3.6: Dome relative humidity sensor correction factor for September 30, 2018.

3.2.4 Standard Evaporation Estimation Techniques

Class A Pan

The U.S. Army Corps of Engineers operates a Class A Evaporation Pan at their Cochiti Lake Ranger Station (see Figure 3.3) and supplied the data used in this study. The Class A Pan is located on the crest of a hill 1,200 m from and 70 m above Cochiti Lake, with continuous evaporation data since 1975. Measurements of the Class A Pan's water level is taken every morning at 08:00. An annual pan coefficient of 0.7 is applied to the Class A Pan's water level measurement in order to account for the higher rate of evaporation due to its evaporation rate being positively correlated to air temperature (Hounam, 1973; Jovanovic et al., 2008; Morton, 1979) and outside the atmospheric boundary layer of the reservoir (Stewart, 1979). In the middle of November, depending on first freeze, through late March or early April, daily winter evaporation values are used, where, in 2018, daily winter evaporation values began on November 12.

The Class A evaporation pan consists of a 22-gauge galvanized iron pan, typically 1.22 m in diameter and 0.254 m deep, on a wood base 0.152 meters above the ground. The Class A Pan's water levels are measured once each day in the morning and is typically filled once a week. By filling the pan once a week, the thermal mass associated with the water in the pan decreases throughout the week, allowing the water to become more susceptible to diurnal temperature changes later in the week, which affects evaporation rates (Hounam, 1973; Jovanovic et al., 2008; Morton, 1979).

Hargreaves-Samani Equation

The Hargreaves-Samani equation (3.5; Hargreaves and Samani, 1985) was originally developed to provide a simple estimate of potential evapotranspiration for regions lacking complete and/or accurate climatological data, but this equation has been shown to be a rough estimation of open-water evaporation rates (Brower, 2018). Equation 3.5 is below:

$$E = 0.0023 * S_o * \sqrt{\delta_T} * (T + 17.8) \quad (3.5)$$

where:

E	is evaporation or evapotranspiration, mm/day,
S_o	is water equivalent of extraterrestrial radiation, mm/day,
δ_T	is daily max. air temperature minus daily min. air temperature, °C,
T	is air temperature, °C,
0.0023	is a calibration coefficient.

The calibration coefficient was determined after eight years of comparing Equation 3.5 to the 29 m^2 weighing lysimeters data at Davis, California. This CFEP study used a polynomial least-squared regression ($R^2 = 0.9997$) equation to represent extraterrestrial radiation, S_o, based on a monthly value from the lookup table in Samani (2019) for northern hemisphere latitude 36. Equation 3.6 is below:

$$S_o = 0.0077m^4 - 0.1919m^3 + 1.211m^2 - 0.2667m + 6.5922 \quad (3.6)$$

where:

m	is the month of the year, decimal month.

Hamon Equation

The Hamon equation (3.7; Hamon, 1961) is similar the Hargreaves-Samani where the only atmospheric variable needed is air temperature, with the saturated vapor density portion of the equation being calculated based on air temperature. This equation was originally developed as a simple technique to estimate evapotranspiration with minimal inputs:

$$E = 0.55\left(\frac{D}{12}\right)^2\left(\frac{SV}{100}\right) * 25.4 \tag{3.7}$$

where:

D	is maximum possible daylight hours, decimal hours,
SV	is saturated vapor density, g/m^3,
0.55	is a calibration coefficient,
25.4	is a conversion to mm/day.

The Hargreaves-Samani (3.5) and Hamon (3.7) equations both require only one atmospheric input, air temperature, with the other input being a proxy for solar radiation and is easily calculated based on the declination of the sun and the latitude of the study location. These two equations have been shown to be generally within 20% of energy-budget equations, which are considerably more difficult and expensive (Harwell, 2012).

U.S. Weather Bureau Equation and Penman Equation

The U.S. Weather Bureau (USWB, which became the National Weather Service in 1970) Equation 3.8 was first proposed in Kohler et al. (1955) as a way to further increase the accuracy of the Class A Pan's evaporation measurements and to theoretically calculate Class A Pan evaporation rates when no pan is present. Equation 3.8 is a modified version of the Penman equation (Penman, 1948) with the inclusion of the 0.7 pan coefficient and with E_{pan} being calculated with Equation 3.9. Equation 3.8 is below:

$$E = 0.7\left[\frac{\Delta}{\Delta+\gamma}Q_n + \frac{\gamma}{\Delta+\gamma}E_{pan}\right] \tag{3.8}$$

where:

Δ	is the slope of saturated vapor pressure curve, kPa/°C,
γ	is the psychrometric constant, kPa/°C,

Q_n	is the effective net radiation, mm/day,
E_{pan}	is the amount of evaporation from a Class A Pan, mm/day,
0.7	is a Class A Pan coefficient.

The slope of the saturated vapor pressure curve, Δ, was calculated using daily average air temperature in Equation 5 on page 10 in Allen et al. (2005), which was based on work done by Murray (1967). The psychrometric constant, γ, is the product of the specific heat of moist air (J/kgC) and barometric pressure (kPa) divided by the product of the ratio of the molecular weight of water (unitless) and the latent heat of vaporization (J/kg). The effective net radiation, Q_n, was calculated using the Equation 2.13 on page 62 in Harwell (2012), where the only inputs are average daily air temperature and daily solar radiation. Lastly, the theoretical amount of evaporation from a Class A Pan, E_{pan}, was calculated with the following equation from Harwell (2012):

$$E_{pan} = (e_s - e_a)^{0.88}\left(0.42 + 0.0029v_p\right) \tag{3.9}$$

where

e_s	is the saturation vapor pressure, mb,
e_a	is the vapor pressure at the temperature of the air, mb,
v_p	is the average wind speed, km/day.

Equation 3.9 was derived in Kohler et al. (1955) to represent Class A Pan evaporation rates and was modified for SI units by Harwell (2012). Two different forms of Equation 3.8 were used in this study and are as follows: 1) using Equation 3.9 with the 0.7 pan coefficient in equation 3.8, called USWB; and 2) using Equation 3.9 without the 0.7 pan coefficient in Equation 3.8, called Penman. Equation 3.8 was originally derived using atmospheric variables

over land, where VPD's are typically larger than over water, requiring the 0.7 pan coefficient correction value. In this study atmospheric variables were collected over the water, eliminating the need for the corrective 0.7 pan coefficient. The Penman version of Equation 3.8 is identical to the Penman equation (Penman, 1948), with the Q_n and E_{pan} being calculated following the steps described above. The atmospheric requirements of the USWB equation and Penman equation are air temperature, relative humidity, wind speed, barometric pressure, and solar radiation.

3.3 Results

3.3.1 CFEP Evaporation Results

The CFEP's estimated evaporation and measured precipitation are shown in Figure 3.7, with the total amount that evaporated during the 201-day study being 1.127 m. A second order polynomial trend line elucidates the seasonal trend in evaporation, with evaporation peaking in June (7.9 mm monthly average) and remaining semi-steady in July, August, and September: 6.89 mm, 5.99 mm (partial month), and 6.45 mm, respectively. In early October, a sharp decline in evaporation was observed with a monthly average of 3.9 mm, a product of the region transitioning from summer monsoonal convection storms to winter frontal storms, as shown in Figure 3.8 below by the consistent values of VPD below 1 kPa. June 24 had the greatest evaporation rate of 12.04 mm; a day dominated by VPD between 4 and 4.8 kPa and with the daily averaged VPD of 3.5 kPa, this was the highest daily averaged VPD during the study's duration. The high variability in daily evaporation rates can be explained by precipitation events, as seen in Figures 3.7 and 3.8, where small evaporation values correspond with low VPD during precipitation events. Additionally, large and small VPD values as seen in Figure 3.8 correspond with peaks and valleys in evaporation rates as seen in Figure 3.7.

Three seasonal trends are shown in Figure 3.8: pre-monsoon, monsoon, and post-monsoon. These seasonal trends are illustrated by the differences in saturated vapor pressure (SVP) and VPD, where similar values of SVP and VPD indicate very dry air with very little moisture present, as seen in May and June. The effect of the monsoon season is shown by the differences between SVP and VPD occurring in early July through September. Finally, the post-monsoon season is shown by the reduction in differences between SVP and VPD in late September and early October.

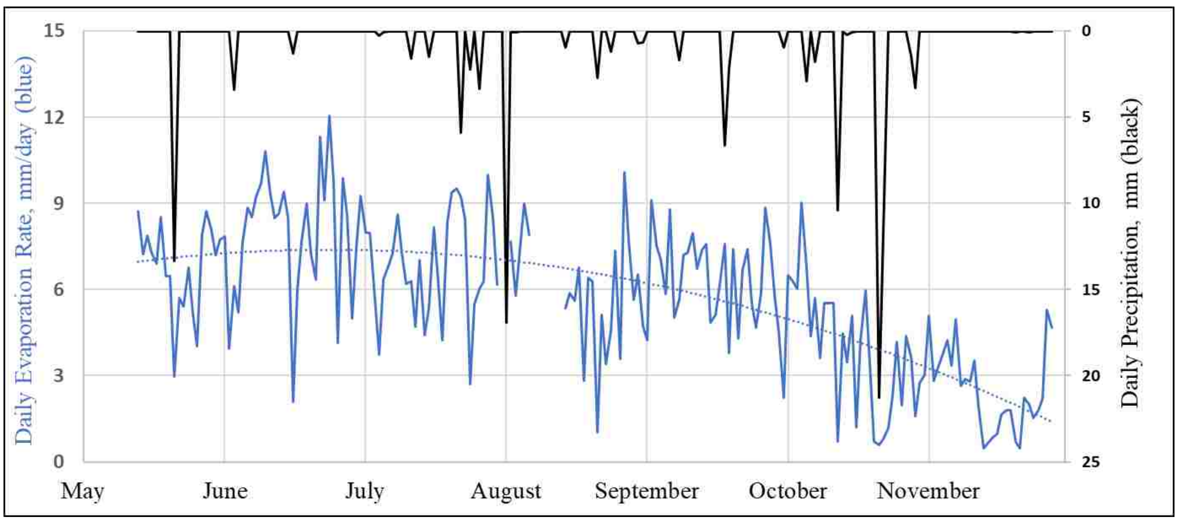

Figure 3.7: CFEP measured daily evaporation rate on Cochiti Lake, NM, USA for the duration of the study (blue line), precipitation (black line), and a second order polynomial trend line.

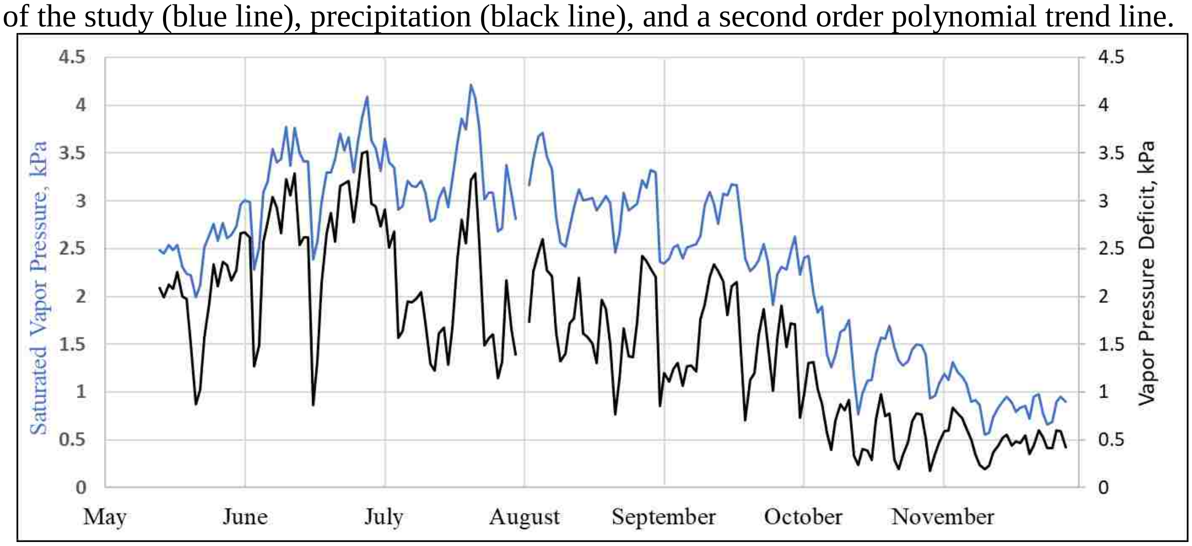

Figure 3.8: Daily saturated vapor pressure (blue line) and vapor pressure deficit (black line), measured at the CFEP on Cochiti Lake, NM, USA.

Wind Direction on Evaporation Rates

By coupling evaporation to wind direction (northerly and southerly), the evaporation rate associated with shore-to-water and water-to-shore winds were determined. The CFEP was placed close to the southern shore of Cochiti Lake where northerly winds had an open-water fetch distance greater than 2,000 m and southerly winds had an open-water fetch distance around 100 m, resulting in different evaporation rates based on from where the wind was coming. The effect of wind direction and VPD on evaporation rates is shown in Figure 3.9, with cumulative evaporation and cumulative evaporation associated with either northerly or southerly winds displayed. Evaporation during a northerly wind period accounted for only 38% of the 1,104 mm that were measured during the 201-day study, with southerly winds accounting for the remaining 62%.

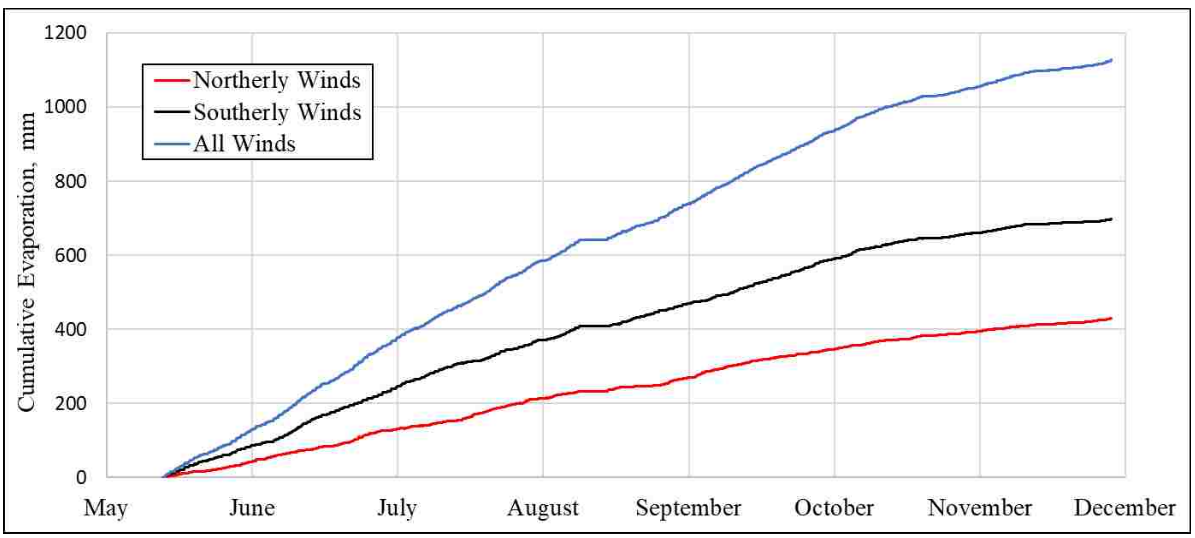

Figure 3.9: Cumulative evaporation rate associated with wind direction during each 15-minute period.

3.3.2 CFEP Validation Results

There was a divergence between evaporation measured by the dome and by the CFEP in the beginning of the day for the first and last validation tests, but the cumulative evaporation results converged toward the end of all three tests (Figure 3.10). The evaporation results from the CFEP on September 30 before 13:00 and on October 21 before 14:45 follow a similar pattern: an increase in evaporation rates in the morning followed by a decrease and negative evaporation rates in the middle of the day, with this pattern emphasized more on the last validation test. Additionally, the evaporation measured by the dome on these two days follows a similar pattern with a gradual increase in evaporation in the morning and then a noticeable increase in evaporation in the afternoon. The results from the October 19 test do not follow either of these patterns; instead, there is a close agreement between the CFEP and dome and a consistent evaporation rate measured by the dome for the duration of the test. The dome measured less cumulative evaporation than the CFEP on the first and last validation tests, and measured more cumulative evaporation on the middle validation test.

Although there was a divergence between the dome and CFEP's measured evaporation, the final cumulative results for all three validation tests had close agreement. Table 3.2 displays the total cumulative evaporation measured by the CFEP and the dome, the difference in evaporation between the two techniques, percent difference, and a dome-to-CFEP ratio. The similar pattern (see Figure 3.10) of evaporation measured by the CFEP on the first and last validation tests was also reflected in the difference of evaporation measured by both tests: -0.17 mm, or a percent difference of -6.17 and -7.54 for the first and last validation tests, respectively. More cumulative evaporation was measured during the first test, even though it had a shorter duration, explaining the slight percent difference from the last test. The middle validation test, which displayed a different evaporation pattern (see Figure 3.10), resulted in the dome measuring more cumulative evaporation than the CFEP: 0.21 mm, or a percent difference of 8.55. The average cumulative evaporation difference between the dome and CFEP was -0.04, or an averaged percent difference of -1.72. Lastly, a dome-to-CFEP ratio was calculated, where values greater than one indicate that the dome measured more evaporation and values less than one indicate that the CFEP measured more evaporation. An average dome-to-CFEP ratio of 0.99 was calculated based on the three validation tests.

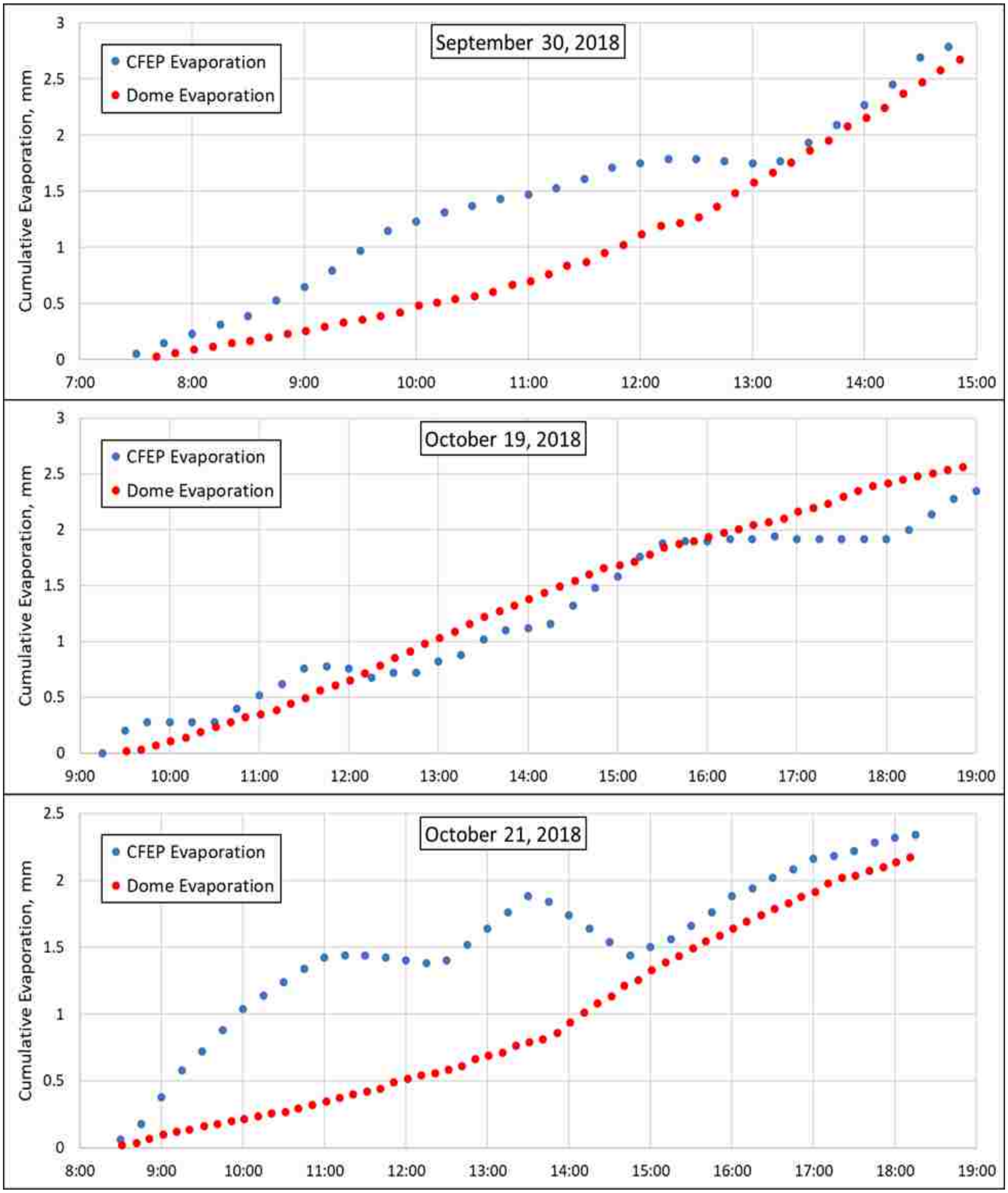

Figure 3.10: Cumulative dome evaporation measurement results (red) and corresponding time CFEP cumulative evaporation results (blue).

Table 3.2: Dome and CFEP Evaporation Results

	Sept. 30 7:40-14:50	Oct. 19 9:30-18:50	Oct. 21 8:30-18:10	Average
Test duration	7:10	9:20	9:40	
CFEP total evaporation (mm)	2.84	2.35	2.34	
Dome total evaporation (mm)	2.67	2.56	2.17	
Difference (dome to CFEP)	-0.17	0.21	-0.17	-0.04
Percent difference (dome to CFEP)	-6.17	8.55	-7.54	-1.72
Dome-to-CFEP ratio	0.94	1.09	0.93	0.99

The following three figures (Figure 3.11, 3.12, and 3.13) are included to explain the anomalous CFEP evaporation measurements during the morning and early afternoon of the first and last validation tests. Figure 3.11 below shows 15-minute averaged solar radiation values measured by the pyranometer on the CFEP. During each of the three validation tests there was no cloud cover present, indicated by the smooth increase and decrease in solar radiation. The maximum amount of solar radiation during each validation test, assuming no cloud coverage, is a function of the sun's declination angle, where a smaller angle corresponds to less solar radiation, as indicated by Figure 3.11.

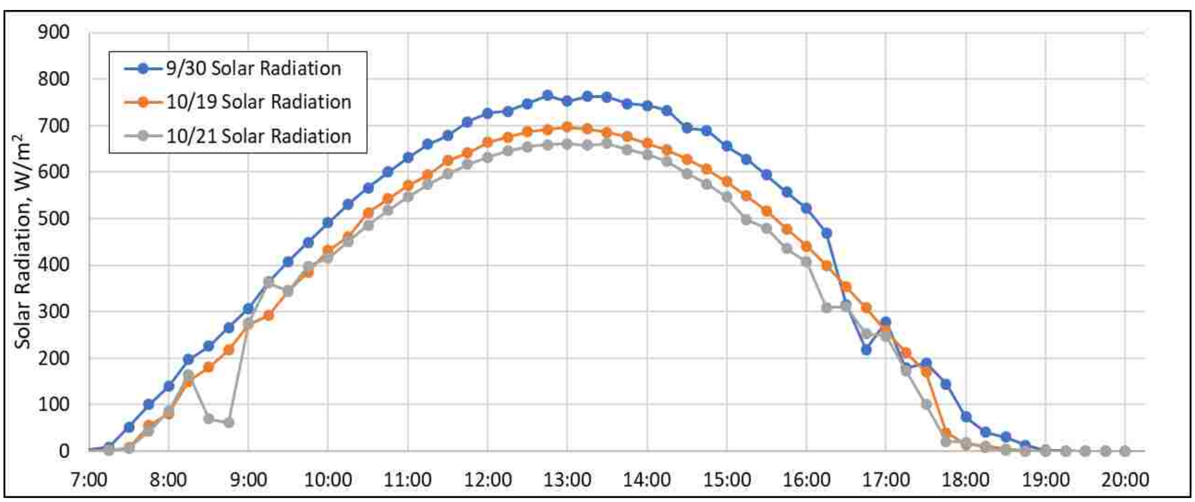

Figure 3.11: Solar radiation measured by a pyranometer on the CFEP.

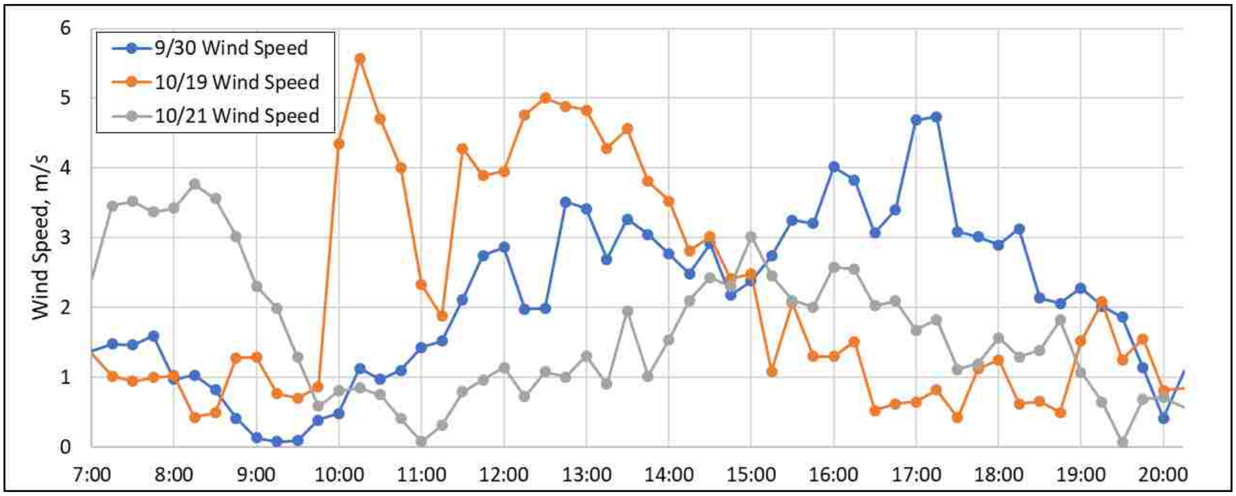

Figure 3.12: Wind speed measured by an anemometer on the CFEP.

The wind patterns for the first and last validation test were similar, with winds under 1 m/s during the beginning of each test and then steadily increasing as the day progressed, whereas the wind pattern during the middle validation started out high with consistent winds greater than 4 m/s in the morning and early afternoon and then decreased toward the end of the validation test. Figure 3.12 displays the averaged 15-minute wind speed measured by the CFEP's anemometer during each validation test. The effect of wind speed on the surface water temperature is shown in Figure 3.13, where on 10/19/18, a day with greater winds in the morning (Figure 3.12), there was a more gradual increase in surface water temperature, whereas on the first and last validation tests there was very little wind in the morning resulting in a sharper increase in water surface temperature in the morning. Figure 3.13 displays the skin-surface water temperature adjacent to the dome measured by an infrared radiometer attached to the validation test boat.

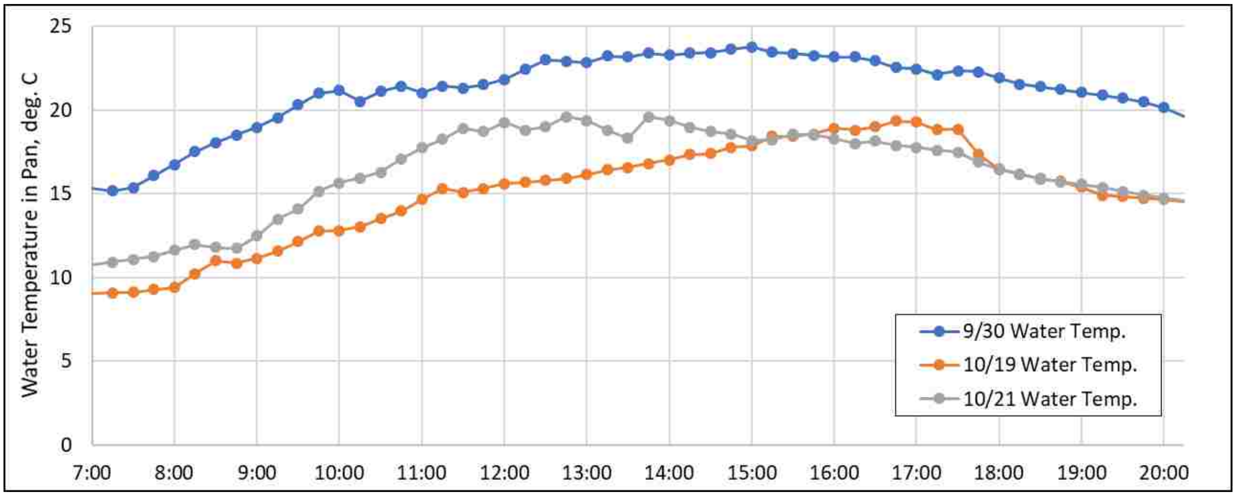

Figure 3.13: Skin-surface water temperature adjacent to the dome measured by an infrared radiometer attached to the validation test boat.

3.3.3 Comparisons between CFEP and Existing Approaches

The evaporation rates from the CFEP were compared to the above four equations and the on-site Class A Pan managed by the U.S. Army Corps of Engineers at their Cochiti Lake Ranger station, which switched to set monthly values on November 12. Five-day averaged evaporation was estimated for the CFEP, Class A Pan, USWB equation, Penman equation, HS equation, and Hamon equation (see Figure 3.14). The CFEP and Class A Pan had closest agreement in evaporation rates for May and June with an averaged difference between the CFEP and Class A Pan being -9 and 0.04 percent, respectively, but the similarities in evaporation rate discontinued in mid-July through October (see Table 3.3). Overestimation of evaporation when compared to the CFEP is represented by percent error difference values greater than zero, and underestimation of evaporation is represented by percent error difference values less than zero. The Penman equation overestimated evaporation when compared to the CFEP in May through August, and underestimated evaporation in September through November. The Penman equation estimated the highest monthly evaporation rate during May through August and began to underestimate evaporation when compared to the CFEP technique in September through November. The total amount of evaporation measured by the five different techniques is as follows: CFEP 1,104 mm; Class A Pan 927 mm; USWB equation 817 mm; Penman equation 1,167 mm; HS equation 805 mm; and Hamon equation 585 mm.

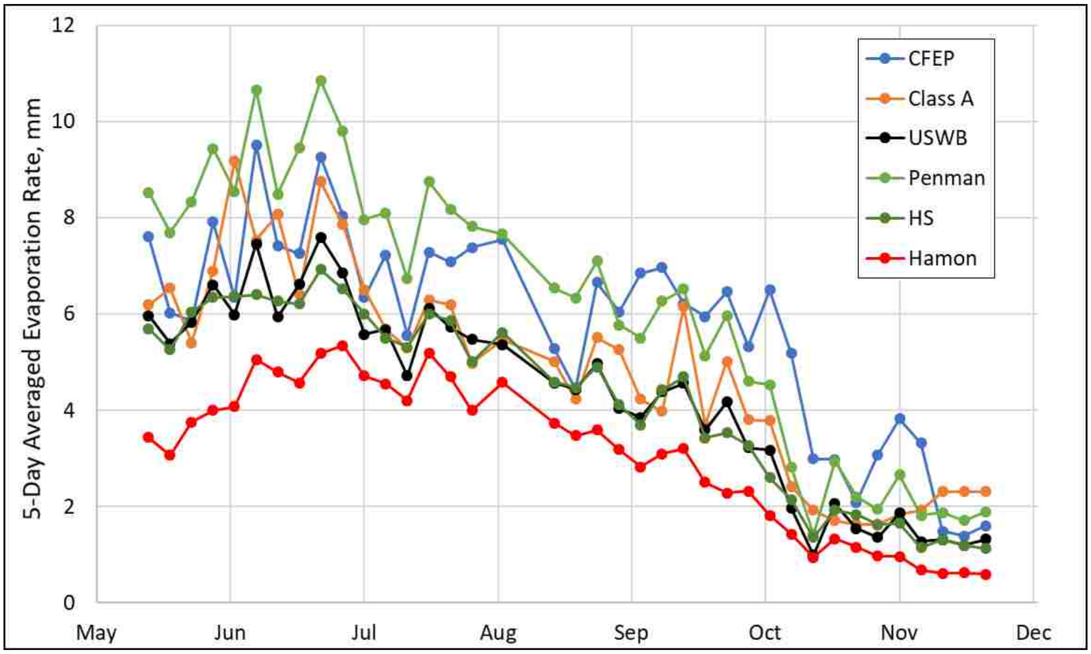

Figure 3.14: 5-day averaged evaporation for the CFEP (Collison Floating Evaporation Pan), Class A Pan, USWB equation (U.S. Weather Bureau), Penman equation, HS equation (Hargreaves-Samani), and Hamon equation.

Table 3.3: Percentage error difference of the CFEP (Collison Floating Evaporation Pan) to Class A Pan, USWB equation (U.S. Weather Bureau), Penman equation, HS equation (Hargreaves-Samani), and Hamon equation. The 25th percentile, median, and 75th percentile were calculated as the absolute percentage error difference.

	Class A (%)	USWB (%)	Penman (%)	HS (%)	Hamon (%)
May	-9	-13	24	-15	-48
June	0.04	-15	22	-19	-39
July	-14	-19	16	-18	-34
August	-13	-19	15	-18	-36
September	-29	-38	-11	-40	-57
October	-40	-40	-28	-48	-64
November	-17	-46	-23	-49	-72
Average	-17	-29	2	-29	-50
25th Percentile	9	15	22	18	36
Median	14	19	15	19	48
75th Percentile	29	46	24	48	64

The agreement in evaporation rate between the CFEP and Class A Pan was very similar during the first part of the study until late August and early September when the CFEP started to consistently measure higher rates of evaporation. The largest percent difference between the CFEP and the Class A Pan was in September and October, 29 and 40 percent, respectively (see Table 3.3 above). This higher evaporation rate in the fall is evident in Figure 3.15 below by the increase in slope of the CFEP's cumulative evaporation compared to the slope of the Class A Pan's cumulative evaporation. A Pearson's correlation coefficient of 0.71 (indicating a strong correlation between daily averaged air temperature at the CFEP and daily evaporation rate from the Class A Pan) was calculated, which is supported by other studies (Hounam, 1973; Jovanovic et al., 2008; Morton, 1979). The close agreement between the HS and USWB is very apparent in Figure 3.15 below, with an average percent difference of 3.3 for the duration of the study.

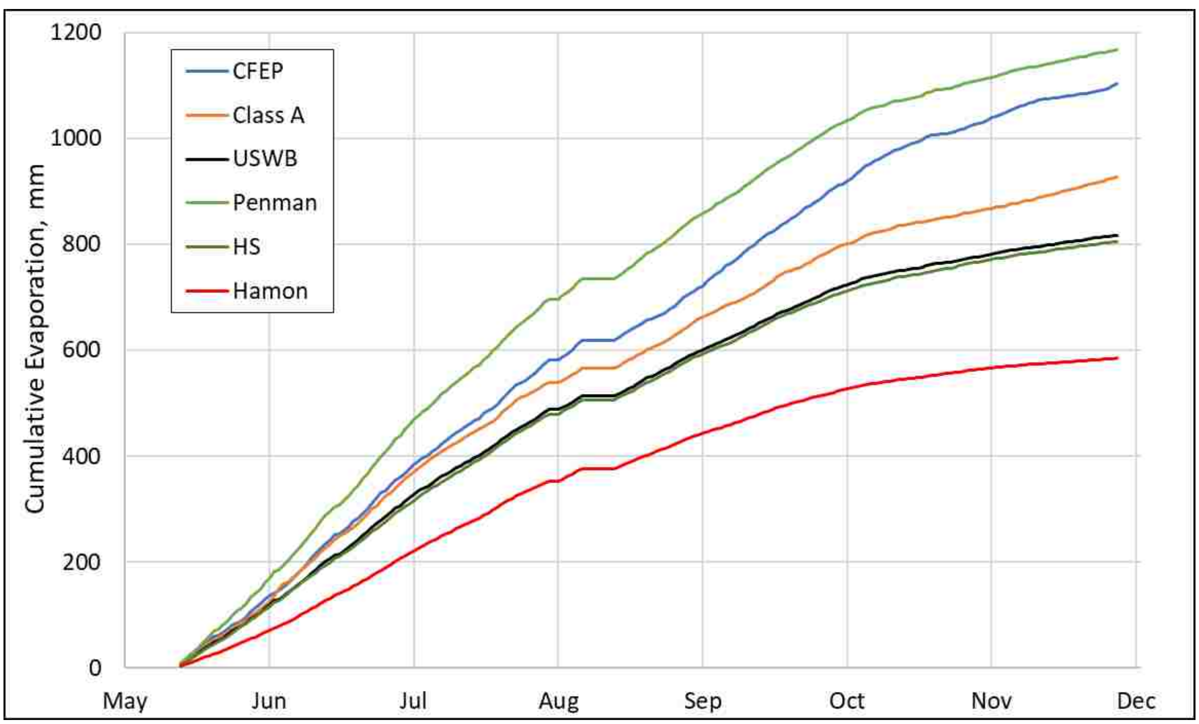

Figure 3.15: Cumulative evaporation for the CFEP (Collison Floating Evaporation Pan), Class A Pan, USWB equation (U.S. Weather Bureau), Penman equation, HS equation (Hargreaves-Samani), and Hamon equation.

The peaks in evaporation measured by the CFEP, Class A Pan, and Penman equation occurred in June, corresponding with the peak air temperatures (see Figure 3.16). The effect of the stored energy in the reservoir being released through evaporation (see Figure 3.17) is shown by the increased values of outgoing radiation between late August and early October, where outgoing radiation values are consistently above the polynomial-least squared regression line during the period in question. This increase in outgoing stored energy is reflected by the higher evaporation rates measured by the CFEP between lake August and early October when compared to the five other techniques, which are not affected by the stored energy within the reservoir.

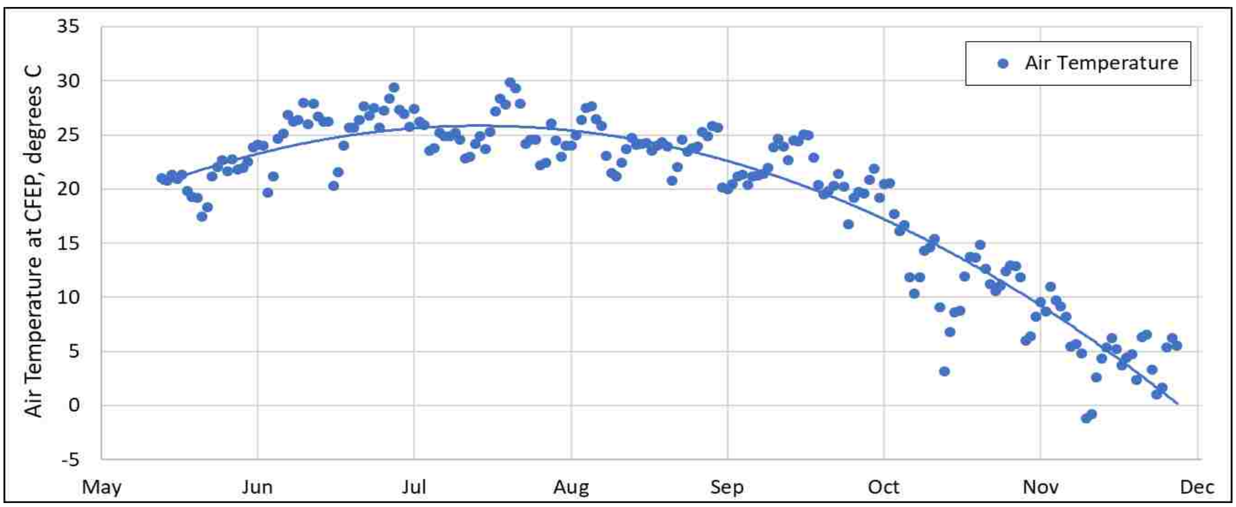

Figure 3.16: Air temperature measured 2 m above the water surface with a polynomial-least squared regression line visualizing the seasonal trend.

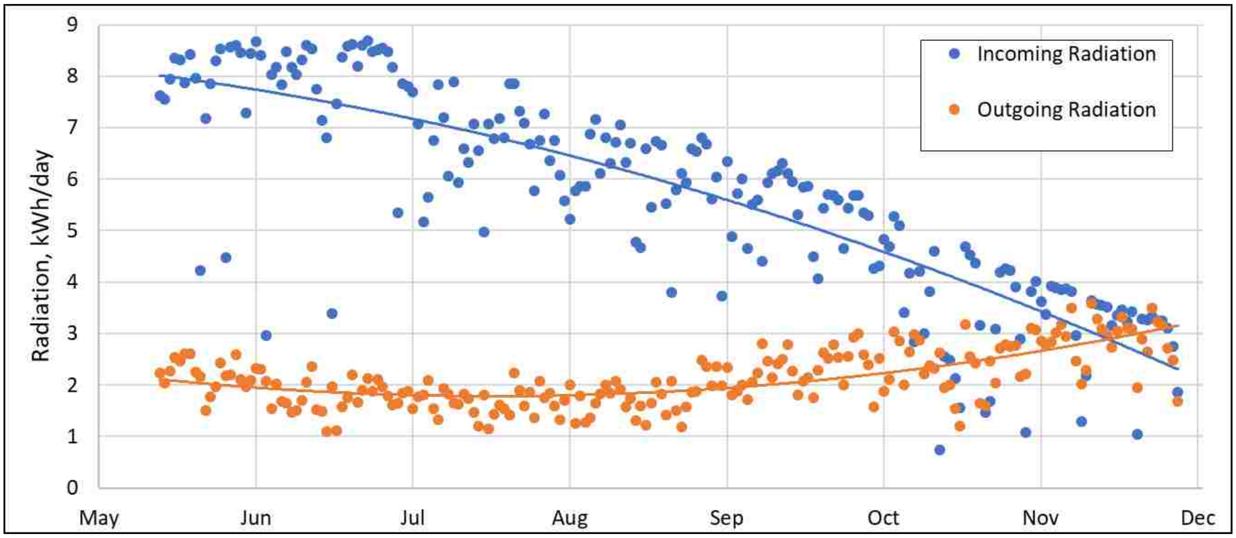

Figure 3.17: Incoming and outgoing radiation measured at the CFEP (Collison Floating Evaporation Pan) with two polynomial-least squared regression lines visualizing the seasonal trend.

The general trend for the five evaporation estimation techniques when compared to the CFEP technique was overestimated evaporation in the beginning of the study and underestimated evaporation at the end of the study. The predominate reason for this trend is that all evaporation techniques evaluated in this study, except for the CFEP technique, do not include heat energy stored and then released from the reservoir. Figure 3.18 below shows the five-day averaged evaporation percent difference between the CFEP and the five other evaporation estimation techniques. The slope of the linear-least squared regression line for the different evaporation estimation techniques are as follows: Class A Pan -0.265; USWB equation -0.167; Penman equation -0.244; HS equation -0.167; and Hamon equation -0.166. The near identical slope of these linear least-squared regression lines indicates that they are each affected by the lack of accounting for stored energy equally.

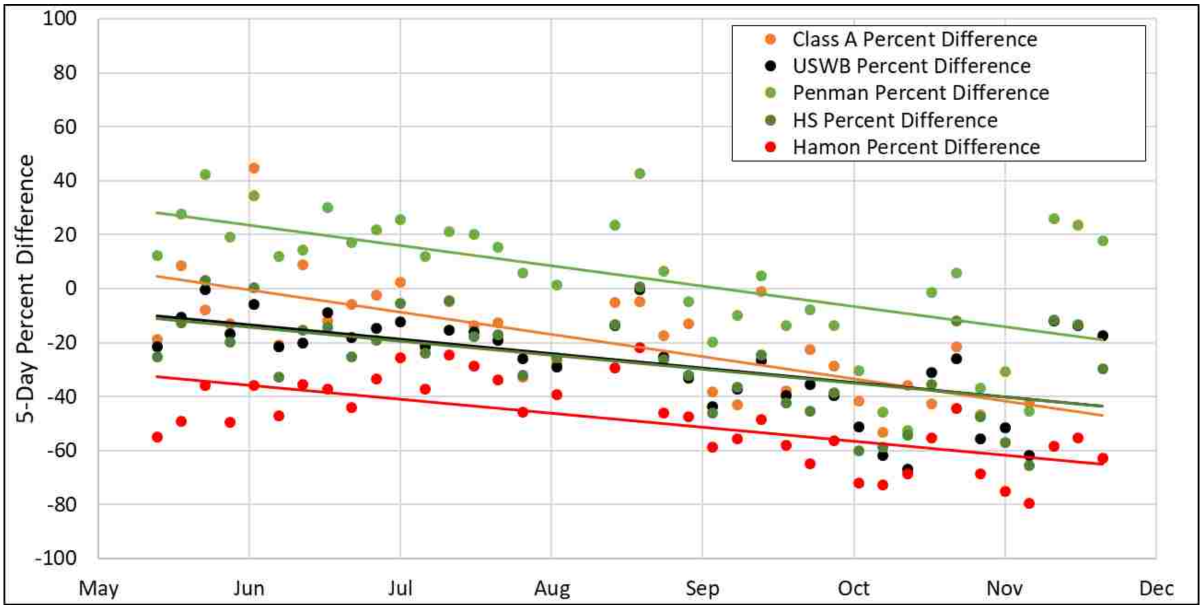

Figure 3.18: 5-day averaged evaporation percentage difference [(B-A)/A]*100, where A are values from the CFEP (Collison Floating Evaporation Pan), and B are values from the following: Class A Pan, USWB equation (U.S. Weather Bureau), Penman equation, HS equation (Hargreaves-Samani), and Hamon equation. Compared to the CFEP, negative percentage errors reflect B values underestimating evaporation and positive percentage errors reflect B values overestimating evaporation.

3.4 Discussion

<u>3.4.1 CFEP Reliability and Wind Direction Affecting Evaporation Rates</u>

The reliability of the CFEP's ability to estimate lake and reservoir evaporation is evident by the near-continuous plot of daily evaporation rates shown in Figure 3.7, with only two gaps in evaporation data due to technical issues unrelated to the normal functionality of the CFEP (human error). The reliability of the CFEP's evaporation estimation during sustained windy conditions was a major concern before conducting this study. The concern was that during sustained wind events on Cochiti Lake, large waves (potentially 1 m in height or greater) would overtop CFEP's wave guard and swamp the evaporation pan. On May 21 sustained 15-minute averaged winds greater than 5 m/s occurred for a period of 15 h (08:00-23:00), peaking at 9 m/s and gusts over 20 m/s. The evaporation pan's water-level height experienced some above average oscillation, but no waves overtopped the evaporation pan. From May 13 through the end of the study there were no indications that the evaporation pan's water level was affected by water entering or leaving during high wind events, with the largest anomalies in water levels being caused by birds landing on and then leaving the evaporation pan.

The general trend of highest evaporation rates in mid-to-late June, then a gradual decrease in evaporation rates through September, and then a sharp decrease in evaporation rates in early October is a product of the North American Monsoon Season (NAMS), with the NAMS typically beginning in early July and lasting until mid-September (Grantz, 2007). The evaporation results of this study match the typical timing of NAMS, with the driest period and highest evaporation rates occurring in June before the NAMS began around the beginning of July 2018 (see Figure 3.8). The onset and departure of the 2018 NAMS is clearly visible in Figure 3.8, with the divergence between SVP and VPD at the beginning of July and then the transition to frontal storm systems in early October.

The high variability of estimated evaporation rates in Figure 3.7 can be explained by sharp decreases in VPD, displayed in Figure 3.8, that correspond with precipitation events. Additional variation in evaporation rates are caused by seasonal changes in SVP and VPD values and summer convection storms occurring in May through September (see Figure 3.8). Consequently, the two largest evaporation rates occur roughly midway between precipitation events that occurred at the beginning, middle, and end of June. Between precipitation events, the desert surrounding Cochiti Lake would begin to dry, as indicated by the gradual increase of VPD a few days after precipitation events, resulting in the two peaks of evaporation rates in June.

The effect of wind direction on evaporation rates was not anticipated. Due to deployment location limitations, the adequate fetch rule was not followed and the CFEP was situated 100 m from the southern shore of Cochiti Lake. The small fetch distance of the southerly winds did not allow the air to become saturated by reservoir evaporation, and when this high VPD air (2+ kPa) reached the CFEP, the evaporation rate increased. The longer fetch distance of the northerly winds allowed the air to become more saturated with water from reservoir evaporation and when this lower VPD air (~1 kPa) reached the CFEP, a smaller evaporation rate associated with the wind speed intensity was recorded. Additionally, as shown in Figure 3.9, the effect wind direction had on cumulative evaporation throughout the entire study is clearly demonstrated, with wind coming from the south accounting for 62% of the evaporation measured during the 201-day study.

3.4.2 CFEP Validity and Potential Errors

Because the major driving forces of evaporation are water temperature and wind speed, the similarities in cumulative evaporation amounts conform to scientific principles, but the evaporation pattern of the evaporation measured by the CFEP is not as straightforward. The atmospheric conditions on the three validation test days were similar to the vast majority of the days during this study, with minimal northerly winds in the morning and stronger southerly winds in the afternoon. During both the first and last validation test, the CFEP estimated high rates of evaporation at the beginning of the validation tests, then a gradual decrease (first test) and larger decrease (last test) in evaporation, indicating an evaporation forcing variable not present in the middle validation test. Since there was no precipitation (negative evaporation) as indicated by solar radiation values shown in Figure 3.11, what caused the estimated evaporation from the CFEP to decrease in the middle of the afternoon or go negative during the first and last validation test? After careful examination of the many variables (air temperature, relative humidity, wind speed and direction, vapor pressure deficit, solar radiation, surface water temperature, and instrument malfunction) three phenomena may explain the majority of the evaporation patterns from the CFEP and the dome: (1) thermal expansion/contraction of the CFEP aluminum, which caused the sharp increase in estimated evaporation during the first and last test; (2) thermal expansion/contraction of the water within the CFEP, which caused the reduction and negative values in estimated evaporation during the first and last test; and (3) high and constant wind conditions, which caused the well-correlated results between the dome and the CFEP in the middle test.

The sharp increase in estimated evaporation measured by the CFEP during the first and last test can be explained by the thermal expansion of the CFEP. The expanding evaporation pan results in an increased volume within the CFEP, and since the water volume is relatively constant, other than the loss of volume due to evaporation, the water level within the pan decreases, displaying a higher evaporation rate. Aluminum (alloy 6061) has a linear thermal expansion coefficient of 23.5×10^{-6} m/mK where every 10° C temperature increase in the evaporation pan's wall increases the volume of the CFEP's evaporation pan by 444 cm^3, decreasing the evaporation pan's water level by 0.0952 mm. However, this is a theoretical maximum since the CFEP is in water, which reduces the thermal expansion of the evaporation pan's wall that is submerged. Although the temperature of the aluminum sides of the pan was not measured, a calculation of thermal loading from the sun on the CFEP's aluminum using the Stefan-Boltzmann law and emissivity of aluminum (0.2) indicates a sharp rise in temperature (+65 °C) with a solar radiation value of 800 W/m^2.

The reduction and negative values in estimated evaporation from the CFEP can be explained by the thermal expansion of water. As the water within the CFEP warms up it expands, with 2.07×10^{-4} m^3/m^3 °C being the coefficient of thermal expansion of water at 15°C.

A change in water temperature within the evaporation pan from 15 to 20°C increases the water level by 0.762 mm (assuming fully mixed water). Since water has almost 4.6 times greater specific heat capacity than aluminum (4.18 vs. 0.91 kJ/kg K), the thermal expansion of the water in the evaporation pan is delayed compared to the thermal expansion of the aluminum CFEP (i.e., the aluminum walls heat up faster than the water). The CFEP's evaporation pan is equipped with a baffle to prevent excessive water movement, which reduces the convective mixing of warmer skin-surface water with cooler water below, further lagging the thermal expansion of the water. When the evaporation pan's water expands, the water level within the evaporation pan increases (displayed as a decreasing, or negative, evaporation rate). Evidence of this lagged thermal expansion of water is apparent in the first and third validation test and displayed in Figure 3.10 by the negative cumulative evaporation rate around noon.

The strong correlation between the CFEP's estimated cumulative evaporation and the dome's evaporation measurements during the middle test is explained by the high and constant wind during the morning and afternoon that day (see Figure 3.12). Wind causes mixing of the warmer surface water with the cooler water below, allowing the water to more gradually warm up (middle test) and preventing the sharp increase in water temperatures seen in the first and last validation (see Figure 3.13). Additionally, the wind during the middle validation test caused more wave action, which further led to three distinct effects: (1) more mixing of the reservoir's surface water to a deeper depth, causing a more gradual increase in surface water temperature; (2) more rocking motion of the CFEP, causing the water within the evaporation pan to become more mixed; and (3) increased splashing of water on the CFEP walls, cooling the aluminum and reducing thermal expansion.

The thermal expansion/contraction of aluminum and water was an unexpected result from this study, which affects the precision and accuracy of the CFEP's evaporation estimation by increasing the spatial variably of 15-min evaporation data (i.e., precision) and the closeness to actual evaporation (i.e., accuracy). The effects of the thermal expansion/contraction of aluminum and water can be ignored by instead taking daily evaporation values at midnight when thermal expansion/contraction is minimal based on the assumption that thermal expansion in the morning and thermal contraction in the evening counteract each other. Even with the inclusion of thermal expansion/contraction, there was high agreement in the final cumulative evaporation, with the average difference in evaporation measured during the three validation tests being -0.04 mm with a range of -0.17 mm to 0.21 mm.

3.4.3 CFEP Comparison

Overall, the Penman equation had the closest agreement to the CFEP technique, especially in July through September, but the agreement between these two techniques diverted in May and June, with the Penman equation overestimating evaporation, and then again in October and November, with the Penman equation underestimating evaporation. It has been shown that the Penman equation typically overestimates evaporation during warmer periods and underestimates evaporation during cooler periods (Allen et. al., 2005; Winter et al., 1995), which is consistent with the findings in this study (see Table 3.3). The average monthly percent error difference between the CFEP and Penman equation was 2% with a range of -28 to 24%. The next closest agreement in estimated evaporation was between the CFEP and Class A Pan technique, with the closest agreement in June, 0.04% difference, and increasing to a percent error difference of -40% in October.

The percent error difference between the CFEP and the Penman equation and the Class A Pan can be explained by seasonally stored energy within the reservoir. From early spring until late summer, when daily averaged air temperatures are greater than daily averaged water temperatures, the reservoir water absorbs heat energy until early fall when this stored energy is released through evaporation. The Penman equation does not account for the storage of heat energy in the warmest months (May through July) and tends to overestimate evaporation. Additionally, with the Class A Pan evaporation rate being correlated to daily averaged air temperatures due to its smaller thermal mass than the reservoir, as the air temperatures decreased, so did the evaporation rate; however, the CFEP's evaporation rate decreased at a slower rate due to the water surrounding the CFEP having a higher thermal mass and cooling down more slowly. The converse would have been true if this study had data for spring evaporation rates when the reservoir is storing energy (heating up), with the Class A Pan and these four equations overestimating evaporation rates (Hounam, 1973; Morton, 1979). Some locations use different pan coefficients to adjust the Class A Pan's evaporation rate accordingly instead of using one annual rate to account for the overestimating of evaporation in the spring and underestimation of evaporation in the fall.

Further evidence of this stored energy not being accounted for in the Class A Pan and the four evaporation equations is shown by the increasing underestimation of evaporation when compared to the CFEP (Figure 3.14), with the largest negative percent different values occurring between September and October. Consequently, the evaporation rate of the CFEP during this time period was also 20-70% greater than the Class A Pan (Table 3.3) and the other four techniques calculated in this study. Underestimating lake and reservoir evaporation amounts in water resource models can lead to inaccurate allocations of water resources, potentially producing shortages in some instances or excess water that is not put toward beneficial use in other instances.

A surprising discovery in this study was the close agreement between the HS and USWB techniques. The HS equation's only on-site measured atmospheric variable is air temperature whereas the USWB equation requires air temperature, humidity, wind speed, and solar radiation. The Hamon equation consistently underestimated evaporation for the whole duration of the project by 30 percent less than the HS and USWB equations, but an adjustment to the calibration coefficient in the Hamon equation can bring this equation's evaporation estimate to within 5 percent difference from the HS equation.

Winter et al. (1995) found that evaporation equations that used solar radiation to determine evaporation consistently overestimate in the spring and underestimate in the fall when compared to an energy-budget evaporation equation. In Rosenberry et al. (2004) where 13 evapotranspiration equations were compared, the Hamon equation (3.7) was within 20% of an energy-budget equation 95% of the time. Lastly, Harwell (2012) found that the Hamon equation (3.7) had an average annual error between 12.9 and 38.1% and that the USWB equation (3.8) had an averaged annual error between 4.7 and 14.1% when compared to five different reservoir Class A Pans spanning between seven and 10 years in duration.

The CFEP technique highlighted the limitations and uncertainties of lake and reservoir evaporation techniques that do not account for the seasonally stored energy within the body of water, which was represented by 28 to 64% underestimation of evaporation during September and October. The current standard method for determining evaporation from Cochiti Lake is the Class A Pan, which, based on the data from this CFEP study, underestimated evaporation by 1.12 MCM (911 acre-feet) during this study's duration, May 13 through November 30,

2018. Based on the 201-day study and on an average reservoir surface area of 5.62 million m^2 (1,388 acres), the CFEP's evaporation rate translates into 6.33 MCM (5,132 acre-feet) of evaporation while the Class A Pan's evaporation rate translates into 5.21 MCM (4,221 acre-feet) of evaporation.

3.5 Conclusion

This study introduced a novel technique, the Collison Floating Evaporation Pan (CFEP), for in-situ estimation of evaporation from lakes or reservoirs that proved to be reliable, accurate, and precise. A pilot deployment of the CFEP on Cochiti Lake, New Mexico, USA was used to demonstrate the durability of the CFEP in a high wind environment. The accuracy and precision of the CFEP was determined through the use of a hemispherical evaporation chamber (dome). The results of this study show that the CFEP is both accurate and precise as demonstrated by the close agreement in evaporation measured by the dome and the CFEP.

Five common evaporation estimation techniques were compared to the CFEP. Because common approaches do not include stored energy, they were unable to capture the higher evaporation rates in the fall, whereas the water within the CFEP's evaporation pan being thermally connected with the reservoir's captured this increased fall evaporation rate. A better understanding of the uncertainties of these equations contributes to the hydrologic sciences by elucidating their strengths and weakness in estimating lake and reservoir evaporation, allowing for corrective actions to be taken which will increase their accuracy and precision. A reduction in the uncertainties associated with lake and reservoir evaporation estimation techniques will improve the accuracy of water supply models, allowing water resource manages to have a firmer grasp on the actual amount of water available.

The CFEP approach provides many advantages over traditional evaporation estimation techniques by not requiring homogeneous fetch. Establishing a new evaporation technique that does not have the limitations and uncertainties associated with deployment locations will enhance the state of science by allowing a wider range of deployment locations that are currently inaccessible. This key advantage of the CFEP allows for deployment in fetch-limited areas, such as smaller lakes and/or channelized reservoirs. Additionally, the CFEP can be deployed near the shore to quantify the effect of shore-to-water winds on lake and reservoir evaporation rates, increasing the state of knowledge of spatially variable evaporation rates.

This quantification of the magnitude of shore-to-lake winds' effect on evaporation rate is substantial, especially in arid or semi-arid environments where it is assumed the VPD of air above the land is greater than the VPD of air over water. The enhanced understanding of the importance of wind on evaporation rates of lakes or reservoirs, where the windward (shore-to-water) side has a quantifiably greater evaporation rate than the leeward (water-to-shore) side, is a substantial addition to hydrologic sciences, as the current standard is to use one evaporation rate for the whole body of water. The additional spatial evaporation information added by not having adequate fetch from the south in this study further highlights the variable rate of evaporation throughout the reservoir and why applying one evaporation value to the whole reservoir can underestimate evaporation amounts by ignoring the greater evaporation rates on the windward side, especially in an arid environment.

Currently, accurate and precise lake and reservoir estimation techniques are limited to well-funded scientific studies, constraining the knowledge of accurate evaporation to a select few locations, limiting the understanding of the evaporation phenomenon and broader application. The CFEP's yearly cost is a quarter of an energy budget or eddy covariance technique, providing a cost-effective alternative for water resource managers who are interested in a more accurate lake or reservoir evaporation estimation technique.

An interesting result from the dome validation tests was the effect of diurnal thermal expansion/contraction of the CFEP's aluminum evaporation pan and the diurnal thermal expansion/contraction of the water within the evaporation pan, where steep increases/decreases in evaporation measured by the CFEP were recorded. These thermal expansion/contraction effects on the CFEP's evaporation rate can be omitted by comparing daily midnight-to-midnight evaporation values when there is no thermal forcing applied to the CFEP.

Future research with the CFEP should focus on further analysis of wind direction associated evaporation rates via the deployment of multiple CFEPs on one lake or reservoir to help improve knowledge of this phenomenon spatially and temporally. Additionally, studies with more dome tests completed at different times of the year will further assess the accuracy and precision of the CFEP. Lastly, measuring the evaporation rate of the CFEP in the early spring, when the reservoir is absorbing heat energy, should be investigated.

Chapter 4: Collison Floating Evaporation Pan Patent

4.1 Patent

The Collison Floating Evaporation Pan was submitted for a U.S. patent in March 2016; a patent, entitled "Floating Evaporation Pan with Adjustable Freeboard and Surrounding Wave-Guard," U.S. 10,082,415 B1 (Collison, 2018), was issued on September 15, 2018 (see Figure 4.1). The CFEP patent is an improvement patent of a prior floating evaporation pan patent by Masoner and Christenson (2007), which was based on the floating evaporation pan used in the Masoner and Stannard (2010) open-water evaporation study. The CFEP patent's main improvements over the prior floating evaporation pan patent include the following: 1) a baffle system within the evaporation pan to help prevent water from sloshing out of the pan; 2) a wave guard surrounding the evaporation pan to help prevent lake or reservoir waves from entering the evaporation pan; 3) an adjustable buoyancy system that allows the freeboard of the CFEP to be adjusted; and 4) an anchoring system that prevents lateral movement of the CFEP while allowing for vertical change. These improvements allow for the CFEP to be placed in larger bodies of water where wind and/or human-induced waves are present, as the prior floating evaporation pan was designed for a body of water 9,000 m^2 where waves were minimal or nonexistent. Another improvement of the CFEP is the material from which it was constructed, 6061 aluminum alloy, which has a thermal conductivity four times greater than the stainless steel from which the prior floating evaporation pan was constructed. This greater thermal conductivity allows for the water within the evaporation pan to be more thermally coupled with the surrounding water, helping to maintain a similar water temperature within the evaporation pan to that of the surrounding water. It was noted in the Masoner and Stannard (2010) study that water temperature within their floating evaporation pan increased at a higher rate during the morning and decreased at a higher rate in the evening than the surrounding water, modifying evaporation rates. Lastly, the volume of the water within the CFEP's evaporation pan is ten times greater than the prior floating evaporation pan, providing a larger thermal mass of water within the evaporation pan, which further reduces the diurnal differences in water temperature between the evaporation pan and surrounding water. An image of the cover page of the CFEP patent is below in Figure 4.1 and the complete patent is in Appendix B: Patent.

(12) **United States Patent**
Collison

(10) **Patent No.: US 10,082,415 B1**
(45) **Date of Patent: Sep. 25, 2018**

(54) **FLOATING EVAPORATION PAN WITH ADJUSTABLE FREEBOARD AND SURROUNDING WAVE-GUARD**

(71) Applicant: **Jacob William Collison**, Albuquerque, NM (US)

(72) Inventor: **Jacob William Collison**, Albuquerque, NM (US)

(*) Notice: Subject to any disclaimer, the term of this patent is extended or adjusted under 35 U.S.C. 154(b) by 43 days.

(21) Appl. No.: **15/081,517**

(22) Filed: **Mar. 25, 2016**

(51) **Int. Cl.**
G01F 23/30 (2006.01)
G01W 1/00 (2006.01)

(52) **U.S. Cl.**
CPC ***G01F 23/303*** (2013.01); ***G01W 1/00*** (2013.01)

(58) **Field of Classification Search**
CPC G01F 23/303; G01W 1/00
USPC 73/61.41
See application file for complete search history.

(56) **References Cited**

U.S. PATENT DOCUMENTS

4,967,789 A * 11/1990 Kypris A01G 25/167 137/413
6,233,953 B1 * 5/2001 Schill F25C 1/142 62/135
7,162,923 B1 * 1/2007 Masoner .... G01W 1/00 73/290 R
8,490,566 B1 * 7/2013 Shivers, III B63B 27/30 114/230.14
2012/0079071 A1 * 4/2012 Stock B01D 1/14 110/250

OTHER PUBLICATIONS

Masoner, et al., "A Comparison of Methods for Estimating Open-Water Evaporation in Small Wetlands", Wetlands, vol. 30, 2010, 513-524.
Masoner, et al., "Differences in Evaporation Between a Floating Pan and Class A Pan on Land", Journal of the American Water Resources Association, vol. 44, No. 3, Jun. 2008, 552-561.

* cited by examiner

Primary Examiner — Son Le
Assistant Examiner — Marrit Eyassu
(74) *Attorney, Agent, or Firm* — Isaac Estrada; Peacock Law P.C.

(57) **ABSTRACT**

An improved evaporation pan assembly and measurement method comprising adjustable buoyancy floats attached to an outer wave-guard that surrounds the evaporation pan. An anchor system preferably restricts lateral movement while allowing for vertical movement with changing fluid levels. Preferably, the evaporation pan assembly further comprises a baffle system within the evaporation pan to prevent sloshing of the fluid within the pan. The height of the body of fluid being evaluated is preferably measured with a guided float assembly within the evaporation pan.

13 Claims, 2 Drawing Sheets

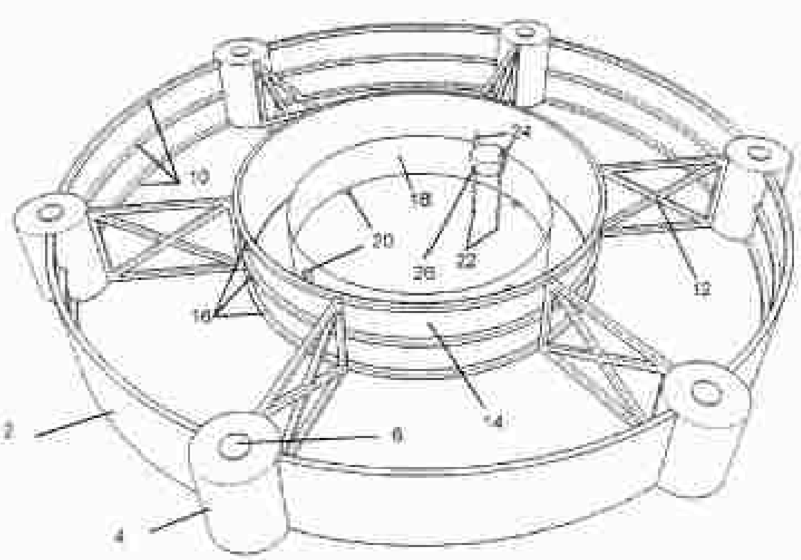

Figure 4.1: Collison Floating Evaporation Pan Patent cover page.

Chapter 5: Summary

Accurate accounting for all gains and losses in a hydrologic system will become increasingly important with anticipated climate shifts toward higher temperatures, less open water, and longer, more severe droughts (Friedrich et al., 2018; Hurd and Coonrod, 2008; Udall and Overpeck, 2017). Open-water evaporative losses are one of the largest consumptive uses of water in many arid and semi-arid areas in the world, and particularly in the Southwestern United States (Bureau of Reclamation, 2012; Friedrich et al., 2018), which is predominately measured by a technology that is inexpensive and easily applied but also known for its inaccuracies.

This study focused on developing, validating, and comparing a new technique for measuring open-water evaporation, the Collison Floating Evaporation Pan (CFEP), U.S. Patent 10,082,415 (Collison, 2018). The objectives for this study were

1. Identify the limitations and potential solutions to evaporation estimation techniques;
2. Design, deploy, and test the reliability and validity of the CFEP and evaluate uncertainties in standard evaporation estimation techniques; and
3. Patented improvements over prior evaporation estimating techniques.

The first phase of this study focused on producing a reliable evaporation measurement from the CFEP. Once a reliable evaporation measurement was established, the accuracy and precision were then tested with a hemispherical evaporation chamber (dome). Once the accuracy and precision of the CFEP was verified, the CFEP's evaporation rates were compared to an onsite Class A Pan, operated by the U.S. Army Corps of Engineers, and four evaporation estimation equations: Hargreaves-Samani, Hamon, Penman, and U.S. Weather Bureau equations.

5.1 Chapter Summaries

5.1.1 Chapter 2

Chapter 2 focused on the limitations of state-of-science and state-of-practice evaporation estimation techniques. Land-based evaporation pans like the Class A Pan, water budgets, and simple evaporation estimation equations were grouped into the state-of-practice category due to their relatively straightforward methods and widespread usage by water resource managers. Eddy covariance, Bowen ratio energy balance, remote sensing, and floating evaporation pans were grouped into the state-of-science category due to their limited usage in only well-funded scientific studies. The major limitations of state-of-practice techniques are their inaccurate estimation of evaporation due to being outside the atmospheric boundary layer (ABL) influence of a body of water and not capturing the effect of stored energy from a body of water. The major limitations of state-of-science techniques are their cost and complexity of use, greatly reducing their usage and durations of studies.

The CFEP was designed to overcome the limitations of both state-of-practice and state-of-science techniques by being affordable, accurate, and straightforward in use. Specifically, the CFEP's fully automated and robust design limits costly field visits and provides longevity, reducing year-on-year costs. The high accuracy of the CFEP is a product of the water within its evaporation pan being thermally coupled with the surrounding lake or reservoir water in addition to being within the atmospheric boundary layer influence of the lake or reservoir. Lastly, how the CFEP measures evaporation is a straightforward process: a water level decrease equals evaporation, providing real-time evaporation rates that require no postprocessing.

5.1.2 Chapter 3

The CFEP was installed on Cochiti Lake, New Mexico in late November 2017; stable and reliable evaporation measurements were established on May 13, 2018, with only two small data gaps due to logger and instrumentation failure. The CFEP measured a total of 1.127 m of evaporation over the 201-day study (May 13 through November 30), with a daily peak evaporation rate of 12.04 mm occurring on June 24 and a daily averaged evaporation rate of 5.6 mm. The results of the three dome tests showed a very close agreement in evaporation measured by the dome and the CFEP, with a percent difference error between the dome and CFEP being as follows: -6.17, 8.55, and -7.54 for September 30, October 19, and October 21, respectively. The average percent difference between the dome and CFEP was -1.72 percent, meaning the CFEP overestimated evaporation on average by 1.72 percent, well within the error rate of ± 5 percent of the dome (Reicosky and Peters, 1977; Reicosky, 1981; Reicosky et al., 1983). The CFEP's evaporation results were then compared to an on-site Class A Evaporation Pan operated by the U.S. Army Corps of Engineers, the Hargreaves-Samani (HS) equation, the Hamon equation, Penman equation, and the U.S. Weather Bureau (USWB) equation.

The evaporation results from the CFEP and the other four techniques diverged in the fall, as the heat energy stored in the reservoir contributed to higher fall evaporation rates that the Class A Pan and all four equations were unable to capture. The current standard method for determining evaporation from Cochiti Lake is the Class A Pan, which, based on the data from this CFEP study, underestimated evaporation by 1.12 MCM (910 acre-feet) during this study's duration, May 13 through November 30, 2018.

5.1.3 Chapter 4

Chapter 4 is a brief summary of the Collison Floating Evaporation Pan patent, U.S. patent number 10,082,415 B1 (Collison, 2018). The CFEP patent is an improvement patent on an existing floating evaporation pan. Specifically, the improvements to the CFEP are the outer wave guard and baffle within the evaporation pan. Both of these improvements were implemented in order to increase the reliability of evaporation measurements, a significant hindrance for prior floating evaporation pans.

5.2 Advancement in Hydrologic Sciences and Broader Impact

This study has shown that the CFEP can be a reliable, accurate, and precise evaporation estimation technique. Because the water level in the CFEP's evaporation pan is identical to the surrounding water, the CFEP can be deployed in fetch-limited locations, such as small lakes or channelized reservoirs, locations currently unavailable to other evaporation estimation techniques. The major advancement in hydrologic sciences provided by this study is the CFEP's ability to estimate spatially variable evaporation rates on lakes and reservoirs. This study showed that the windward side (shore-to-water winds) of a reservoir in an arid environment can experience at least twice the evaporation rate as the leeward side (water-to-shore winds).

Currently, a single value of estimated evaporation rates is applied to the entire lake or reservoir, potentially significantly underestimating evaporation in arid environments. Underestimating lake and reservoir evaporation amounts in water resource accounting models can lead to inaccurate allocations of water resources. These inaccuracies can lead to expensive compact delivery disputes, misuse of limited water resources, and less water available for beneficial use. As projected water supplies decrease and water demands increase, these inaccurate water allocations need to be corrected in order to make water systems more efficient.

A major efficiency improvement to water resource systems is storing water where evaporative losses are the smallest instead of storing water where it is most convenient, which is the current practice. One example of storing water where it is convenient is Elephant Butte Reservoir (EBR) in NM, USA. During periods of low available water, the vast majority of water is required to be stored in EBR per Rio Grande Compact regulations under Article VII (Rio Grande Compact, 1938). Elephant Butte Reservoir is also the location of the highest evaporation rate in the Middle Rio Grande Basin, with an annual evaporation rate of 2.86 m. Farther north in the Middle Rio Grande Basin are reservoirs capable of storing extra water, which have annual evaporation rates around 1.32 m. By storing water in these northern reservoirs, a potential annual water savings of 50-105 MCM (40-85k acre-feet) could be achieved (Pelz, 2017). Currently, in the Middle Rio Grande Basin when there is plenty of water, excess water is allowed to be stored in reservoirs with lower evaporative losses, but when water is scarce, it is stored in the location with highest evaporative losses. If this major inefficiency is corrected, a significant amount of extra water will be available for beneficial uses.

Storing water where evaporation is the lowest is the concept of conservation at the source (Friedrich et al., 2018). In order for conservation at the source methodologies to be implemented, a significant number of water laws and compacts need to be changed. The majority of these water laws and compacts were implemented in the early 1900s, when demand was less and more water was available, so efficiency was sacrificed for convenience. Additionally, the high inaccuracies of commonly used evaporation estimation techniques provide questionable evaporation rates, limiting the certainty of reducing evaporative losses by applying conservation at the source methodologies.

Water resource managers depend on accurate and reliable lake and reservoir estimated evaporation in order to properly manage water, but due to budget constraints, accuracy is sacrificed for reliability. Current state-of-science evaporation estimation techniques can cost between $150-300k + per year depending on location of deployment, instrumentation used, maintenance schedule, and data processing needs. Further, they are complicated in practice and require significant postprocessing of data in order to estimate evaporation. This significant cost, when compared to the $10-30k per year cost of operating a Class A Pan, limits the most accurate evaporation estimation techniques to well-funded and short-duration scientific studies. The cost per year of the CFEP is estimated to be $40-70k, significantly less than the state-of-science techniques, but as or more accurate. The CFEP fills the niche between inexpensive and easily applied, but inaccurate, and expensive and complicated, but accurate by being inexpensive, easily applied, and also accurate.

By filling this niche, water resource managers will have access to an affordable and accurate water estimating technique, which will greatly enhance hydrologic science and have broader impacts. Knowing accurate evaporation rates at considerably more locations will result in a better understanding of evaporation losses based on different climatological regions, geographical regions, and operations practices.

5.3 Future Research

Future research can further establish the CFEP as an accurate and reliable technique for determining open-water evaporation rates. This can be accomplished by improvements to the CFEP's design and instrumentation, and by studies at different locations and seasons.

5.3.1 Improvements to the CFEP

The CFEP can be improved via a more stable way to measure water level from within the evaporation pan. The current method, a float attached to a linear-potentiometer, has unwanted vertical oscillation during high wind events, adding uncertainty to the water-level measurements' accuracy and precision. Different water-level measurement techniques will be tested in future studies.

5.3.2 Lake Powell, Elephant Butte, and Caballo Lake Studies

There is currently a CFEP deployed on Lake Powell, USA in conjunction with the Desert Research Institute (DRI). DRI has two barges on Lake Powell, each equipped with the instrumentation necessary to compute both an energy-budget estimation of evaporation and an eddy covariance technique. The CFEP is attached to the barge in Warm Creek, Lake Powell; the project started in November 2018 and will continue through December 2021. The CFEP located on Cochiti Lake will be relocated to Elephant Butte Reservoir during the fall of 2019, and a new CFEP will be constructed for Caballo Lake (25 km south of Elephant Butte) and deployed around the same time period. These two CFEPs will be deployed for at least one year and will be compared to the eddy covariance towers operated by New Mexico State University. Over the next few years, these three different CFEPs will be validated with additional dome tests throughout the year and compared to more sophisticated evaporation estimation techniques to determine more extensively the accuracy and precision of the Collison Floating Evaporation Pan.

References

Agam, N., and Berliner, P.R., 2006, Dew formation and water vapor adsorption in semi-arid environments, a review, J. of Arid Envir. V 65, I 4, p. 572-590.

Alkaeed, O., Flores, C., Jinno, K., and Tsutsumi, A., 2006, Comparison of several reference evapotranspiration methods for Itoshima Peninsula Area, Fukuoka, Japan, Faculty of Engr. Kyushu Univ. Vol 66, No. 1, March.

Allen, R.G., Pereira, L.S., Raes, D., Smith, M., 1998, Crop evapotranspiration-guidelines for computing crop water requirements-FAO irrigation and drainage paper 56, FAO – Food and Agriculture Organization of the United Nations, Rome, Vol. 300, No. 9.

Allen, R.G., Walter, I.A., Elliott, R.L., Howell, T.A., Itenfisu, Daniel, Jensen, M.E., and Snyder, R.L., 2005, The ASCE standard reference evapotranspiration equation: American Society of Civil Engineers, Reston, Va., 216 p.

Allen, R.G., Tasumi, M., and Trezza, R., 2007, Satellite-based energy balance for mapping evapotranspiration with internalized calibration (METRIC) – model, J. Irrig. Drain Eng., 113(4):380-394.

Alvarez, V. M., Baille, A., Martínez, J. M., and González-Real, M. M., 2006, Efficiency of shading materials in reducing evaporation from free water surfaces. Agric. Water Manage., 84, 229–239, https://doi.org/10.1016/j.agwat.2006.02.006.

Baldocchi, D.D., 2003, Assessing the eddy covariance technique for evaluating carbon dioxide exchange rates of ecosystems: past, present, and future: Global Change Biology, v. 9, no. 4, p. 479–492.

Bell, S.A., Carroll, P.A., Beardmore, S.L., England, C., and Mander, N., 2017, A methodology for study of in-service drift of meteorological humidity sensors, Metrologia 54 S63.

Blanken, P.D., Rouse, W.R., Culf, A.D., Spence, C., Boudreau, L.D., Jasper, J.N., Kochtubajda, B., Schertzer, W.M., Marsh, P., and Verseghy, D., 2000, Eddy covariance measurements of evaporation from Great Slave Lake, Northwest Territories, Canada: Water Resources Research, v. 36, no. 4, p. 1,069–1,077.

Bird, B.R., Stewart, W.E., and Lightfoot, E.N., 2007, Transport Phenomena, 2nd ed. John Wiley and Sons Inc. 928pg.

Bowen, I.S., 1926, The ratio of heat losses by conduction and by evaporation from any water surface: Physics Review, v. 27, p. 779–787.

Brower, A.L, 2018, ET tool box, evapotranspiration toolbox for the Middle Rio Grande, a water resources decision support tool, version 4.0, online access January 2019: https://www.usbr.gov/uc/albuq/water/ETtoolbox/ettoolbox.pdf.

Brutsaert, W.H., 1982, Evaporation into the atmosphere: Boston, Mass., D. Reidel Publishing, 299 p.

Brutsaert, W., Sugita, M., 1992, Application of self-preservation in the diurnal evolution of the surface energy budget to determine daily evaporation, Journal of Geophysical Research Atmospheres 97(D17).

Bureau of Reclamation, September 2012, Colorado River Basin, Consumptive Uses and Losses Report 2001-2005, Revised.

Bureau of Reclamation, December 2012, Colorado river basin water supply and demand study, executive summary.

Chapman, Andrew, 2016, Types of drones: multi-rotor vs fixed-wing vs single rotor vs hybrid VTOL, DRONE magazine, issue 3, June.

Chu, C.R., Li, M.H., Chang, Y.F., Liu, T.C., and Chen, Y.Y., 2012, Wind-induced splash in Class A evaporation pan. J. Geophys. Res., 117, D11101, https://doi.org/10.1029/2012JB009146.

Cleugh, H.A., Leuning, R., Mu, Q., Running, S.W., 2006, Regional evaporation estimates from flux tower and MODIS satellite data, Remote Sensing of Environment, 106, 285-304.

Collison, J. W., 2018, Floating evaporation pan with adjustable freeboard and surrounding wave-guard. U.S. Patent 10,082,415 September 25, 2018.

Crilley, D.M., and Collison, J.W., 2015, A water-budget approach to estimating potential groundwater recharge from two domestic sewage disposal fields in eastern Bernalillo County, New Mexico, 2011–12: U.S. Geological Survey Scientific Investigations Report 2015–5060, 32 p., http://dx.doi.org/10.3133/sir20155060.

Dalton, J., 1802, Experimental essays on the constitution of mixed gases; on the force of steam or vapour from water and other liquids in different temperatures, both in a Torricellian vacuum and in air; on evaporation and on the expansion of gases by heat, Mem. Proc. Manchester Lit. Phil. Soc., 5, 535-602.

Davis, J. R., 2001, Alloying: understanding the basics, ASM International, p 351-416, DOI:10.1361/autb2001p351

Doorenbos, J., Pruitt, W.O., 1977, Food and Agriculture Organization Irrigation and Drainage Paper, Guidelines for predicting crop water requirements, Rome.

DRI, 2019, Western regional climate center, Evaporation Station, accessed Feb. 2019, https://wrcc.dri.edu/Climate/comp_table_show.php?stype=pan_evap_avg

Duan, Zheng, 2014, Estimating water balance components of lakes and reservoirs using various open access satellite databases, Delft University of Technology

Ebaid, H.M.I., Ismail, S.S., 2010, Lake Nasser evaporation reduction study, Journal of Advanced Research, 1, 315-322.

Eichinger, W.E., Nichols, J., Prueger, J.H., Hipps, L.E., Neale, C.M.U., Cooper, D.I., and Bawazir, A.S., 2003, Lake evaporation estimation in arid environments, IIHR Report No. 430, July 2003.

Elsawwaf, M., Willems, P., Pagano, A., and Berlamont, J., 2010, Evaporation estimates from Nasser Lake, Egypt, based on three floating station data and Bowen ratio energy budget, Theor. Appl. Climatol. 100:439-465.

Famsworth, R.K., Thompson, E.S., and Peck, E.L., 1982, Evaporation atlas for the contiguous 48 United States: NOAA Technical Report NWS 33.

Federal Energy Management Program, 2017, Water and wastewater annual price escalation rates for selected cities across the Unites States, U.S. Dept. of Energy, Office of Energy Efficiency & Renewable Energy, September.

Fick, A., 1855, Poggendorff's Annalen, Phil. Mag. S.4, Vol. 10, 30-39, 59-86 (in English).

Foken, Thomas, 2008, Micrometeorology: Berlin-Heidelberg, Springer, 306 p.

Follansbee, Robert, 1934, Evaporation from reservoir surfaces. In Transactions, Vol. 99, pp. 704-715. American Society of Civil Engineers, New York, NY.

Friedrich, K., Grossman, R.L., Huntington, J., Blanken, P.D., Lenters, J., Holman, K.D., Gochis, D., Livneh, B., Prairie, J., Skeie, E., Healey, N.C., Dahm, K., Pearson, C., Finnessey, T., Hook, S.J., and Kowalski, T., 2018, Reservoir evaporation in the western United States, current science, challenges, and future needs, American Meteor. Society Jan. 2018 pg. 167-187.

Garcia, C.A., Johnson, M.J., Andraski, B.J., Halford, K.J., and Mayers, C.J., 2008, Portable chamber measurements of evapotranspiration at the Amargosa Desert Research Site near Beatty, Nye County, Nevada, 2003–06: U.S. Geological Survey Scientific Investigations Report 2008–5135, 10 p.

Gianniou, S.K., and Antonopoulos, V.Z., 2007, Evaporation and energy budget in Lake Vegoritis, Greece, J. of Hydrology, 345, 212-223.

Grantz, K., Rajagopalan, B., Clark, M., and Zagona, E., 2007, Seasonal shifts in the North American monsoon, Amer. Met. Soc. Journal of Climate, V20, 1923-1935.

Grayson, R.B., Argent, R., Nathan, R.J., McMahon, T.A., and Mein, R.G., 1996, Hydrological recipes: estimation techniques in Australian hydrology. Cooperative Research Centre for Catchment Hydrology, 125 pp.

Greenwood, E.A.N., and Beresford, J.D., 1979, Evaporation from vegetation in landscapes developing secondary salinity using the ventilated chamber technique—I. Comparative transpiration from juvenile Eucalyptus above saline ground-water seeps: Journal of Hydrology 42, p. 369-382.

Hales, L.Z., 1981, Floating breakwaters: state-of-the-art literature review, U.S. Army, Corps of Engineers, Coastal Engineering Research Center. Technical Report No. 81-1.

Hamon, W.R., 1961, Estimating potential evapotranspiration, Journal of the Hydraulics Division, ASCE. 87 (HY3):107-120.

Harbeck, G.E., 1962, A practical field technique for measuring reservoir evaporation utilizing mass-transfer theory, U.S. Geol. Surv. Prof. Pap., 272-E, 101–105.

Hargreaves, G.H., 1975, Moisture availability and crop production, Trans. Am. Soc. Agric. Eng. 18(5):980-984.

Hargreaves, G.H., and Allen, R.G., 2003, History and evaluation of Hargreaves evapotranspiration equation, J. Irrig. Drain Engr, 129(1): 53-63.

Hargreaves, G.H., and Samani, Z.A., 1985. Reference crop evapotranspiration from temperature. Appl. Eng. Agric. 1(2), 96–99.

Harwell, G.R., 2012, Estimation of evaporation from open water—A review of selected studies, summary of U.S. Army Corps of Engineers data collection and methods, and evaluation of two methods for estimation of evaporation from five reservoirs in Texas: U.S. Geological Survey Scientific Investigations Report 2012–5202, 96 p.

Hassan, M., 2013, Evaporation estimation for Lake Nasser based on remote sensing technology. Ain Shams engineering journal, 4, 593-604.

Herting, A., Farmer, T., Evans, J., 2004, Mapping of the evaporative loss from Elephant Butte Reservoir using remote sensing and GIS technology.

Horst, T.W., and Weil, J.C., 1994, How far is far enough?: The fetch requirements for micrometeorological measurement of surface fluxes, Journal of Atmospheric and Oceanic Technology, Vol. 11, page 1018-1025

Hounam, C.E., 1973, Comparison between pan and lake evaporation, World Meteorological Organization, Technical Note No. 126, 52p.

Huntjens, P., Pahl-Wostl, C., Rihoux, B., Schlüter, M., Flachner, Z., Neto, S., Koskova, R., Dickens, C., 2011, Adaptive water management and policy learning in a changing climate: a formal comparative analysis of eight water management regimes in Europe, Africa, and Asia, Env. Pol. And Gov. 21, 145-163.

Hurd, B.H. and Coonrod, J., 2008. Climate change risks New Mexico's waterways: its byways and its flyways. Water Resources IMPACT 10(4).

Irmak, S., Irmak, A., Allen, R.G., and Jones, J. W. 2003, Solar and net radiation-based equations to estimate reference evapotranspiration in humid climates. Journal of Irrigation and Drainage Engineering. ASCE. 129(5):336-347.

Jensen, Marvin E., 2010, Estimating evaporation from water surfaces, CSU/ARS Evapotranspiration Workshop, Fort Collins, CO, March 15.

Johnson, H.D., Brown, E.G., and Robie, R.B., 1979, Evaporation from water surfaces in California. State of California Department of Water Resources, Bulletin 73-79.

Jovanovic, B., Jones, D.A., and Collins, D., 2008, A high-quality monthly pan evaporation dataset for Australia, Climatic Change, 87:517-535.

Kaimal, J.C., and Finnigan, J.J., 1994, Atmospheric boundary layer flows, their structure and measurement: New York, Oxford University Press, 289 p.

Kamath A., Chella, M. A., Bihs, H., and Arntsen, A.O., 2015 Evaluating wave forces on groups of three and nine cylinders using a 3D numerical wave tank, Engineering Applications of Computational Fluid Mechanics, 9:1, 343-354.

Klink, M., 2006, Evaporation estimation using a floating pan, Clemson University Masters Theses, Paper 40.

Koch, W., Lange, O. L., and Schulze, E.D., 1971, Ecophysiological investigations on wild and cultivated plants in the Negev Desert—I. Methods; A mobile laboratory for measuring carbon dioxide and water vapor exchange: Oecologia 8, p. 296-309.

Koh, L.P., and Wich, S.A., 2012, Dawn of drone ecology: low-cost autonomous aerial vehicles for conservation, Trop. Conserv. Sci. Vol 5 (2): 121:132

Kohler, M.A., 1954, Lake and pan evaporation, pp. 127-148, In: Water-Loss Investigations: Lake Hefner Studies, Tech. Rep., Geological Survey Prof. Paper 269, 170 pp.

Kohler, M.A., Nordenson, T.J., and Fox, W.E., 1955, Evaporation from pans and lakes: U.S. Weather Bureau Research Paper 38, 82 p.

Kormann, R., and Meixner, F., 2001, An analytical footprint model for non-neutral stratification: Boundary-Layer Meteorology, v. 99, no. 2, p. 207–224.

Kumambala, P.G., and Ervine, A., 2010, Water balance model of Lake Malawi and its sensitivity to cimate change. Open Hydrology Journal.

Lee, T.M., and Swancar, A., 1997, Influence of evaporation, ground water, and uncertainty in the hydrologic budget of Lake Lucerne, a seepage lake in Polk County, Florida. Water-Supply: Paper 2439, US Geological Survey.

Lenters, J.D., Kratz, T.K., and Bowser, C.J., 2005, Effects of climate variability on lake evaporation: results from a long-term energy budget study of Sparkling Lake, northern Wisconsin (USA). J Hydrol 308:168–195

Lenters, J. D., Anderton, J.B., Blanken , P., Spence, C., and Suyker, A.E., 2013, Assessing the impacts of climate variability and change on Great Lakes evaporation. In: 2011 Project Reports. D. Brown, D. Bidwell, and L. Briley, eds. Available from the Great Lakes Integrated Sciences and Assessments (GLISA) Center:

Liu, Z., and Higgins, C.W., 2015, Does temperature affect the accuracy of vented pressure transducer in fine-scale water level measurements?, Geosci. Instrum. Method. Data Syst., 4, 65-73.

Lowe, L., Webb, J.A., Nathan, R.J., Etchells, T., and Malano, H.M., 2009, Evaporation from water supply reservoirs: An assessment of uncertainty. J. Hydrol., 376, 261–274, https://doi.org/10.1016/j.jhydrol.2009.07.037.

Majidi, M., Alizadeh, A., Farid, A., Vazifedoust, M., 2015, Estimating evaporation from lakes and reservoirs under limited data condition in a semi-arid region, Water Resources Manage, 29:3711-3733.

Masoner, J.R., and Christenson, S.C., 2007, Adjustable floating open-water evaporation pan, U.S. Patent 7,162,923 B1, January 16, 2007.

Masoner, J.R., and Stannard, D.I., 2010, A comparison of methods for estimating open-water evaporation in small wetlands. Society of Wetland Science, 30:513-524.

Mauder, M. and Foken, T., 2006, Impact of post-field data processing on eddy covariance flux estimated and energy balance closure, Met. Zeitschrift, Vol 15, No. 6, 597-609

Monteith, J.L., 1965, Evaporation and the environment, in The State and Movement of Water in Living Organisms, edited by G.E. Fogg, pp. 205-234, Cambridge Univ. Press, London.

Moreo, M.T., and Swancar, A., 2013, Evaporation from Lake Mead, Nevada and Arizona, March 2010 through February 2012: U.S. Geological Survey Scientific Investigations Report 2013–5229, 40 p

Morton, F.I., 1979, Climatological estimates of lake evaporation. Water Resources Research, 15:64-76.

Murray, F.W., 1967, On the computation of saturation vapor pressure, J. Appl. Meteorol., 6:203-204.

Myers, Tom, 2013, Loss rates from Lake Powell and their impacts on management of the Colorado River, JAWRA 1-2, DOI: 10.1111/jawr.12081

National Inventory of Dams, Washington DC, U.S. Army Corps of Engineers, Federal Emergency management Agency, http://nid.usace.army.mil, accessed January 2019.

Özgür, E., and Koçak, K., 2015, The effects of atmospheric pressure on evaporation, Acta Geobalcanica, Vol 1, 17-24.

Papadopulos, S.S. and Associates, 2000, Middle Rio Grande water supply study, Boulder, Colorado.

Pahl-Wostl, C., 2007, Transitions towards adaptive management of water facing climate and global change. Water Resour. Manage. 21:49-62.

Pelz, Jen, 2017, The Rio Grande, rethinking rivers in the 21st century, WildEarth Guardians, Santa Fe, NM.

Penman, H.L., 1948, Natural evaporation from open water, bare soil, and grass, Proc. R. Soc., London, Vol A193:120-145.

Penman, H.L., 1963, Vegetation and hydrology, Tech. Comm. 53. Commonwealth Bureau of Soils, Harpenden, England.

Peterson, K., Hanson, A., Roach, J., Randall, J., Thomson, B., 2019, A dynamic statewide water budget for New Mexico: phase III-Future scenario implementation, NM WRRI Technical Completion Report No. 380

Piper, B.S., Plinston, D.T., & Sutcliffe, J.V., 1986, The water balance of Lake Victoria. Hydrological Sciences Journal, 31, 25-37

Priestly, C.H.B., and Taylor, R.J., 1972, On the assessment of surface heat flux and evaporation using large-scale parameters, Monthly Weather Review, 100:81-82.

Puckridge, D.W., 1978, A comparison of evapotranspiration measurements of crop communities using lysimeters and assimilation chambers: Australian Journal of Soil Research 16, p. 229-236.

Rayner, D.P. 2005, Australian synthetic daily Class A pan evaporation. Queensland Department of Natural Resources and Mines.

Reicosky, D.C., 1981, A research tool for evapotranspiration measurements for model validation and irrigation scheduling: Proceedings, American Society of Agricultural Engineers, Irrigation Scheduling Conference, Chicago, p. 74-80.

Reicosky, D.C., and Peters, D.B., 1977, A portable chamber for rapid evapotranspiration measurements on field plots: Agronomy Journal 69, p. 729-732.

Reicosky, D.C., Sharratt, B.S., Ljungkull, J.E., and Baker, D.G., 1983, Comparison of alfalfa evapotranspiration measured by a weighing lysimeter and a portable chamber: Agricultural Meteorology 28, p. 205-211.

Rientjes, T.H.M., Perera, B.U.J., Haile, A.T., 2011, Regionalization for lake level simulation - the case of Lake Tana in the Upper Blue Nile, Ethiopia. Hydrology and Earth System Sciences, 15, 1167-1183.

Rio Grande Compact, 1938, Rio Grande Compact Commission Report, https://www.usbr.gov/uc/albuq/water/RioGrande/pdf/Rio_Grande_Compact.pdf, accessed January, 2019.

Rosenberry, D.O., Stannard, D.I., Winter, T.C., and Martinez, M.L., 2004, Comparison of 13 equations for determining evapotranspiration from a prairie wetland, Cottonwood Lake area, North Dakota, USA: Wetlands, v. 24, no. 3, p. 483–497.

Rosenberry, D.O., Winter, T.C., Buso, D.C., and Liken, G.E., 2007, Comparison of 15 evaporation methods applied to a small mountain lake in the northeastern USA, Journal of Hydrology, 340, 149-166.

Russell, J.M., & Johnson, T.C., 2006, The water balance and stable isotope hydrology of Lake Edward, Uganda-Congo. Journal of Great Lakes Research, 32, 77-90

Samani, Z., 2019, Estimating solar radiation and evapotranspiration using minimum climatological data (Hargreaves-Samani equation), Assoc. Prof. Civil Engr. Dept. New Mexico State University, online only, accessed January 19, 2019, http://www.zohrabsamani.com/research_material/files/Hargreaves-samani.pdf

Saugier, B., 1976, Sunflower. In J.L. Montieth (ed.) vegetation and the Atmosphere, v. 2: London, Academic Press, p. 87-118.

Savoca, M.E., Senay, G.B., Maupin, M.A., Kenny, J.F., and Perry, C.A., 2013, Actual evapotranspiration modeling using the operational Simplified Surface Energy Balance (SSEBop) approach: U.S. Geological Survey Scientific Investigations Report 2013-5126, 16 p., http://pubs.usgs.gov/sir/2013/5126.

Senay, G.B.; Bohms, S., Singh, R.K., Gowda, P.H., Velpuri, N.M., Alemu, H., and Verdin, J.P., 2013, Operational evapotranspiration mapping using remote sensing and weather datasets: a new parameterization for the SSEB approach. USGS Staff -- Published Research. Paper 739.

Sene, K.J., 2000, Theoretical estimates for the influence of Lake Victoria on flows in the upper White Nile. Hydrological Sciences Journal, 45, 125-145

Setegn, S.G., Chowdary, V.M., and Mal, B.C., 2011, Water balance study and irrigation strategies for sustainable management of a tropical Ethiopian lake: A Case Study of Lake Alemaya. Water Resources Management, 25, 2081-2107

Sharma, M.L., 1985, Estimating Evapotranspiration, in Advances in Irrigation: Wembley, Australia, Academic Press, v. 3, p. 213-281.

Sivapragasam, C., Vasudevan, G., Maran, J., Bose, C., Kaza, S., and Ganesh, N., 2009, Modeling evaporation-seepage losses for reservoir water balance in semi-arid regions, Water Res. Manage. 23:853-867.

Stannard, D.I., 1988, Use of a hemispherical chamber for measurement of evapotranspiration: U.S. Geological Survey Open-File Report 88–452, 18 p.

Stannard, D.I., Gannett, M.W., Polette, D.J., Cameron, J.M., Waibel, S., and Spears, J.M., 2013, Evapotranspiration from wetland and open-water sites at Upper Klamath Lake, Oregon, 2008-2010: U.S Geological Survey Scientific Investigations Report 2013-5014, 65 p., http://pubs.er.usgs.gov/publication/sir20135014.

Stewart, R. W., 1979, The atmospheric boundary layer, Third IMO Lecture, World Meteor. Org. No. 523

Tanny, J., Cohen, S., Assouline, S., Lange, F., Grava, A., Berger, D., Teltch, B., and Parlange, M. B., 2008, Evaporation from a small water reservoir: Direct measurements and estimates. J. Hydrol., 351, 218–229, https://doi.org/10.1016/j.jhydrol.2007.12.012.

Trask, J. C., 2007, Resolving hydrologic water balances through novel error analysis, with focus on inter-annual and long-term variability in the Tahoe Basin. Ph.D. dissertation, University of California, Davis, 378 pp.

Troen, I.B., and Mahrt, L., 1986, A simple model of the atmospheric boundary layer; sensitivity to surface evaporation, Boundary-layer Met. 37, 129-148.

Turnipseed, D.P., and Sauer, V.B., 2010, Discharge measurements at gaging stations: U.S. Geological Survey Techniques and Methods book 3, chap. A8, 87 p.

Udall, B. and Overpeck, J., 2017, The twenty-first century Colorado River hot drought and implications for the future, Water Resour. Res., 53, 2404– 2418, doi:10.1002/2016WR019638.

U.S. Environmental Protection Agency (USEPA), 2009, National lakes assessment: a collaborative survey of the nation’s lakes. EPA 841-R-09-001. U.S. Environmental Protection Agency, Office of Water and Office of Research and Development, Washington, D.C.

Velpuri, N.M., Senay, G.B., and Asante, K.O., 2012, A multi-source satellite data approach for modelling Lake Turkana water level: calibration and validation using satellite altimetry data. Hydrology and Earth System Sciences, 16, 1-18

Winter, T.C., 1981, Uncertainties in estimating the water balance of lakes: Water Resources Bulletin, v. 17, no. 1, p. 82–115.

Winter, T.C., Rosenberry, D.O., and Sturrock, A.M., 1995, Evaluation of 11 equations for determining evaporation from a small lake in the north central United States, Water Res. Research, Vol 31, No. 4, p. 983-993, April.

Winter, T.C., Buso, D.C., Rosenberry, D.O., Likens, G.E., Sturrock, A.M., and Mau, D.P., 2003, Evaporation determined by the energy-budget method for Mirror Lake, New Hampshire. Limnol Oceanogr 48(3):995–1009

Wurbs, R.A, and Ayala, R.A., 2014, Reservoir evaporation in Texas, USA, J. Hydrol., 510, 1-9.

Young, H.D., and Sears, F.W., 1992, University Physics, 8th ed, Addison-Wesley Pub. Co. 1132p

Appendix A: Evaporation Pan History

Prior to the 1934 American Society of Civil Engineers symposium on "Evaporation from Water Surfaces," an assortment of evaporation estimation methods was in use. These methods varied in size, shape, and location, which hampered efforts to compare evaporation rates from multiple reservoirs and lakes. This symposium was tasked with determining a standardized method for measuring evaporation. Three main types of pans were compared: the Class A Pan, the Colorado Sunken Pan, and the USGS floating pan. The Colorado Sunken Pan was shown to be more accurate than the Class A Pan, but the reliability of the evaporation measurements was questionable because of debris being blown into the pan due to the top of the pan being level with the ground surface. The USGS floating pan was shown to be the most accurate way to measure evaporation, but the reliability of data due to loss or addition of water to the pan during high wave activity could not be accounted for. Additionally, the difficulty of daily access (having to boat out to the USGS floating pan) resulted in gaps in the record, reducing the reliability of records. This symposium determined that Class A Pans should be the standard method because of the ease of access, low cost of instillation, reliability of data, and expansive records, even though it was the least accurate method investigated (Follansbee, 1934).

The Class A Pan consists of a 22-gauge galvanized iron pan, typically 1.22 meters in diameter and 0.254 meters deep, on a wood base 0.152 meters above the ground. The Colorado Sunken Pan is a 0.914 meters square, 18-gauge galvanized iron pan between 0.457 and 0.914 meters deep with all but the top 50-152 mm of the pan above the surface of the ground, where the water level within the pan is level with the surrounding ground. For both the Class A Pan and Colorado Sunken Pan, water levels are typically measured once each day in the morning and filled once a week. By filling the pan once a week, the thermal mass associated with the water in the pan decreases through the week, allowing the water to be more susceptible to diurnal temperature changes later in the week, affecting evaporation rates.

Lastly, the USGS Floating Evaporation Pan is a 0.914 meters square and 0.457 meters deep pan made from 18-gauge galvanized iron surrounded by a raft supported by floatation barrels with all but the top 76 mm of the pan above the water level, where the water level within the pan is level with the surrounding water. Measurements from the USGS Floating Evaporation Pan are completed by counting the number of calibrated cups (each cup adds 0.254 mm to the pan) in order to bring the water level within the pan to a set level. Additionally, during a rain event over a floating pan, the water that splashes in and the water that splashes out of the pan are considered to be equal to each other and, thus, cancel each other out whereas water can only splash out of a land-based pan indicating an evaporation loss. Due to the location of the USGS Floating Evaporation Pan, the middle of a reservoir, daily measurements were more difficult to obtain and often resulted in missed measurements (Follansbee, 1934).

The reliability limitations of each of the aforementioned pans was the deciding factor for the 1934 ASCE Symposium's decision to recommend the Class A Pan as the standard. The Colorado Sunken Pan had reliability issues related to debris blowing into the pan and the USGS Floating Evaporation Pan had the problem of not being able to account for waves over topping the pan or water splashing out of the pan (Follansbee, 1934). Thus, the Class A Pan was chosen despite its own shortcomings.

One such shortcoming with the Class A Pan relates to the fact that the heat capacity of land-based pans varies substantially from lakes and reservoirs. The available energy within a land-based pan for evaporation is susceptible to diurnal variations in weather whereas in larger bodies of water, the available energy for evaporation changes on a seasonal basis. This difference in heat capacity further decreases the ability of land-based pans to estimate lake or reservoir evaporation accurately on a daily basis. In order to overcome this limitation of evaporation from land-based pans, a pan coefficient needs to be applied. Typically, a pan coefficient around .70 is used for annual estimation (Follansbee, 1934; Kohler, 1954). Kohler (1954) reported that the use of a 0.70 pan coefficient on annual evaporation rates should be within 10 to 15 percent of actual evaporation of the body of water of interest.

The most common technique for estimating lake and reservoir evaporation in the U.S. is the Class A Pan. The U.S. is not alone in using the Class A Pan as its main source of lake and reservoir evaporation estimation; the Food and Agriculture Organization of the United Nations recommends a Class A Pan when data is not sufficient to use the Penman-Monteith equation (Allen et al., 1998; Doorenbos and Pruitt, 1977; Monteith, 1965). Additionally, Australia has used the Class A Pan as its standard since the 1910s and has produced a method that creates synthetic daily Class A Pan evaporation data, based on many years and locations of Class A Pan data, in order to estimate areas lacking Class A Pan data (Rayner, 2005). Clearly, Class A Pan's are still widely used and are the accepted, standard technique for measuring estimated evaporation rates. However, issues with accuracy still remain, which is a severely limiting factor to its continued use as the climate only becomes drier and hotter. As the climate shifts towards hotter and drier conditions in the Southwestern U.S. (Friedrich et al., 2018; Udall and Overpeck, 2017), conditions in which Class A Pans tend to greatly overestimate evaporation (Eichinger et al., 2003; Jovanovic et al., 2008), a replacement technique for estimating evaporation is needed.

Appendix B: Collison Floating Evaporation Pan Patent

US010082415B1

(12) **United States Patent**
Collison

(10) **Patent No.:** **US 10,082,415 B1**
(45) **Date of Patent:** **Sep. 25, 2018**

(54) **FLOATING EVAPORATION PAN WITH ADJUSTABLE FREEBOARD AND SURROUNDING WAVE-GUARD**

(71) Applicant: **Jacob William Collison**, Albuquerque, NM (US)

(72) Inventor: **Jacob William Collison**, Albuquerque, NM (US)

(*) Notice: Subject to any disclaimer, the term of this patent is extended or adjusted under 35 U.S.C. 154(b) by 43 days.

(21) Appl. No.: **15/081,517**

(22) Filed: **Mar. 25, 2016**

(51) **Int. Cl.**
G01F 23/30 (2006.01)
G01W 1/00 (2006.01)

(52) **U.S. Cl.**
CPC ***G01F 23/303*** (2013.01); ***G01W 1/00*** (2013.01)

(58) **Field of Classification Search**
CPC G01F 23/303; G01W 1/00
USPC 73/61.41
See application file for complete search history.

(56) **References Cited**

U.S. PATENT DOCUMENTS

4,967,589 A * 11/1990 Kypris A01G 25/167 137/413
6,233,953 B1 * 5/2001 Schill F25C 1/142 62/135
7,162,923 B1 * 1/2007 Masoner .... G01W 1/00 73/290 R
8,490,566 B1 * 7/2013 Shivers, III B63B 27/30 114/230.14
2012/0079971 A1 * 4/2012 Stock B01D 1/14 110/250

OTHER PUBLICATIONS

Masoner, et al., "A Comparison of Methods for Estimating Open-Water Evaporation in Small Wetlands", Wetlands, vol. 30, 2010, 513-524.
Masoner, et al., "Differences in Evaporation Between a Floating Pan and Class A Pan on Land", Journal of the American Water Resources Association, vol. 44, No. 3, Jun. 2008, 552-561.

* cited by examiner

Primary Examiner — Son Le
Assistant Examiner — Marrit Eyassu
(74) *Attorney, Agent, or Firm* — Isaac Estrada; Peacock Law P.C.

(57) **ABSTRACT**

An improved evaporation pan assembly and measurement method comprising adjustable buoyancy floats attached to an outer wave-guard that surrounds the evaporation pan. An anchor system preferably restricts lateral movement while allowing for vertical movement with changing fluid levels. Preferably, the evaporation pan assembly further comprises a baffle system within the evaporation pan to prevent sloshing of the fluid within the pan. The height of the body of fluid being evaluated is preferably measured with a guided float assembly within the evaporation pan.

13 Claims, 2 Drawing Sheets

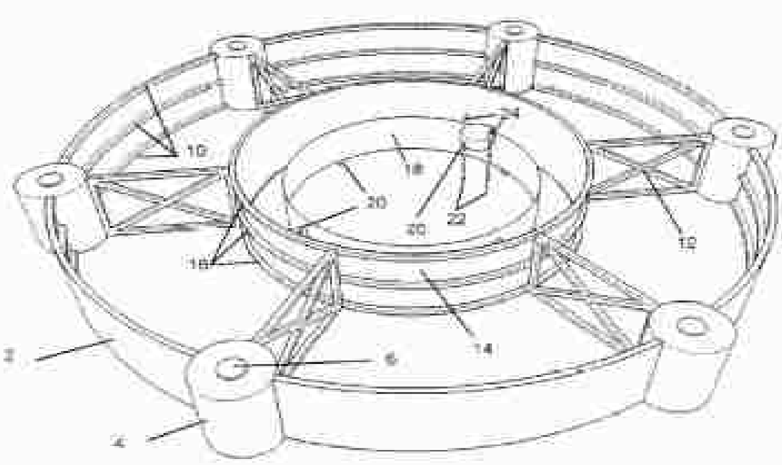

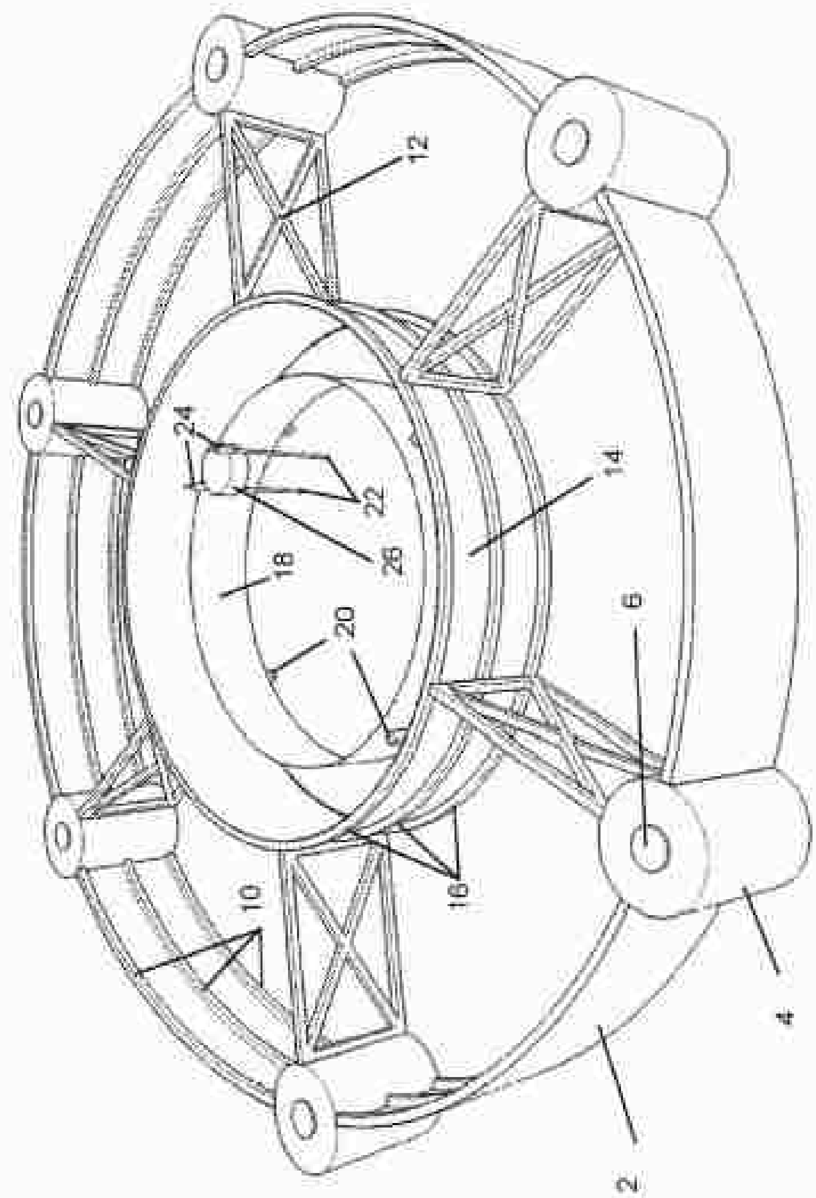

FIG. 1

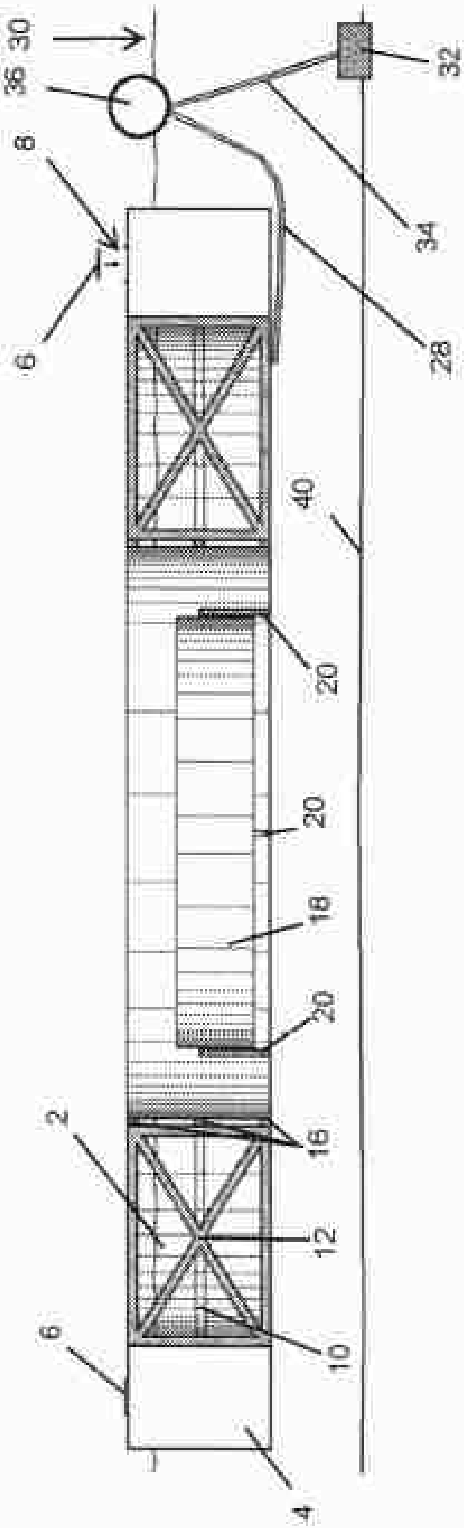

FIG. 2

FLOATING EVAPORATION PAN WITH ADJUSTABLE FREEBOARD AND SURROUNDING WAVE-GUARD

STATEMENT REGARDING FEDERALLY SPONSORED RESEARCH OR DEVELOPMENT

Not Applicable

BACKGROUND OF THE INVENTION

Field of the Invention (Technical Field)

Embodiments of the present invention relate in general to methods and apparatuses for measuring evaporation rates for a fluid within a body of fluid, and more particularly to methods and apparatuses that carry out such measurement through a floating evaporation pan within the larger body of the fluid of interest.

Description of Related Art

Knowing the amount of evaporation from a body of fluid is critical for its proper management. Typically, the largest unknown in the management of large bodies of fluid (e.g., lakes and reservoirs) is the amount of fluid lost to evaporation. There are many methods of measuring the evaporation rate, each with its own advantages and disadvantages, with the most common method being a land-based evaporation pan. Under normal operation conditions, a land-based evaporation pan is situated near a large body of fluid, elevated above the ground on a wooden platform, and the fluid-level within the pan is measured periodically to determine the evaporation rate.

There are several problems associated with obtaining accurate evaporation rates using a land-based evaporation pan. Due to the pan being placed on land, the fluid temperature within the pan could be far greater than the fluid temperature in the larger fluid body being evaluated, causing evaporation to be overestimated. The higher evaporation rates within a land-based pan are due in part to the increased advection of heat energy through the metal, sun-exposed sides of the land-based pan, which increases the temperature of the fluid in the land-based pan. Additionally, the land-based pan has a substantially smaller boundary layer than a large fluid body (e.g., a reservoir or lake) that is in the range of tens of centimeters for the land-based pan compared to hundreds of meters for the large fluid body. Since both boundary layers go from saturation vapor pressure at the surface of the fluid to ambient vapor pressure at the top of the boundary layer, the land-based pan has a much steeper vapor pressure gradient within that layer, resulting in greater evaporation from the land-based pan.

There is a known method developed to overcome the problems with evaporation measurement with land-based pans in which an adjustable floating open-water evaporation pan is used. The pan floats in the body of fluid being measured. By putting the pan in the body of fluid being measured, the increased advection of energy through the sides of the pan is greatly reduced and the atmospheric boundary conditions in the evaporation pan closely resemble that of the surrounding fluid body. This floating evaporation pan works well in environments where there is only minor wave action, such as wetlands, small ponds, and/or lagoons. Wave action can have two major adverse impacts on the height of the fluid within the pan: 1) wind or human generated waves can overtop the side of the evaporation pan adding fluid to the pan; and, 2) wind or human generated wave action can cause a sloshing disturbance within the pan where fluid within the pan can overtop into the surrounding body of fluid. In both cases, the measurement of evaporation within the pan is now invalid for the time period where fluid was added or removed, reducing the reliability of the floating evaporation pan.

There is a long felt need for apparatuses and methods to obtain more accurate and reliable evaporation rate readings in large, open bodies of fluids where there is wind or human generated wave action. Embodiments of the present invention solve this problem by providing methods and apparatuses that more accurately measure evaporation rate.

BRIEF SUMMARY OF THE INVENTION

Embodiments of the present invention comprise a floating evaporation pan that has adjustable buoyancy floats attached to an outer wave-guard surrounding the evaporation pan. In one embodiment, in addition to the surrounding wave-guard, there is a full-circumference splash guard attached to the outer-top of the evaporation pan. Furthermore, within the pan there preferably is a baffle system that reduces fluid sloshing. Lastly, the freeboard (the distance from the surface of the fluid to the top of the apparatus) of the pan can be adjusted with the adjustable buoyancy floats so that the fluid level within the pan can be slightly lower than the fluid level of the surrounding body. The addition of the outer wave-guard surrounding the evaporation pan, a full-circumference splash guard, the baffle system within the evaporation pan, and the fluid level within the pan being lower than the surrounding fluid enhance the accuracy and reliability of evaporation measurements for the embodiments of the present invention.

Accordingly, it is the objective of the present invention to provide an improved evaporation pan assembly that allows for more accurate and reliable evaporation rate calculations than current land-based or floating evaporation pans.

The embodiments of the present invention meet the objective for more accurate and reliable evaporation rate measurements in large, open bodies of fluid with the incorporation of techniques and methods that greatly reduce the disturbance of evaporation measurements from wave action. There preferably is a wave-guard equally spaced between the buoyancy floats, which deflects the energy of waves away from the floating evaporation pan. The wave-guard and buoyancy floats preferably surround the evaporation pan at equal distances and provide an area of calm fluid adjacent to the evaporation pan. By allowing for this area of calm fluid between the wave-guard and the pan, the overall width of the apparatus is increased, reducing the rocking motion of the invention. The reduction of rocking motion of the apparatus further prevents fluid from being added or removed from within the evaporation pan. The baffle system within the evaporation pan dampens sloshing created by the rocking of the apparatus. Preferably surrounding the evaporation pan is a structural brace that preferably serves as an exterior splash guard. An anchoring system is preferably also present to prevent rotation and movement of the apparatus in a large body of fluid. This anchoring system preferably prevents the lateral movement of the apparatus while allowing for vertical movement to accommodate for changing fluid elevation of the larger body of fluid. The fluid level within the evaporation pan is preferably maintained slightly lower than that of the surrounding body of fluid by use of a pump that is controlled by a guided-float within the evaporation pan. The sun-exposed sides of the evaporation pan preferably absorb energy from the sun, heating up the sides. This increased energy is preferably dissipated into the surrounding fluid body before it is dissipated to the fluid within the evaporation pan due to the slightly higher body of fluid level surrounding the evaporation pan. The freeboard of the wave-guard is preferably controlled with the adjustable buoyancy floats through the addition of weight (fluid, sand, gravel, etc.) to the buoyancy floats. Once the proper freeboard is established for the apparatus, the remaining hollow in the buoyancy floats is preferably filled with expanded polystyrene. The addition of the expanded polystyrene preferably prevents the invention from sinking even if the buoyancy floats are punctured. These techniques and methods significantly increase the reliability of evaporation rate measurements providing for an extremely accurate measurement of the evaporation rate within the body of fluid being evaluated.

Further scope of applicability of the present invention will be set forth in part in the detailed description to follow, taken in conjunction with the accompanying drawings, and in part will become apparent to those skilled in the art upon examination of the following, or may be learned by practice of the invention. The objects and advantages of the invention may be realized and attained by means of the instrumentalities and combinations particularly pointed out in the appended claims.

BRIEF DESCRIPTION OF THE SEVERAL VIEWS OF THE DRAWINGS

The accompanying drawings, which are incorporated into and form a part of the specification, illustrate one or more embodiments of the present invention and, together with the description, serve to explain the principles of the invention. The drawings are only for the purpose of illustrating one or more preferred embodiments of the invention and are not to be construed as limiting the invention. In the drawings:

FIG. 1 is a perspective view of an embodiment of the present invention; and

FIG. 2 is a cross-sectional view of the embodiment of FIG. 1.

DETAILED DESCRIPTION OF THE INVENTION

In the following detailed description, numerous specific details are set forth in order to provide a thorough understanding of the embodiments of the invention. However, it will be understood by one of ordinary skill in the art that the embodiments may be practiced without these specific details. For instance, well known operation or techniques may not be shown in detail. Technical and scientific terms used in this description have the same meaning as commonly understood to one of ordinary skill in the art to which this subject matter belongs.

Embodiments of the invention comprise an improved floating evaporation pan assembly that has built-in protections from wave action. An open-body container (hereinafter "evaporation pan") is preferably surrounded by a wave-guard, preventing wave action disturbance of evaporation rate measurements to improve the reliability of said measurements. One embodiment of the wave-guard comprises a vertical wall at the height of, or taller than, the wall of the evaporation pan. The wave-guard may be attached to adjustable buoyancy floats (hereinafter "floats") at preferably equal spacing surrounding the evaporation pan. In a preferred embodiment, the floats are designed to provide additional buoyancy for the evaporation pan so that the evaporation pan can never sink. The floats preferably have an access port on the top for the addition of weight that is at the same density as, or denser than, the surrounding body of fluid. After the desired freeboard of the wave-guard and evaporation pan are obtained, expanded polystyrene is optionally added to each float to fill in the remaining hollow. The expanded polystyrene preferably provides sufficient buoyancy to prevent the evaporation pan from sinking, even if the integrity of the floats is compromised by penetration of the floats, and filling with the surrounding body of fluid. The evaporation pan is preferably attached to the floats through spacing-braces. These spacing-braces preferably provide an area of calm fluid body surrounding the evaporation pan and add rigidity to the whole apparatus. Preferably, within the evaporation pan itself, there is an adjustable baffle system for the reduction of sloshing and a guided-float for the measurement and control of the fluid level in the evaporation pan.

In one embodiment, the apparatus is preferably anchored in such a manner that its lateral movement is minimized if not eliminated while also allowing for its vertical movement so that the apparatus can move up or down with the level of the surrounding body of fluid. This anchoring system allows the apparatus to be fixed at a known location and prevents its rotation so that any instrumentation installed on the apparatus will not cast a shadow on the evaporation pan. In a preferred embodiment, the anchor system will consist of one or more (e.g., three) mooring systems attached to the spacing-braces around the evaporation pan. Mooring systems are well established in the art and one such system is described herein as an example. A typical mooring system consists of an anchor, to be selected by one skilled in the art, an anchor line connecting the anchor to the buoy on the surface of the fluid, and a pickup line, which connects the buoy to the object being moored.

Referring to FIGS. 1 and 2, in one embodiment, floating evaporation pan system 1 preferably comprises evaporation pan 14, a plurality of wave-guards 2, and a plurality of floats 4 to provide buoyancy for the apparatus to float on the surface 30 of a body of fluid. Each float 4 preferably comprises one removable cap 6 to cover or fit in opening 8. These floats 4 are preferably positioned substantially approximately equidistant from each other and surround evaporation pan 14 to maintain a level operation of the apparatus. Each float 4 is preferably attached to one spacing-brace 12 and to two wave-guards 2. Preferably, spacing-braces 12 attach the outer structure comprising the wave-guards 2 and floats 4 to evaporation pan 14. Spacing-braces 12 preferably provide sturdiness for the apparatus in an environment with wave action and allow a separation between the wave-guards 2 and evaporation pan 14. Additionally, spacing-braces 12 preferably provide a durable location to attach one or more pickup lines 28 for each mooring system. Each wave-guard section 2 is optionally reinforced with one or more wave-guard bracing 10. Wave-guard bracings 10 preferably provide durable attachment points between wave-guards 2 and floats 4.

In one embodiment, evaporation pan 14 preferably comprises bracing 16 attached, for example, to its outer, vertical surface. Bracing 16 preferably provides rigidity for evaporation pan 14. In one embodiment, the uppermost brace 16 comprises a splash guard, which is preferably disposed above the surrounding fluid body level, and further provides a durable location for spacing-braces 12 to attach.

Preferably, within evaporation pan 14 there is a baffle system. In one embodiment, this baffle system comprises baffle **18** and baffle supports **20**. Baffle **18** is preferably connected to baffle supports **20**, which are preferably adjustable, and are preferably perpendicularly attached to the interior bottom of evaporation pan **14**.

The system preferably also comprises a guided-float assembly comprising a plurality of guide-rods **22**. In one embodiment, guide-rods **22** are attached perpendicularly to the bottom of evaporation pan **14**. The system preferably further comprises guide-tubes **24** that slide over the guide-rods **22**. Preferably, guide-tubes **22** are attached to guided-float **26**. In one embodiment, guided-float **26** preferably rises and falls with the fluid level within evaporation pan **14** and is preferably attached to a linear displacement measurement device. The type of linear displacement measurement device selected by one skilled in the art is not shown because the type selected may vary, as well as the type of mounting system for such a measurement device.

The mooring system preferably comprises anchor **32** that resides on bed **40** of the fluid body being evaluated. Attached to anchor **32** is anchor line **34** that preferably connects anchor **32** to mooring buoy **36** on the surface of the fluid body. Pickup line **28** preferably connects spacing-brace **12** on the apparatus to mooring buoy **36**.

In one embodiment, the apparatus is made of a suitable material (e.g., aluminum or other fluid resistant material) to prevent galvanic corrosion, excluding caps or plugs **6**. The construction material should be fluid resistant, durable, and non-reactive to the body of fluid being evaluated.

In describing attachments between the elements herein, any known method of attaching the elements may be employed by one skilled in the art. Examples of attachment methods include the use of drilling holes and employing screws and bolts, using pins and/or adhesives, or using welding techniques.

In operation, the embodiment for an apparatus described above is preferably used as follows. The apparatus is preferably assembled on level land and then moved to the study location once the mooring system is installed. Evaporation pan **14** is preferably filled with fluid from the surrounding body of fluid to a level less than that of the surrounding body of fluid. Floats **4** are preferably then filled with sand until the apparatus is level and at the proper freeboard level. The proper freeboard level is achieved when wave over-topping of evaporation pan **14** is minimized and wind flow disturbance along the surface of body **30** of fluid is minimized. When the desired freeboard and level is achieved, expanded polystyrene is optionally added to the remaining hollow space in each float **4**, followed by securing the cap or plug **6** into opening **8** of each float. Finally, the fluid-level within evaporation pan **14** is preferably measured at certain time intervals by one skilled in the art by means of the guided float assembly and the above mentioned linear displacement measuring device, providing the information necessary to calculate the evaporation rate of the body of fluid being evaluated.

INDUSTRIAL APPLICABILITY

The invention is further illustrated by the following non-limiting examples.

Example 1

An apparatus as described above was constructed of marine grade aluminium, 6061-T6 alloy. There were six floats spaced 60 degrees from each other with wave-guard segments attached between the floats. The floats and wave-guards formed a circular-ring surrounding the evaporation pan. The circular-ring shape of the floats and wave-guard aided in the stability of the apparatus and deflected energy imposed on the apparatus from waves in the body of fluid being evaluated. The spacing-braces attached the circular-ring formed by the floats and wave-guard segments to the evaporation pan. The length of the spacing-braces was sufficiently long to prevent splashing on the wave-guards from being ejected into the evaporation pan. Three mooring systems were attached to the bottom of the spacing-braces where the spacing-braces attached to a float approximately every 120 degrees, and each extending outward from the apparatus along the vector formed by the spacing-brace that it was attached to. One mooring system comprised an anchor on the bed of the fluid body being evaluated, an anchor line, a mooring buoy, and a pickup line.

The preceding example can be repeated with similar success by substituting the generically or specifically described components and/or operating parameters of this invention for those used in the preceding examples. Note that in the specification and claims, "about" or "approximately" means within twenty percent (20%) of the numerical amount cited. Although the invention has been described in detail with particular reference to these preferred embodiments, other embodiments can achieve the same results. Variations and modifications of the present invention will be obvious to those skilled in the art and it is intended to cover in the appended claims all such modifications and equivalents. The entire disclosures of all references, applications, patents, and publications cited above are hereby incorporated by reference.

What is claimed is:

1. An apparatus for determining the evaporation rate of an open body of fluid, comprising:

an open container comprising a vertical wall surrounding the periphery of said open container;

a baffle system mounted within said open container and said baffle system configured to reduce sloshing of fluid out of the evaporation pan;

a wave-guard system connected to said open container with spacing-braces, wherein said spacing braces space away said wave-guard system from said open container and comprising wave-guard bracings and a wave-guard vertical wall at least as tall as said vertical wall of said container, said wave-guard system entirely surrounding said open container;

a buoyancy system; and

an anchor assembly preventing lateral movement of said apparatus while allowing vertical movement thereof.

2. The apparatus of claim 1 wherein said buoyancy system comprises buoyancy floats surrounding said open container disposed approximately equidistant from each other.

3. The apparatus of claim 2 wherein said wave-guard system connected to said buoyancy floats forms a circular ring surrounding said open container.

4. The apparatus of claim 1 wherein said open container comprises a circular shape.

5. The apparatus of claim 1 further comprising a guided-float assembly comprising one or more guide-rods attached to a bottom surface of said open container, and a guided float.

6. The apparatus of claim 1 further comprising an anchor securing said apparatus at a fixed location within the body of fluid and preventing lateral movement.

7. A method of determining a rate of evaporation of an open body of fluid comprising the steps of:

providing an evaporation pan;

filling the evaporation pan with the body of fluid to be evaluated;

providing a wave-guard element both extending away from and entirely surrounding the evaporation pan to protect the evaporation pan from waves in the body of fluid;

reducing sloshing of fluid out of the evaporation pan with a baffle system; and

measuring the level of the fluid in the evaporation pan at selected time intervals to determine the rate of evaporation of the fluid.

8. The method of claim 7 further comprising attaching adjustable buoyancy floats providing adequate flotation for the evaporation pan.

9. The method of claim 7 further comprising attaching a guided-float assembly within the evaporation pan before filling the evaporation pan with fluid from the surrounding body of fluid.

10. The method of claim 7 further comprising attaching the wave-guard element to the evaporation pan with a plurality of spacing-braces.

11. The method of claim 7 further comprising supporting the wave-guard element by a plurality of buoyancy floats.

12. The method of claim 7 further comprising providing a plurality of anchoring systems preventing rotational and horizontal movement.

13. The method of claim 7 wherein the evaporation pan is filled with fluid from the body of fluid being evaluated to a level less than that of the surrounding body of fluid.

* * * * *